

Carbonaceous Species in Atmospheric Aerosols: Sources and Temporal Variability

A THESIS

submitted for the Award of Ph. D. degree of

MOHANLAL SUKHADIA UNIVERSITY

in the

Faculty of Science

By

Kirpa Ram



Under the Supervision of

PROFESSOR M. M. Sarin

SENIOR PROFESSOR

**Physical Research Laboratory,
Ahmedabad-380 009, India.**

**MOHANLAL SUKHADIA UNIVERSITY
UDAIPUR**

2010

D E C L A R A T I O N

I Mr. **Kirpa Ram**, S/o: Mr. **Ram Raj**, resident of **A-1, PRL residences, Navrangpura, Ahmedabad – 380 009**, hereby declare that the research work incorporated in the present thesis entitled “**Carbonaceous Species in Atmospheric Aerosols: Sources and Temporal Variability**” is my own work and is original. This work (in part or in full) has not been submitted to any University for the award of a Degree or a Diploma. I have properly acknowledged the material collected from secondary sources wherever required. I solely own the responsibility for the originality of the entire content.

Date:

(Kirpa Ram)

C E R T I F I C A T E

I feel great pleasure in certifying the thesis entitled “**Carbonaceous Species in Atmospheric Aerosols: Sources and Temporal Variability**” by Kirpa Ram under my guidance. He has completed the following requirements as per Ph.D. regulations of the University

- (a) Course work as per the university rules.
- (b) Residential requirements of the university
- (c) Regularly submitted six monthly progress report
- (d) Presented his work in the departmental committee
- (e) Published/accepted minimum of one research paper in a referred research journal.

I am satisfied with the analysis of data, interpretation of results and conclusions drawn.

I recommend the submission of thesis.

Date: 2010

Name and Designation of supervisor

*Countersigned by
Head of the Department*

To my Grand parents

&

Sister Anjani

Acknowledgements

After spending the most valuable five years of my life and remembering those sweet and eventful years at the Physical Research Laboratory (PRL), Ahmedabad, India; I realize that there are many without whom this thesis would not have been a reality. To me, this thesis is by far the most challenging and significant scientific accomplishment in my career. With deep sense of gratitude and respect, I wish to express my sincere thanks and appreciation to my thesis supervisor, Prof. M.M. Sarin – a person who believes in the perfection, for introducing me to the field of Atmospheric Chemistry. His enthusiasm, integral view of handling a research project, timely planning and his mission for providing “high quality research with great perfection”, has taught me very important lesson of life. His constant and enormous support, inspiration and encouragement throughout my Ph. D. period have helped to bring out the best from me in the form a thesis. He is an immense source of inspiration and I am extremely grateful to him for providing me this opportunity. I am greatly indebt to him in making me what I am today.

I thank Prof. J. N. Goswami, the Director, and Prof. Utpal Sarkar, the Dean, Physical Research Laboratory, for providing me all the necessary facilities to carry out my thesis work.

I would like to thank Prof. S. Krishnaswami who inspired me to do good work and keeping me awake all the time. It was a great opportunity and privilege for me to work in the foundation made by him. The scientific discussions with him were simply outstanding and amazing which helped me to bring out the best from me. I am extremely benefited by his class, ways of expression and talking, and am highly indebt to him for the encouragement provided to me during my research tenure at PRL, both professional and personal.

The course work taught by Profs. J. N. Goswami, M.M. Sarin, R. Ramesh, A. K. Singhvi, S.K. Bhattacharya, S.A. Haider, Drs. S.K Singh, J.S. Ray and D. Benargee during the first year at PRL was extraordinary and knowledgeable. This course work has provided an overview of the use of various tools and techniques which I use to read in text books in my early education. I wish to thank all of them for the excellent and outstanding course taught to me at PRL in the various fields’ of fundamental research.

The suggestions from the core scientific committee of PRL, constituting Profs. S. Rindani, R. Ramesh, S.A. Haider, Drs. S. Ramachandran, D.A. Angom Singh and D. Benargee were always helpful. I specially thank Prof. Shyam Lal, Dr. S. Ramachandran and Dr. B. Bapat for the scientific discussion at various stages of my research work. I thank Dr. P. Sharma for the help provided in the early time of my stay at PRL.

My research journey at PRL started with a project carried out under the supervision of Dr. Sunil K. Singh during the course work. I am extremely benefited by this project and learnt the basics of chemistry and experiments. With great respect and gratitude, I thank Dr. S.K. Singh for providing me an excellent opportunity. I can not forget to thank Dr. Ravi Bhushan (Ravi Daa) – a friend, philosopher, and a person with great sense of humanality whom you can always trust. He can always find time to talk to you and always ready to help. I am extremely thankful to him for

the help, care and support provided to me in the Laboratory. I wish to thank Dr. R. Rengarajan and Mr. A.K. Sudheer for helping me in doing the experimental work during my early time. The scientific discussion and advices from them were very helpful. To run a good laboratory, one would always wish to have a person like Mr. J. P. Bhavsar (Bhavsar Bhai). Whatever scientific material/equipment you look for in the Laboratory, you should first ask Bhavsar Bhai. I thank Bhavsar Bhai for his help and support. My special thanks to all the members of our atmospheric research group (Ashwini, Timmy, Prashant and Srinivas). I wish to thank my closest friends (Gyana, Rahaman, Vineet, Jayati and Pal) for their help and support in the Laboratory. Thanks to Ms. Sneha Acharya for the help in computer related work. I thank Mrs. Pauline Josheph for all the help, care and support provided to me. I thank all the family members of the Chemistry group for a nice and comfortable company during trips of holidays. I specially thank Mrs. Renu Singh and Mr. Markandeya for inviting us at all the festivals and happy occasions and providing a homely environment.

I thank all the faculties, scientists and staff members of the Geosciences Division. My special thanks to Profs. A.K. Shinghavi, R. Ramesh, S. K. Bhattacharya, S.V.S. Murty, Drs. M.G. Yadava, Kuljeet Kaur, Vinay K. Rai, Navin Juyal, A.D. Shulkla, Som K. Shrama, K. Rao and R.D. Deshpande for their help and kind support during my stay at PRL. I must thank Pranav Bhai, Deepak Panda, T.A. Rajesh, T.K. Sunil Kumar, Venkat Ji, Manan and Lakhan bhai for helping in instrumental related problems.

The time spent at PRL hostel with my closed friends will be an unforgettable moment of my life. I must thank all of my seniors (Drs. Rohit Srivastava, Shreyas Managave, Ritesh K. Mishra, P. Morthekai, Sanat Das, Uma Kota, Rajesh Kushwaha, Salman Silotri, Jayant, H. Zeen Devi and A. S. Maurya), my batch-mates (Gyana, Naveen, Sumita, Alok, Bhavik, Vishal, Harnider, Manan, Sumanta, Shuchita, Lokesh, Brejesh, Sanjeev, Ram, Rohan and Arvind) and junior-mates (Rohit, Amjad, Naveen Chauhan, Rabiul, Neeraj, Ashish, Tapas, Sunil, Arun, Surichi, Moumita, Arvind Suxena, Chinmay, Iman, Patra, Suman, Ashok, Praveen, Anand, Sandeep, Srikant, Soumya, Subrata, Suratna, Vimal, Yogita, Zulfikar and Arvind Rajpurohit). It was a great pleasure for me to have seniors and friends like you all. Thank you all my dear friends for making my stay very pleasant at PRL. The discussions at tea-time were always awesome and one would not like to miss tea-time at PRL.

I was inspired by the good quality of research work done by our seniors. I thank Drs. N. Rastogi, D. Ganguly, A. Mishra, L. Sahu, R. K. Mishra, Ashutosh K. Singh, Santosh K. Rai. My special thank to Dr. N. Rastogi who taught me a lot on the experimental techniques before he left PRL. The scientific discussions with Drs. D. Ganguly, L. Sahu and A. Mishra were always fruitful and I learned a lot from them.

I take this opportunity to thank all the members of PRL work shop. I specially thank Mr. G.P. Ublae, Vishnu Patel, Bankim, Jayanti bhai for the help and fulfilling the requirement to carry out my research work at various stages. I must thank Jitu Bhai, Rakesh, Jokhakar Ji, Sivadasan Ji and all the members of electric sections for their help and support. I thank all the members of the

administration department for their help and support for admin related works. My special thanks to Deekshitullu Ji, Ghanshyam Bhai, Ranganathan Ji, Bhupendra Ji, Senthil Bhai, Pradeep, Hemal Bhai, Mrs. Nandini Rao, Usha Ji for their help and support at various levels.

I must thank all the members of the Computer center, Subedar and Dolakia Ji, Tejas, Jigar, Alok, Mishra Ji and Kailash for the help in computer related problems. The help from Mrs. Nishtha A. Kumar, Uma Ji, Thakore Bhai and all the supporting staffs of PRL library is thankfully acknowledged.

I am glad to acknowledge Dr. S.N. Tripathi and his group members (Sanjay Baxala, Jai Devi, Sumit Misra, Harish Ji and Hari Shanker) and for the help provided in the collection of aerosol samples at Kanpur. The discussions with Dr. Tripathi were always fruitful. Thanks to Dr. P. Hegde for help in the aerosol sample collection at Manora Peak and providing the meteorological data of the study period.

With great respect and gratitude, I wish to thank all the faculties, scientists, staff members and the students of PRL, whose names are missing, for their love, care and support provided during my stay at PRL.

My journey at PRL was very eventful and was often falling sick at regular intervals. I wish to thank our PRL medical doctors, Dr. (Mrs.) Sheetal Patel and Dr. Sameer Dani, and staff members who kept me in good health.

I am highly indebted to my parents (Shree Ram Raj and Smt. Shanti Devi) and grand parents, who always have been a source of inspiration and motivation to me. They never let me down throughout my study period and taught me the real meaning of hard work and honesty by setting up their own examples. I dedicate this thesis to my grand parents, who left us in my early days of education. I thank to my elder sisters (Late Smt. Anjani and Smt. Laxmi) and brothers (Prashant and Shushant) for their love, care and support in my life. I would like to share this moment of achievement and happiness with my entire family, friends (Jainendra, Anil, Sunil, Navneet, Gaya, Vimlendra, Shekhar, Ashok, Shravan and Shailesh) and closed members.

I am grateful to my wife Preeti and son, Hrithivk for their moral support and patience provided to me throughout the research work. I remember the days when I have to work late night in the Laboratory but it was a great support from them without any complaint. Without their support, care and understanding it would have been impossible to complete my research work. I hope they will continue their encouragement and support in the same way in future too.

In the last, I thank all the persons who have, directly or indirectly, helped me during my Ph. D. Thesis.

Kirpa Ram

ABSTRACT

This thesis presents a comprehensive study of the chemical and optical properties of ambient aerosols (with emphasis on carbonaceous species) collected from high-altitude sites (Manora Peak and Mt Abu) and an urban location (Kanpur) in the Indo-Gangetic Plain (IGP). The mass concentrations of OC, EC and WSOC at an urban site are an order of magnitude higher than those at the high-altitude sites. The source variability, emission strength, secondary aerosol formation and boundary layer dynamics, all contribute significantly to the seasonal trend in the mass concentrations of carbonaceous species at Kanpur. Based on the chemical tracers (K^+ concentration, K^+/OC : $A_v = 0.06 \pm 0.03$ and OC/EC ratios: $A_v = 7.8 \pm 3.4$), biomass burning emission (wood-fuels and agricultural waste) has been identified as a major source of carbonaceous aerosols. The $WSOC/OC$ ratios vary within a narrow range (~ 0.35 – 0.40) at Kanpur during wintertime; whereas the elevated ratios (~ 0.55) during summertime suggest significant contribution from secondary organic aerosols. The highly acidic environment (SO_4^{2-} and NO_3^- aerosols) over IGP, during the wintertime, may significantly alter the morphological features of EC. In addition, the secondary aerosol formation and their hygroscopic growth (through nucleation/coagulation) can enhance the scattering properties of aerosols, a process that can be invoked for the poor visibility over northern India during the wintertime.

A novel approach is also proposed for the determination of absorption coefficient (b_{abs}) and mass absorption efficiency (σ_{abs}) of EC using simultaneous measurements of optical-attenuation (at 678 nm) in the thermo-optical EC-OC analyzer. At Manora Peak and Mt Abu, b_{abs} is 13.7 ± 7.3 and 5.8 ± 4.3 Mm^{-1} respectively; and that at urban site (Kanpur) is 42.7 ± 17.9 Mm^{-1} . The σ_{abs} varies from 4.3 to 20.9 m^2g^{-1} , unlike the constant conversion factor used in optical instruments for the determination of BC concentration. The *in-situ* measurements of optical properties along with the aerosol chemical composition (this study) are useful for the inter-comparison with other techniques/measurements.

Keywords: *Elemental and organic carbon (EC, OC), water-soluble OC (WSOC), OC/EC and WSOC/OC ratios, secondary organic aerosols, aerosol absorption coefficient (b_{abs}), mass absorption efficiency of EC (σ_{abs}), Indo-Gangetic Plain (IGP)*

CONTENTS

List of Tables

List of Figures

Chapter-1	Introduction	1-14
1.1	Atmospheric aerosols and Earth's radiation budget	1
1.2	Sources, size-distribution and residence time of aerosols	2
1.3	Chemical composition and optical properties of aerosols	3
1.4	Importance of atmospheric aerosols	5
1.4.1	Impact on heterogeneous-phase chemistry	5
1.4.2	Effect of aerosols on air-quality, visibility and hydrological cycle	6
1.4.3	Atmospheric aerosols as a source of nutrients to the Ocean and effect on human health	7
1.5	A review of studies from Indo-Gangetic Plain (IGP)	8
1.6	Rationale and objective of the present study	9
1.7	Thesis outline	13
Chapter-2	Material and Methods	15-34
2.1	Site description and ambient aerosol sampling	15
2.2	Site description	16
2.2.1	Kanpur: an urban site in the Indo-Gangetic Plain (IGP)	16
2.2.2	Manora Peak and Mt Abu: the high-altitude sites in India	16
2.3	Ambient aerosol sampling	17
2.3.1	Aerosol sampling at Kanpur	17
2.3.2	Aerosol sampling at Manora Peak and Mt Abu	18
2.4	Analytical methods	19
2.4.1	Determination of particulate matter (PM) mass	20
2.4.2	Analysis of OC and EC using a thermal-optical EC-OC analyzer	20
2.4.3	Analysis of water-soluble organic carbon (WSOC)	26
2.4.4	Analysis of water-soluble inorganic species (WSIS)	27
2.4.5	Analysis of bicarbonate (HCO_3^-)	27
2.4.6	Determination of aerosol absorption coefficient (b_{abs}) and mass absorption efficiency of EC (σ_{abs})	29
Chapter-3	Aerosol characteristics over urban and high-altitude sites	35-48
3.1	Introduction	35
3.2	Results and Discussion	36
3.2.1	Characterization of sources of aerosols using the tracer approach	36

3.2.2	Seasonal variability in PM ₁₀ mass at Kanpur	38
3.2.3	Total suspended particulate (TSP) mass and long-range of transport of aerosols at high-altitude sites	40
3.2.4	Aerosol optical depth at Manora Peak	45
3.3	Summary	47
Chapter-4	Carbonaceous aerosols at an urban site (Kanpur) in the Indo-Gangetic Plain	49-69
4.1	Introduction	49
4.2	Results and Discussion	50
4.2.1	Meteorological details and back trajectory analysis	50
4.2.2	Mass concentrations of carbonaceous species (OC and EC): Spatio-temporal variability	54
4.2.3	The OC/EC ratios and characterization of sources of carbonaceous aerosols	58
4.2.4	Mass concentrations of WSOC	60
4.2.5	The WSOC/OC ratios and secondary organic aerosol (SOA) formation	62
4.2.6	Estimation of secondary organic carbon (SOC)	65
4.2.7	Fractional contribution of the absorbing EC to aerosol mass	66
4.2.8	Inter-comparison of mass concentrations of OC and EC over Indian Regions	67
4.3	Summary	69
Chapter-5	Carbonaceous aerosols at high-altitude sites in India	70-83
5.1	Introduction	70
5.2	Results and Discussion	71
5.2.1	Meteorological details at Manora Peak	71
5.2.2	Temporal and spatial variability in mass concentrations of carbonaceous species	73
5.2.3	The OC/EC ratio	77
5.2.4	Water-soluble organic carbon (WSOC) and WSOC/OC ratio	79
5.2.5	Estimation of secondary organic carbon (SOC)	80
5.2.6	Inter-comparison of mass concentrations of OC and EC with other high-altitude sites	82
5.3	Summary	82
Chapter-6	Aerosol absorption properties over Indian regions	84-102
6.1	Introduction	84
6.2	Results and Discussion	86
6.2.1	Optical-attenuation and surface EC concentration	86
6.2.2	Inter-comparison of attenuation coefficient derived by the EC-OC analyser (b _{ATN-ECOC}) and the Aethalometer (b _{ATN-}	89

	Aeth)	
6.2.3	Spatial and temporal variation of absorption coefficient (b_{abs})	91
6.2.4	Site-specific mass absorption efficiency of EC (MAE, σ_{abs}): Temporal variability and influence of different emission sources	95
6.3	Summary	102
Chapter-7	Synthesis and scope of future research	103-108
7.1	Synthesis	103
7.2	Scope of future research	106
	References	109-131
	List of Publications	132-134
	Appendix	135-135

List of Tables

Table	Contents	Pages
2.1	List of the sampling sites, time-period and frequency of sample collection	16
2.2	Temperature cycles and purging gas conditions for the analysis of OC and EC using thermal-optical EC-OC analyzer	21
2.3	Average blank concentrations, detection limits and reproducibility of carbonaceous species	25
2.4	Average blank concentrations, detection limits and reproducibility of water-soluble inorganic species	29
2.5	Measured optical parameters and related uncertainties	34
4.1	Meteorological data during the sampling period at Kanpur	52
4.2	Monthly-averaged mass concentrations of OC, EC, TCA, WSOC and their ratios at Kanpur	55
4.3	Seasonal-average mass concentrations of OC, EC, TCA, WSOC and their ratios at Kanpur	56
4.4	The average and range of K^+/OC and K^+/EC ratios in aerosols from the Indian, Chinese sites, savanna and agricultural waste burning emissions	60
4.5	Comparison of OC, EC (or BC) mass concentrations and OC/EC ratios over Indian regions	68
5.1	Monthly average concentrations of TSP, OC, EC, TCA and WSOC along with the OC/EC and WSOC/OC ratios at Manora Peak during the sampling period (Feb 2005-July 2008)	77
6.1	Attenuation coefficient (b_{ATN}): Inter-comparison of Aethalometer and EC-OC analyzer	90
6.2	Absorption coefficient (b_{abs}) and site-specific mass absorption efficiency (σ_{abs}) of EC at different geographical locations in northern India	91
6.3	Spatio-temporal variability in mass absorption efficiency (MAE, σ_{abs}): Inter-comparison with literature-based studies	100

List of Figures

Figures	Contents	Pages
1.1	Components of atmospheric aerosols	4
2.1	A map of the sampling sites in India	15
2.2	Schematic flow-chart diagram for measurements of chemical and absorption properties of aerosols	19
2.3	The schematic diagram of the thermo-optical EC-OC analyzer	20
2.4	A real-time thermograph of a sample ran on EC-OC analyzer	22
2.5	Scatter plots for repeat measurements of OC, EC, TC and WSOC	25
2.6	Scatter plots for repeat measurements of water-soluble inorganic species	28
3.1	Scatter plots between (a) OC and K^+ for Oct-Nov and Dec-Feb and (b) OC and K^+ for March and April – June; (c) PM_{10} and Ca^{2+} for March and April – June and (d) PM_{10} and Ca^{2+} for Dec-Feb and Oct-Nov at Kanpur	38
3.2	Monthly-averaged concentrations of (a) PM_{10} and (b) mass fractions of TCA and WSIS at Kanpur	39
3.3	Temporal variability in the mass concentrations of (a) TSP, (b) water-soluble Ca (Ca^{2+}) and (c) carbonate carbon (CC) at Manora Peak	41
3.4	Scatter plots between TSP and carbonate carbon at (a) Mt Abu and (b) Manora Peak, the two high-altitude sites in India.	42
3.5	Temporal variability in the mass concentrations of TSP and carbonate carbon at Mt Abu	43
3.6	Back-trajectory analyses of air-masses reaching at Mt Abu and Manora Peak, the two high-altitude sites in India	44
3.7	The monthly mean aerosol optical depth (AOD @ 500 nm) at Manora Peak	46
3.8	Temporal variability of monthly-averaged AOD and TSP mass concentrations at Manora Peak	47
4.1	Wind-rose plot at Kanpur	51
4.2	Five-day back trajectory analyses at Kanpur	53
4.3	Temporal variability of the concentrations of carbonaceous species: (a) EC, (b) OC, (c) WSOC and (d) WSOC/OC ratios at Kanpur	54
4.4	Temporal variability of: (a) PM_{10} ; mass concentrations of (b)TCA, (c) WSIS and (d) fractional contribution of TCA and	57

	WSIS to PM ₁₀ during the sampling period	
4.5	Scatter plots between WSOC and OC at Kanpur and other sites in the IGP	61
4.6	Bar diagram of monthly averaged WSOC/OC ratios at Kanpur	62
4.7	Bar diagram of average WSOC/OC ratios at Kanpur and other urban sites	63
5.1	Monthly-averaged data of rainfall, temperature, wind-speed and wind-direction at Manora Peak	72
5.2	Temporal variability in the concentrations of (a) OC, (b) EC, (c) WSOC, (d) OC/EC and (e) WSOC/OC ratio at Manora Peak	74
5.3	Temporal variability of OC and EC mass concentrations at Mt Abu	75
5.4	Box plots of TSP, OC, EC and OC/EC ratio from Manora Peak and Mt Abu	76
5.5	Scatter plots between (a) OC and EC; and (b) WSOC and OC at Manora Peak	78
6.1	Linear relationships between optical-attenuation (ATN) and surface EC concentration	88
6.2	Inter-comparison of attenuation coefficient derived from the two different instrumental techniques	91
6.3	Spatial variability of the absorption coefficient, mass absorption efficiency and EC mass concentrations for the different sampling sites in India	92
6.4	Temporal variability in the absorption coefficient (b_{abs}), EC mass concentration and mass absorption efficiency (σ_{abs}) at Manora Peak	94
6.5	Scatter plot between b_{abs} and EC concentration	96
6.6	The monthly averaged values of b_{abs} , σ_{abs} and EC mass concentrations at Manora Peak	97

INTRODUCTION

1.1 Atmospheric aerosols and Earth's radiation budget

Atmospheric aerosols, an important component of the atmosphere, are derived from a variety of sources (natural and anthropogenic) and are composed of wide-range of particles having different chemical composition, size (0.001 μm to 100 μm), shape and optical properties. They are mainly confined to the lower troposphere wherein intense vertical and horizontal mixing takes place. As a consequence, large-scale temporal and spatial heterogeneity in aerosol loadings of the atmosphere is observed. The abundance of aerosols in the atmosphere is either quantified by their total mass concentration ($\mu\text{g m}^{-3}$) or by an optical measurement referred to as aerosol optical depth (AOD). The latter parameter is defined as the vertical integral of the fraction of incident light scattered or absorbed over the entire height of the atmosphere. The absorption and/or scattering of the solar radiation and the estimates of atmospheric radiative forcing due to the long-lived greenhouse gases are well constrained in the magnitude with a high level of scientific understanding [IPCC, 2007]. According to the newer estimates of the IPCC, it is well recognized estimated that net radiative forcing due to carbon dioxide (CO_2), methane (CH_4) and nitrous oxide (N_2O) is $+2.30 \text{ W m}^{-2}$ (range: $+2.07$ to $+2.53 \text{ W m}^{-2}$). In contrast, atmospheric aerosols have short residence time (few days to a week) and are projected to have a regional to global impact on the radiation budget. The total direct radiative forcing due to aerosols is of the order of -0.5 W m^{-2} (range: -0.9 to -0.1 W m^{-2}) and an indirect radiative forcing of -0.7 W m^{-2} (range: -1.8 to -0.3 W m^{-2}) [IPCC, 2007]. Atmospheric aerosols, thus, produce a net cooling effect (negative forcing), however

these estimates carries a large degree of uncertainty and the level of scientific understanding still remains medium to low [IPCC, 2007]. The large uncertainty in the estimation of radiative forcing is mainly attributed to the relative increase in the concentrations of absorbing black carbon and considered to be much larger than the overall increase in the abundance of scattering anthropogenic aerosols [Myhre, 2009].

1.2 Sources, size-distribution and residence time of aerosols

Natural and anthropogenic emissions are the main sources of atmospheric aerosols. The natural sources of aerosols include the wind-blown dust, sea-salts and volcanic eruptions (episodic events) whereas emissions from fossil-fuel (vehicular, industrial and coal-based) and biomass burning (wood-fuel and agricultural-waste) are among the major anthropogenic sources of aerosols. Atmospheric aerosols can also be formed through the oxidation of volatile organic compounds (VOCs) yielding low volatile species (called as secondary organic aerosols; SOAs) which can coagulate to either form aerosols or directly condense onto pre-existing particles. The secondary inorganic aerosols (SO_4^{2-} and NO_3^-) are formed by the oxidation of their precursor gases (SO_2 and NO_2 , respectively) in the atmosphere [Seinfeld and Pandis, 1998]. However, a small fraction of SO_4^{2-} aerosols are derived from the sea-salts [Chester, 1990].

The specific knowledge of the size-distribution of atmospheric aerosols is essential in order to understand their interaction with the solar radiation and various heterogeneous reactions [Seinfeld and Pandis, 1998]. The size-distribution of atmospheric aerosols exhibits a bi-modal distribution and is classified into two main categories: fine-mode ($< 2.5 \mu\text{m}$) and coarse-mode ($> 2.5 \mu\text{m}$) particles. The fine-mode aerosols are further sub-divided into two categories: ultra-fine (0.01 to 0.1 μm , e.g. mainly combustion generated aerosols or fumes) and sub-micron particles (0.1 to 2.5 μm , e.g. biological particles and bacteria). Sub-micron particles are important because of their high scattering efficiency, long residence time and that they can act as cloud-condensation nuclei (CCN). In addition, their large surface area makes them an important constituent for the heterogeneous-phase chemistry. On the other hand,

coarse-mode aerosols contribute to the maximum aerosol mass and aerosol optical depth (AOD).

Atmospheric aerosols are removed from the atmosphere either by gravimetric settling (dry deposition) or by the scavenging with rain-water (wet deposition). Dry deposition of atmospheric aerosols critically depends on their sizes (Stoke's law) and hence, smaller particles have larger residence time in the atmosphere and vice-versa. The residence time is defined as the average time spent by an aerosol in the atmosphere before it is removed. In general, the life-time of atmospheric aerosols varies from a few days to weeks [Seinfeld and Pandis, 1998] and thus, have local to regional effects on aerosol chemistry, transport, radiative forcing and climate.

1.3 Chemical composition and optical properties of aerosols

The chemical composition of atmospheric aerosols is highly variable on spatial and temporal scales. Their chemical composition depends upon the geographical location, types (urban, rural or high-altitude), sources and their emission strength, meteorological conditions and transport patterns of aerosols toward the sampling sites. Over urban and rural atmosphere, carbonaceous aerosols contributes to the majority (~30-50%) of the aerosol mass followed by water-soluble inorganic species (WSIS) and mineral aerosols [Andreae *et al.*, 2008; Fuzzi *et al.*, 2006; Guo *et al.*, 2010; Kanakidou *et al.*, 2005; Rengarajan *et al.*, 2007; Tare *et al.*, 2006]. Aerosols at high-altitude locations are strongly governed by the long-range transport and hence, their chemical composition is governed by the transport patterns, secondary formation and chemical processing in the atmosphere [Carrico *et al.*, 2003a; Cong *et al.*, 2008; Cozic *et al.*, 2008; Decesari *et al.*, 2010; Hegde *et al.*, 2007; Kumar and Sarin, 2009]. For example, Zhang *et al.* [2007] have reported that ~95% of total organic aerosols at remote locations consists of oxygenated organic aerosols compared to ~64% at urban and ~83% at urban downwind sites. Decesari *et al.* [2010] have reported that ~55% of total organic carbon (OC) was water-soluble at a high-altitude site, National-climate observatory-Pyramid (NCO-P, ~5079 m amsl), located in the Himalaya. Over the coastal and oceanic regions, sea-salt aerosols

contribute significantly to the aerosol mass [Kumar *et al.*, 2008]. The heavy metals (Pb, Cd, Zn, Ni etc) are relatively abundant when the sampling sites are located closer to industrial areas. Fig. 1.1 illustrates the principal components of the atmospheric aerosols.

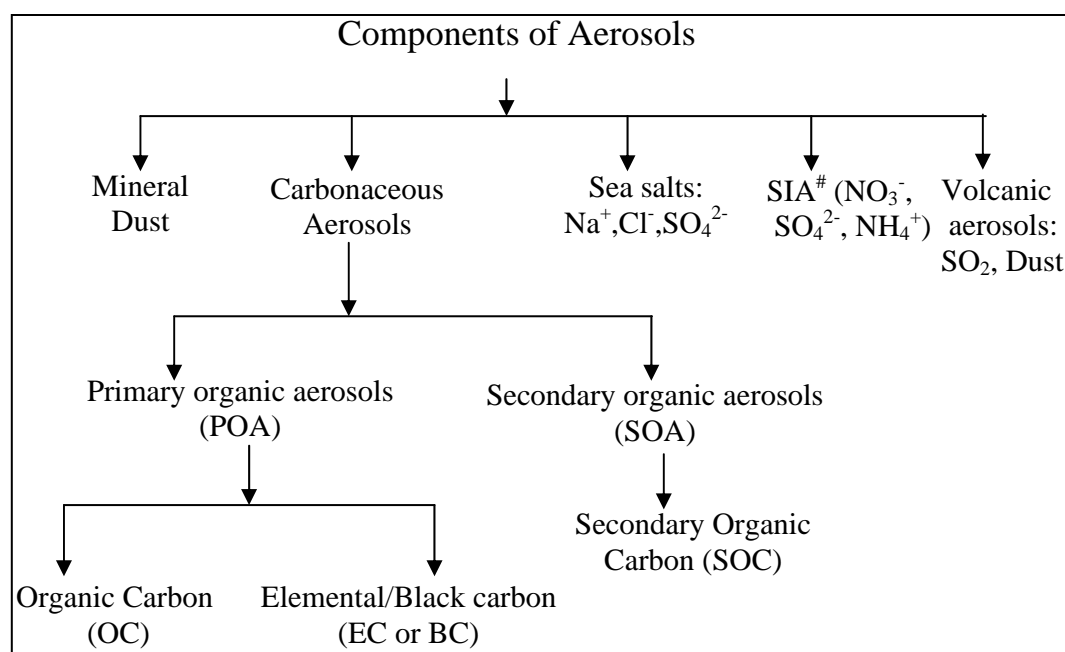


Fig. 1.1: Components of atmospheric aerosols (#SIA refers to secondary inorganic aerosols).

Atmospheric aerosols undergo chemical and physical transformations during transport and thus, they lose their original identity and rarely exist as a single component in the atmosphere. Instead, they are composed of a mixture of species derived from a number of sources and their optical properties are governed by the mixing state. The mixing state of an aerosol is defined as how various components are distributed among each other in a given aerosol population. In general, two types of the mixing states have been suggested: external mixing (particles have retained their original identity and can be treated as an individual species) and internal mixing (all the particles of the same size in a given aerosol population has uniform composition and do not behave as an individual species). Thus, the extent of mixing

can be defined as ‘to what extent an aerosol has retained its original composition’. The external mixing can be considered as a hypothetical case and may be true for freshly emitted aerosols which have not undergone any chemical and physical transformations. Through the chemical transformations and the aging, aerosols tend to become more of internally mixed nature [Cozic *et al.*, 2008]. The internal mixing increases the absorption signal for the given amount of BC as high as 50% [Bond *et al.*, 2006] and thus, the mixing state can significantly affect the estimation of radiation budget [Jacobson, 2001; Satheesh and Ramanathan, 2000].

1.4 Importance of atmospheric aerosols

1.4.1 Impact on heterogeneous–phase chemistry

The knowledge of the chemical composition, size-distribution and optical properties of atmospheric aerosols is essential to estimate the radiative and climatic effects [Maenhaut, 2008]. Since many of the atmospheric chemical reactions can modify the size-distribution, chemical composition and optical properties of aerosols, there is an increasing interest to understand the atmospheric chemistry on a regional to global scale. Several heterogeneous reactions act as a sink and/or source for reactive gaseous species (e.g. NO_x, O₃ and SO₂ etc) in the troposphere. In this regard, carbonaceous aerosols provide an active surface for heterogeneous reactions involving reactive species such as HNO₂, O₃, NO_x and OH radicals [Ammann *et al.*, 1998; Lary *et al.*, 1997; Lary *et al.*, 1999]. For example, Ammann *et al.* [1998] have reported that heterogeneous production of HNO₂ from NO₂ on suspended soot particles can be ~10⁵ to 10⁷ times faster in polluted environments. The photolysis of HNO₂ directly produces hydroxyl (OH) radicals which can modify the day-time photochemistry. Furthermore, the reactions of HNO₂ on soot particles lead to the production of tropospheric O₃ [Lary *et al.*, 1997].

Several studies suggest uptake of the acidic species (SO₂, HNO₃, H₂SO₄ etc) on mineral surfaces. For example, Rastogi and Sarin [2006] have provided a direct evidence for the neutralization of acidic species by mineral dust from an urban site (Ahmedabad) located in a semi-arid region of western India. Song *et al.* [2007] have

investigated the reaction probability of sulfate and nitrate precursors and their chemical evolution onto dust particles in East-Asia. *Geng et al.* [2009] have found gypsum (CaSO_4) particles in Asian dust samples collected over the marine boundary layer (MBL) of the Bohai Sea and the Yellow Sea. They suggested that either these particles were of the soil-origin or heterogeneous reaction products of CaCO_3 with airborne sulphuric acid and/or gaseous SO_2 . Furthermore, they also observed (C, N, O) rich-droplets and nitrate-containing secondary particles and suggested that Asian dust are an important carrier of gaseous nitrogen species, especially NO_x and/or HNO_3 . The chemical processing of mineral aerosols enhances the solubility of mineral dust and can change the mixing state of aerosols (from external to internal) which further can lead to an increase in the absorption characteristics and CCN activities [*Geng et al.*, 2009; *Manktelow et al.*, 2010].

1.4.2 Effect of aerosols on air-quality, visibility and hydrological cycle

Atmospheric aerosols, derived from natural and anthropogenic emission sources, significantly affect the air quality, visibility, atmospheric chemistry and Earth's radiation budget [*IPCC*, 2007]. The formation of secondary aerosols, in conjunction with the airborne particles of primary origin, has been recently recognized as a dominant process contributing to air pollution over urban areas and mega-cities [*Dall'Osto et al.*, 2009; *Guo et al.*, 2010; *Lee and Sequeira*, 2002; *Zhang et al.*, 2010]. Furthermore, the hygroscopic growth of secondary aerosols enhances the scattering property and decreases the visibility [*Malm et al.*, 1996]. The visibility is directly linked to aerosol extinction coefficient (b_{ext}), defined as the sum of scattering and absorption coefficients (i.e. $b_{\text{ext}} = b_{\text{scat}} + b_{\text{abs}}$), and is related to the abundances of anthropogenic ionic species [*Cheung et al.*, 2005; *Malm et al.*, 1996]. An extensive fog-haze weather formation during wintertime (Dec-Feb) over entire Indo-Gangetic Plain (IGP) in northern India is an ideal example of the reduction in the visibility due to the presence of high level of pollutants [*Ali et al.*, 2004; *Badarinath et al.*, 2007; *Gautam et al.*, 2007; *Nair et al.*, 2007; *Ramanathan and Ramana*, 2005; *Tare et al.*, 2006].

Secondary organic aerosols (SOAs) mainly exist in submicron size and are hygroscopic in nature. These two characteristics of SOAs make them an important component for the cloud activation processes, hydrological cycle and indirect effect of aerosols by acting as cloud-condensation nuclei (CCN) [Haywood and Boucher, 2000; Sun and Ariya, 2006]. Optical properties of clouds are controlled by the availability and hygroscopicity of atmospheric particles which can serve as cloud condensation nuclei [Ramanathan *et al.*, 2001; Schwartz *et al.*, 2002]. The fine-mode aerosols, derived from anthropogenic emissions, can lead to an increase in the CCN number concentration [Andreae and Crutzen, 1997]. The increase in the CCN number concentration leads to reduction in the cloud-droplet size and precipitation [Rissman *et al.*, 2004]. On the other hand, this also increases the reflectivity of the solar radiation resulting in a higher cloud-albedo (known as the first indirect climatic effect of aerosols). Thus, it is very important to know the composition of CCN population and hygroscopicity of aerosols to understand the cloud-droplet formation and precipitation processes [Haywood and Boucher, 2000; Rosenfeld *et al.*, 2007; Wang *et al.*, 2009].

1.4.3 Atmospheric aerosols as a source of nutrients to the Ocean and effect on human health

Atmospheric aerosols contain key elements such as iron (Fe), phosphorous (P), nitrogen (N) and Silica (Si) and serve as an important source of nutrients to the ocean [Jickells *et al.*, 2005]. The long-range transport of mineral aerosols and chemical transformation processes can further enhance the solubility and their deposition can modify the productivity, ocean-biogeochemistry and ocean-cycle [Mahowald *et al.*, 2005; Mahowald *et al.*, 2009]. The semi-arid regions of Thar Desert (in western India) and deserts in the Middle East can be the dominant source of mineral dust. Furthermore, Kumar *et al.* [2010] have recently highlighted that Fe derived from combustion sources (biomass burning and fossil-fuel) is an additional source of soluble-iron (Fe^{2+}) and could be a source of Fe^{2+} deposition to the two adjacent oceans (the Bay of Bengal and the Arabian Sea).

Atmospheric aerosols are very small in size and hence, they can easily enter into human lungs, especially fine-aerosols. It has been observed that fine-particulate matter are directly correlated with severe health effects such as cardiovascular, respiratory (e.g. Asthma), and allergic diseases [Nel, 2005]. In urban areas, traffic-related air pollution of fine-aerosols and gaseous species (nitrogen oxides, carbon monoxide and ozone) is one of the prime suspects of allergic and respiratory diseases. The incomplete combustion of diesel and petroleum compounds produces soot particles and unburnt hydrocarbons. Some of the unburnt hydrocarbons contain volatile, semi-volatile organic compounds (VOCs and SVOCs, respectively) and poly-aromatic hydrocarbons (PAHs) which are carcinogenic and mutagenic in nature [Lighty et al., 2000; Mauderly and Chow, 2008]. Furthermore, atmospheric chemical reactions of PAHs with NO_x , OH radical and O_3 can produce hazardous nitrated- and oxygenated-PAH derivatives [Albinet et al., 2008].

1.5 A review of studies from Indo-Gangetic Plain (IGP)

A large number of studies, based on the satellite and ground-based measurements of physical and optical properties of aerosols, have been performed over the IGP in order to assess their radiative impact [Dey and Tripathi, 2008; Ganguly et al., 2009; Ganguly et al., 2006; Nair et al., 2007; Singh et al., 2004; Singh et al., 2005]. These studies have reported large heterogeneity and spatiotemporal variability in the optical properties of aerosols and attributed them to local emission sources, meteorological conditions and transport of aerosols. The naturally derived aerosols (mainly mineral dust) originating from Pakistan, Afghanistan and the Thar Desert (in western India), contribute significantly to the aerosol loading and aerosol optical depth (AOD) during summer months (April-June). For example, Jethva et al. [2005] have reported that AOD values ranged from 0.6-1.2 (at 550 nm) during summer with relatively low fine-mode aerosol fraction (FMAF) values (<0.4) suggesting the dominance of coarse-mode particles over the IGP.

It has been speculated that anthropogenically derived aerosols (carbonaceous and inorganic aerosols) contribute significantly to the aerosol mass loading over

northern India during the wintertime (Dec-Feb). For example, *Tare et al.* [2006] have suggested that fine-mode aerosols contributed as much as 83% of the total aerosol mass at Kanpur during Dec 2004. However, there are no measurements of carbonaceous species reported in the IGP, except those of black carbon (BC) using an Aethalometer. *Tripathi et al.* [2005a] have reported that BC mass concentration at Kanpur varied from 6 to 20 $\mu\text{gC m}^{-3}$ during the field campaign (Dec 2004) and resulted in a low value of 0.76 for single scattering albedo (SSA). During the same field campaign, *Ganguly et al.* [2006] have reported that BC mass concentration was as high as 60 $\mu\text{gC m}^{-3}$ at Delhi (an urban location) with an average value of 29 ± 14 $\mu\text{gC m}^{-3}$ resulting in further low value of 0.68 for SSA.

The INDOEX (Indian Ocean Experiment) study has reported the presence of high level of pollutants over the Indian Ocean, enriched in BC (mixed with sulfate and organics) and transport of aerosols from south and South-east Asia during the wintertime (Jan-March 1999) [*Lelieveld et al.*, 2001]. More recently, *Ramanathan et al.* [2007] have observed a vertically extended atmospheric brown clouds (ABC), between 0.5 to 3 km, over the Indian Ocean. Using a general circulation model, it is suggested that warming trends in the lower atmosphere, due to the ABC, could be equivalent to the recent increase in the greenhouse gases.

1.6 Rationale and objective of the present study

Carbonaceous aerosols, consisting of organic carbon (OC) and elemental carbon (EC), are the major components of atmospheric particulate matter (PM) and constitute ~30 – 70 % of the fine-aerosol mass over an urban atmosphere [*Cao et al.*, 2003; *Fuzzi et al.*, 2006; *Hoyle et al.*, 2007; *Kanakidou et al.*, 2005; *Rengarajan et al.*, 2007]. Although EC is a minor component of atmospheric aerosols (2-10% of PM), it is a major particulate absorbing species of solar radiation [*Jacobson*, 2001; *Ramanathan and Carmichael*, 2008]. Furthermore, the relative amount of OC and EC in the atmosphere and OC/EC ratios are important parameters for the assessment of direct/indirect impacts of aerosols on the regional scale radiative forcing [*Novakov et al.*, 2005].

The OC/EC ratios currently used in the radiative transfer models are largely derived based on the emission inventories of organic aerosols. However, these ratios depend on the fuel type, quantity and more importantly on their combustion efficiency [Bond *et al.*, 2007; Streets *et al.*, 2004]. These parameters are highly variable depending on the geographical location. The real-time and long-term measurements on carbonaceous aerosols from south-Asia, particularly over Indian regions, are rather sparse, limited to only a few months of data and are inadequately represented in the literature [Chowdhury *et al.*, 2007; Miyazaki *et al.*, 2009; Ram and Sarin, 2010; Rengarajan *et al.*, 2007; Sheesley *et al.*, 2003]. Thus, there is a need for a systematic and long-term measurement of carbonaceous aerosols from the south-Asian region. Recently, Ganguly *et al.* [2009] have argued in favour of ground-based and long-term measurements of carbonaceous aerosols for their better parameterization and validation of optical properties retrieved from the satellite data.

A significant fraction of OC can also be derived from secondary organic aerosol (SOA) formation in the atmosphere and is referred to as secondary organic carbon (SOC). Most of the SOCs are soluble in water [Kondo *et al.*, 2007; Weber *et al.*, 2007], can act as cloud condensation nuclei (CCN) [Novakov and Penner, 1993; Sun and Ariya, 2006] and, thus, have an indirect climatic effect through the changes in the cloud-albedo [Haywood and Boucher, 2000]. In this regard, the measurements of water-soluble organic carbon (WSOC) and organic acids (carboxylic acids) content in atmospheric aerosols are rather essential.

The real-time measurements of black carbon (BC) via optical methods (using an Aethalometer) have been extensively performed over Indian regions in order to establish the spatio-temporal variability [Babu and Moorthy, 2002; Babu *et al.*, 2002; Badarinath *et al.*, 2007; Ganguly *et al.*, 2006; Latha and Badarinath, 2003; Ramachandran and Rajesh, 2007; Tripathi *et al.*, 2005a; Tripathi *et al.*, 2005b; Venkataraman *et al.*, 2005]. The optical methods rely on measuring the change in attenuation of light (ΔATN) at a given wavelength through the filter embedded with aerosols and use of a constant factor (referred as attenuation cross-section, σ_{ATN}) to infer the BC mass concentration. These online methods are based on the basic

assumption that absorption is solely due to BC and σ_{ATN} remains constant during the course of measurements [Bond and Bergstrom, 2006; Snyder and Schauer, 2007]; however, none of these assumptions are strictly valid. The absorption at a given wavelength may be sensitive to aerosol species other than BC mass [Bond and Bergstrom, 2006; Snyder and Schauer, 2007]. A number of studies reported in the literature invoke that σ_{ATN} is variable on a spatial scale, even shows diurnal variation [Snyder and Schauer, 2007] and changes from sample to sample [Liousse et al., 1993]. More importantly, the data on σ_{ATN} reported in the literature are based on absorption measurements via optical method and EC from a thermal method [Allen et al., 1999; Bond and Bergstrom, 2006; Liousse et al., 1993; Snyder and Schauer, 2007]. The variability in σ_{ATN} has been interpreted in terms of emission sources, mixing state of aerosols, their chemical-composition and use of more than one protocol for the determination of EC by thermal method.

Carbonaceous aerosols over south-Asian region, originating from a variety of anthropogenic emission sources (vehicular exhaust, biomass burning and fossil-fuel emissions) [Gustafsson et al., 2009; Rengarajan et al., 2007; Venkataraman et al., 2005], are gaining considerable importance because of their potential impact on regional climate [Menon et al., 2002; Ramanathan and Carmichael, 2008; Ramanathan et al., 2007]. The climate-relevant optical parameters such as BC mass fraction, absorption and scattering coefficients (b_{abs} and b_{scat} , respectively) and attenuation cross-section (σ_{ATN}), depends on the source, analytical measurements and have different chemical and optical properties [Bond and Bergstrom, 2006; Martins et al., 1998; Schwarz et al., 2008]. The assessment of radiative forcing is associated with the largest uncertainty arising due to the lack of reliable measurements of these optical parameters on a regional scale [Schmid et al., 2006]. Thus, a systematic study on the measurement of optical properties of atmospheric aerosols from Indian regions is essential for the estimation of their radiative and climatic impact on a regional scale.

With this rationale, this thesis work aims to study the chemical composition and optical properties of ambient aerosols over Indian regions, with an emphasis on

carbonaceous aerosols. Bulk-aerosols, $PM_{2.5}$ and PM_{10} (particulate matter with aerodynamic diameter <2.5 and $10 \mu\text{m}$, respectively) have been collected from an urban (Kanpur) and two high-altitude sites (Manora Peak and Mt Abu). The aerosol sampling was carried out during Jan 2007-March 2008 (PM_{10} samples) and Oct 2008-April 2009 ($PM_{2.5}$ and PM_{10}) at Kanpur. The bulk-aerosol sampling at Manora Peak was conducted during Feb 2005-July 2008 (~42 months) and that from Mt Abu was performed during May 2005-Feb 2006.

The Indo-Gangetic Plain (IGP), extending from (21.75°N , 74.25°E) to (31.0°N , 91.5°E), is one of the most populated and polluted regions in northern India. The entire Gangetic Plain experiences extreme variability in the climate over the annual seasonal cycle with dense fog and haze weather conditions during wintertime [Das *et al.*, 2008; Gautam *et al.*, 2007; Ramachandran *et al.*, 2006; Ramanathan and Ramana, 2005]. During the wintertime (Dec-Feb), a shallow boundary layer height, typically 500-800m [Nair *et al.*, 2007], leads to an efficient trapping of aerosols. Furthermore, the Himalayan mountains act as a demarcation line for the dispersion and movement toward the north direction and thus, direct the downwind flow of aerosol plumes to the Bay of Bengal (BOB). The sampling site at Kanpur (26.5°N , 80.3°E , 142 m amsl) represents an urban environment and is located at the centre of the IGP. The sampling site is affected by local emissions (biomass burning, vehicular exhaust and fossil-fuel combustion) and transport of aerosols from the urban areas located upwind in the north-western parts of the IGP. Thus, ambient aerosol sampling at Kanpur provides an ideal opportunity to understand the chemical characteristics and optical properties of aerosols associated with the changes in the emission sources and their emission strength, boundary layer dynamics and secondary aerosol formation.

The high-altitude site (Manora Peak; 29.4°N , 79.5°E , ~2000 m above mean sea level, amsl), located at the foot-hills of the Shivalik range of mountains in the central Himalaya, represents a relatively cleaner site and is less influenced by anthropogenic emissions. The major sources of carbonaceous aerosols include biomass burning emission (used for cooking and residential heating purposes) and the

advective transport of polluted air-masses from the Indo-Gangetic Plain. In addition, Manora Peak and Mt Abu are influenced by the atmospheric transport of mineral aerosols from the Thar Desert (in western India) during summer months (April-June). Thus, both the sampling sites provide ideal locations to study the chemical characteristics and optical properties of aerosols under the influence of long-range atmospheric transport of mineral aerosols. Furthermore, the aerosol sampling from high-altitude sites is advantageous in order to understand the evolution/transformation and changes in the mixing state of aerosols through heterogeneous reactions occurring on mineral surfaces during their transport processes.

OBJECTIVES

- 1. To characterize primary and secondary carbonaceous species, their sources and spatial variability over urban and high-altitude sites in northern India.**
- 2. To assess the impact of anthropogenically derived ionic species on the chemical composition of urban aerosols over the Indo-Gangetic Plain.**
- 3. To study spatio-temporal variability in the absorption properties of carbonaceous aerosols.**

1.7 THESIS OUTLINE

- ❖ **Chapter 1** provides an introduction to atmospheric aerosols, chemical and optical properties and their important role in the Earth's radiation budget and hydrological cycle. A review of previous research work done over the Indo-Gangetic Plain is presented in chapter-1. The rationale and objective of the thesis study is also defined in this chapter.
- ❖ **Chapter 2** describes the sampling sites, aerosol sampling and analytical procedures adopted for the chemical and optical measurements used in the study.

- ❖ **Chapter 3** reports on the spatial and temporal variabilities in the aerosol mass and aerosol optical depth (AOD) over urban and high-altitude sites in India. The chemical characterization and sources of aerosols are discussed with the help of mass concentrations of selected chemical tracers (Ca^{2+} , K^+ , K^+/OC and OC/EC ratios) and air mass back trajectory analyses.
- ❖ **Chapter 4:** The analytical data, results and discussion on sources of aerosols, spatio-temporal variability of carbonaceous species (EC, OC and WSOC), at an urban location (Kanpur) are presented in this chapter. A comparison of the data from other urban and rural sampling locations in the Indo-Gangetic Plain is also presented in this chapter.
- ❖ **Chapter 5:** The analytical data, results and discussion on carbonaceous species and their ratios from the two-high-altitude sites (Manora Peak and Mt Abu) are presented in this chapter.
- ❖ **Chapter 6:** This chapter describes results and discussion on aerosol absorption properties, their spatial and temporal variability over Indian regions.
- ❖ **Chapter 7:** This chapter summarizes important findings of present thesis study and their implications in assessing the radiative and climatic impacts of atmospheric aerosols on a regional scale. A discussion on the scope of future research is provided in chapter 7.

MATERIAL AND METHODS

2.1 Site-description and ambient aerosol sampling

The aerosol sampling sites, in northern and western India, are shown in Fig. 2.1 and their characteristics and geographical locations are summarized in Table 2.1. The time-period of the aerosol sampling, frequency and number of samples collected are also listed in Table 2.1.

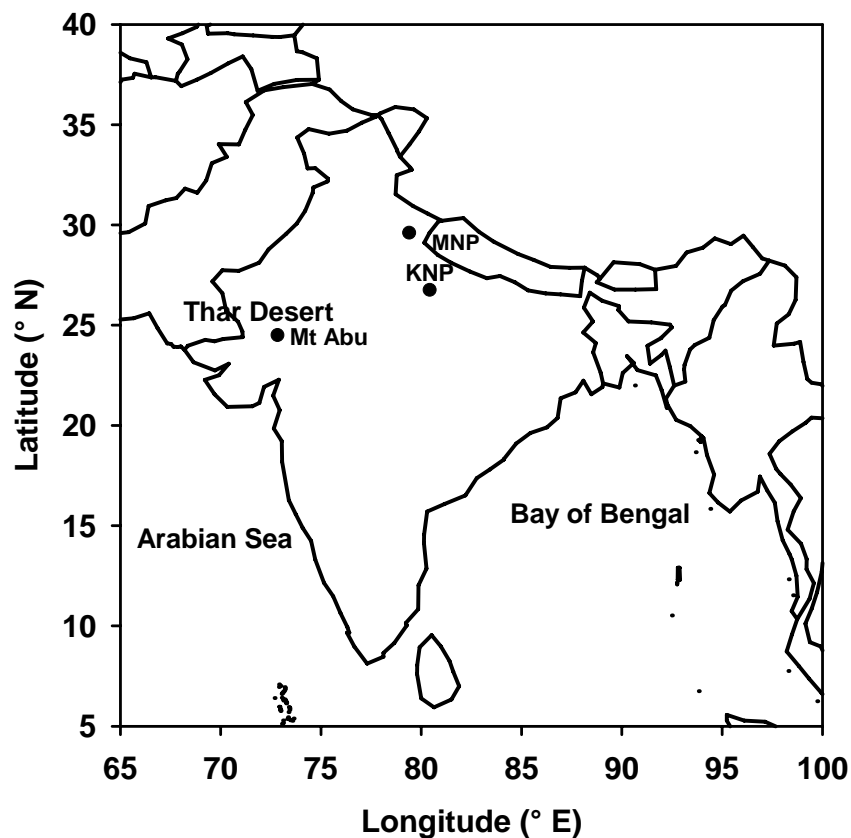


Fig. 2.1: A map of the sampling locations (shown by filled-circles) in the Indo-Gangetic Plain (IGP): Kanpur (KNP, urban) and Manora Peak (MNP, high-altitude). The location of Thar Desert and sampling site, (Mt Abu, high-altitude), in western-India is also shown.

Table 2.1: List of the sampling sites, types and their geographical location, time-period and frequency of sample collection. ‘n’ represents number of aerosol samples collected from different sampling locations.

Sampling site	Type	Lon ° N	Lat ° E	Elevation m amsl [#]	Time-period	Sampling frequency	n	Aerosol type
Kanpur					Jan 2007-Feb 2008	every fifth-day	66	PM ₁₀
Kanpur	urban	26.5	80.3	142	19-30 Oct 2008	Daily (day-night)	34	PM _{2.5} /PM ₁₀
Kanpur					Nov 2008-April 2009	every fifth-day	56	PM _{2.5} /PM ₁₀
Manora Peak	high-altitude	29.4	79.5	1950	Feb 2005-July 2008	two samples/month	86	Bulk
Mt Abu	high-altitude	24.6	72.7	1700	May 2005-Feb 2006	every-week	41	Bulk

amsl[#]: above mean sea level

2.2 Site description

2.2.1 Kanpur: an urban site in the Indo-Gangetic Plain (IGP)

The sampling site at Kanpur (26.5 °N, 80.3 °E, 142 m above mean sea level) is located in central part of the Indo-Gangetic Plain (IGP) and represents a typical urban environment. The sampling site is influenced by emissions from biomass burning (agriculture waste and wood-fuel), vehicular exhausts and industrial activities. The impact of biomass burning on the regional air quality is more pronounced during the wintertime (Dec-Feb) due to crop harvesting season and the common practice of wood-fuel burning for domestic use. The strength of biomass burning sources considerably decreases during summer (April-June) relative to the emissions from vehicular exhausts and coal-fired industries, representing the major sources of carbonaceous species. In addition to the regional emissions, sampling site is located downwind of the major polluting sources in northern India. The lower boundary layer height during winter (Dec-Feb) and Himalayan mountain range confines the aerosols within lower atmosphere. The relative humidity (RH) remains high (>80 %) during wintertime, and as a result complex foggy-hazy weather conditions prevail over the entire IGP.

2.2.2 Manora Peak and Mt Abu: high-altitude sites

Manora Peak (29.4°N, 79.5°E) is located at an altitude of ~2000 m amsl in the Shivalik range of mountains along the central Himalaya (Fig. 2.1). The

sampling site at Mt Abu (24.6 °N, 72.7 °E, 1680 m amsl) lies in a semi-arid region of western India (annual rainfall ~ 600-700 mm occurring only during the south-west monsoon; July-Sep) and is located on the highest peak in the southern end of Aravali mountain range. The sampling sites are relatively free from anthropogenic activities within the immediate vicinity. The major source of carbonaceous aerosols includes biomass burning emission used for cooking and heating purposes and transport of polluted air-masses from the Indo-Gangetic Plain (IGP) during wintertime (Dec-Feb) [Dumka *et al.*, 2006]. During summer (April-June), long-range transport of mineral aerosol dominate the atmospheric loading with a relative decrease in the abundances of carbonaceous species due to reduced biomass burning emission strength [Ram *et al.*, 2008]. The two types of aerosols and their emission strengths impart a strong seasonal and inter-annual variability in the chemical and optical properties of ambient aerosol at Manora Peak and Mt Abu.

2.3 Ambient aerosol sampling

All the ambient-aerosol samples (bulk, PM_{2.5} and PM₁₀) were collected onto pre-combusted (at 450 °C for ~6 hrs) tisuquartz filters (PALLFLEX™, 2500QAT-UP; size: 20.0 cm × 25.4 cm) (Table 2.1). The filters had a collection efficiency of 99.9% for the particles up to size 0.3 µm. All filters were wrapped in Al-foils and sealed in a polyethylene zip-lock bags and stored at ~4 °C until the analysis.

2.3.1 Sampling at Kanpur

PM₁₀ samples (particulate matter with aerodynamic diameter <10 µm) were collected, during Jan 2007-Feb 2008, from Kanpur using a high-volume sampler (APM 450, Environtech Pvt. Ltd., New Delhi, India) operated at a flow rate of $1.0 \pm 0.1 \text{ m}^3 \text{ min}^{-1}$. Aerosol sampling was set-up on the third-floor of the Environmental Engineering Laboratory (~15 m above ground level) of the Indian Institute of Technology campus. The sampler was periodically calibrated to check on the variations in the flow rate, if any. All samples (n=66) were collected during daytime, integrated for ~8-10 hrs and the volume of air sampled ranged from

~500-600 m³. The sampling frequency was one sample every fifth-day during Jan-Feb and Oct-Dec 2007; the frequency was increased to two samples per week during March-June 2007, when mineral dust is most abundant. July-Sep months represent wet-season when south-west monsoon rain causes efficient washout of the atmosphere and no aerosol samples were collected during July-Sep period. Thus, out of these 66 samples, 22 samples were collected during wintertime (Dec-Feb), 9 samples during March, 25 samples during summer (April-June) and 10 samples during post-monsoon (Oct-Nov).

Aerosol samples (PM_{2.5} and PM₁₀; particulate matter less than 2.5 μm and 10 μm aerodynamic diameter respectively) were collected simultaneously by operating two high-volume samplers (Thermo Andersen; USA). The sampler inlets have an effective cutoff-size of 50% and were operated at a flow rate of 1.1 ± 0.1 m³ min⁻¹. The flow rates were maintained by a volume-flow controller (VFC) and samplers were calibrated periodically (once in a month). Ambient air was filtered through pre-combusted tissuquartz filters and a total of 34 samples were collected spread over a period of 12 days (19-30th Oct 2008). Of these, 20 samples (10 pairs of PM_{2.5} and PM₁₀) were collected during day-time (08:30 to 17:30 hrs, local time) and 14 (7 pairs of PM_{2.5} and PM₁₀) during night-time (18:30 to 07:30 hrs, local time). Furthermore, a total of 56 aerosol samples (28 pairs of PM_{2.5} and PM₁₀) were collected during Nov 2008-April 2009. The sampling frequency was one sample every fifth-day for the entire sampling period. In addition, a number of samples collected during the land-campaign (Dec 2004) from Hisar (urban), Allahabad (urban) and Jaduguda (rural), in the Indo-Gangetic Plain (IGP) of northern India, have been used for the inter-comparison of measured chemical species and optical parameters.

2.3.2 Sampling at Manora Peak and Mt Abu

Bulk-aerosol samples were collected using a high-volume sampler (model APM 230, Environtech Pvt. Ltd., New Delhi, India) operated at a flow rate of 1.0 ± 0.1 m³ min⁻¹ for about 24 hrs in order to filter nearly 1500 m³ of air. The aerosol sampling, at Manora Peak, was started from Feb 2005 and was continued till July 2008. Overall, the sampling frequency was maintained at one sample every two

weeks, except when the sampling frequency was increased to one sample per week (during Dec 2007-March 2008). A total of 86 aerosol samples were collected during the sampling period spanned over 42 months (Table 2.1). Of these, 38 samples were collected during wintertime (Dec-March), 20 samples during summer (April-June), 17 samples during monsoon (July-Sep) and 11 samples during post-monsoon (Oct-Nov). A total of 41 bulk-aerosol samples were collected from another high-altitude site, Mt Abu, in western India during May 2005-Feb 2005.

2.4 Analytical methods

Ambient aerosols were analyzed for the particulate matter (PM) mass, the concentrations of elemental carbon (EC), organic carbon (OC), water-soluble OC (WSOC), water-soluble inorganic constituents (cations: Na^+ , K^+ , NH_4^+ , Ca^{2+} and Mg^{2+} and anions: Cl^- , SO_4^{2-} and NO_3^-). The measurements of optical parameters include aerosol absorption coefficient (b_{abs}) and mass absorption efficiency of EC (σ_{abs}). The measurements of the chemical species and optical properties in the aerosol samples are shown in a schematic flow-chart given below (Fig. 2.2).

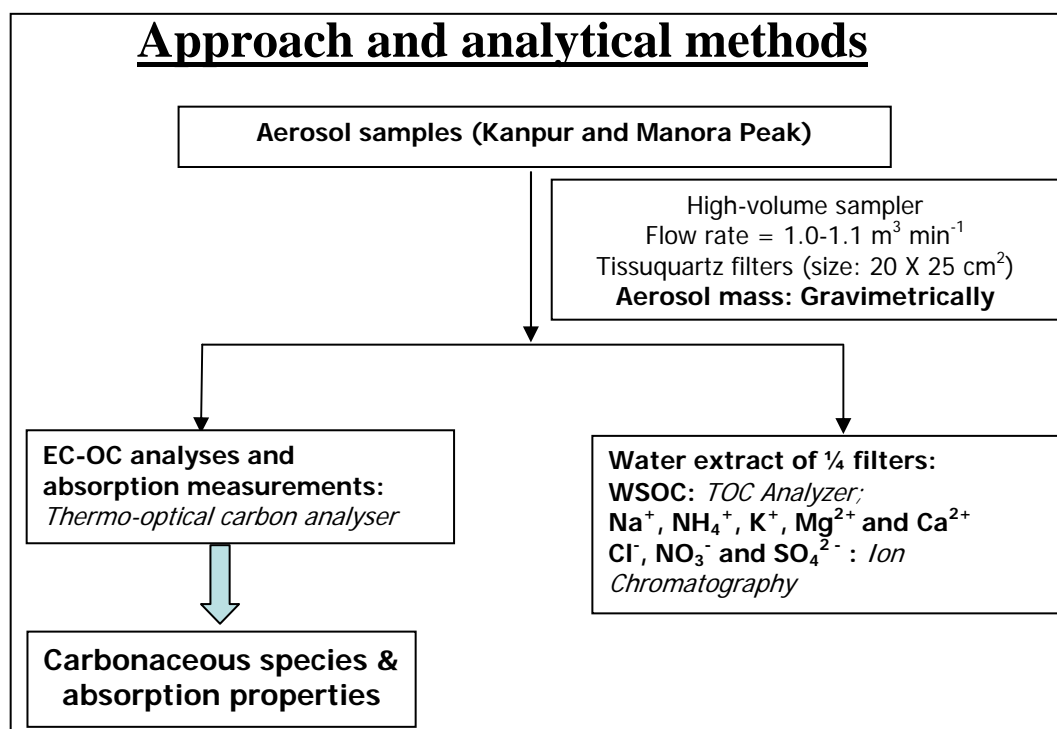


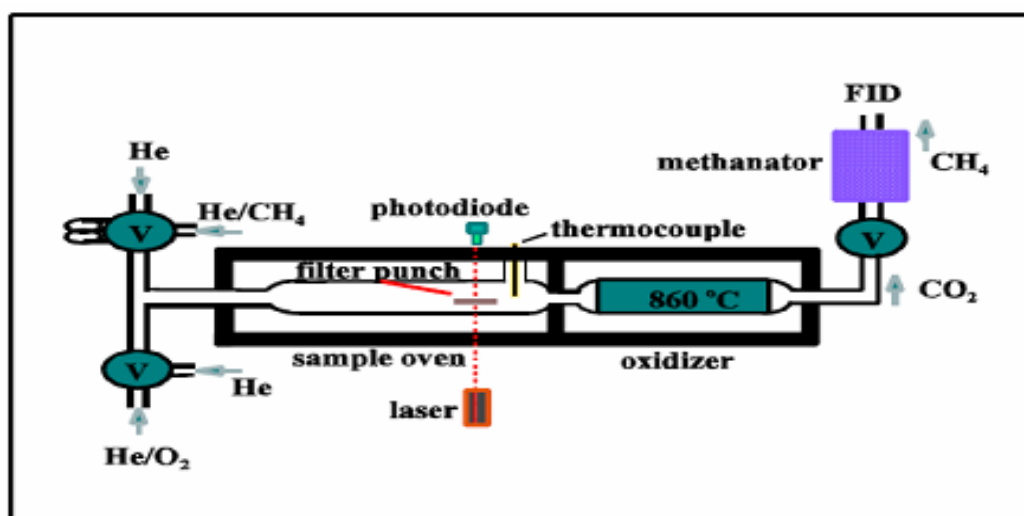
Fig. 2.2: A schematic flow-chart diagram for measurements of chemical and absorption properties of aerosols.

2.4.1 Determination of particulate matter (PM) mass

Particulate matter (PM) mass was assessed gravimetrically by weighing the filters before (blank filter weight, w_0) and after the sampling (total weight, w_t) on an analytical balance with a precision of 0.1 mg (Sartorius, model LA130S-F). Prior to weighing, filters were equilibrated for ~ 12 hrs at $22 \pm 1^\circ\text{C}$ and relative humidity (RH) of $35 \pm 5\%$. The total suspended particulate (TSP) matter ($\mu\text{g m}^{-3}$) was obtained by dividing the sample weight ($w_t - w_0$, in unit of μg) by the volume of air filtered (in unit of m^{-3}). The volume of air was determined by multiplying the sampler's flow rate ($\text{m}^3 \text{min}^{-1}$) with the total sampling time (min).

2.4.2 Analysis of OC and EC using a thermal-optical EC-OC analyzer

The thermo-optical EC-OC analyzer mainly consists of sample oven, Manganese dioxide (MnO_2) oxidizer and a methanator. The typical schematic diagram of OC/EC analyzer is shown in Fig. 2.3.



Schematic of Thermal-Optical Instrument

Fig. 2.3: The schematic diagram of the thermo-optical EC-OC analyzer (adopted from Sunset Laboratory manual).

The measurements of organic carbon (OC) and elemental carbon (EC) by a thermal-optical carbon-aerosol analyzer can be divided into three main parts:

- I. Thermal evaluation and quantification of evolved carbon fractions
- II. Determination of the split-point between OC and EC and correction for pyrolyzed carbon (PC), and

III. Correction for carbonate carbon (CC)

A rectangular aliquots of filters (area = 1.5 cm²) is kept in the sample oven and concentrations of organic carbon (OC) and elemental carbon (EC), deposited on the filter, is analyzed by a thermal-optical carbon-aerosol analyzer (Sunset Laboratory, Forest Grove, OR) using NIOSH-5040 (National Institute of Occupational Safety and Health) method based on thermal-optical transmittance (TOT) protocol [Birch, 1998; Birch and Cary, 1996]. The analytical procedure for OC-EC consists of two-stage thermal analyses. In the first stage, OC is volatilized from the aerosol sample in an inert atmosphere (100% He) through a step-wise heating (room temperature to 310 °C for 80 s, 310 °C to 475 °C for 60 s, 475 °C to 615 °C for 60 s, 615 °C to 870 °C for 60 s; Table 2.2). All the thermally desorbing organic compounds and pyrolysis products, present in aerosol samples, are then purged into a manganese dioxide (MnO₂) oxidizing oven. The oxidizing oven temperature is maintained at 860 °C and the carbon fragments flowing through MnO₂ oven are quantitatively converted to CO₂ gas. The thermograph provides four OC fractions (OC₁, OC₂, OC₃, OC₄) during the first heating cycle (Table 2.2).

Table 2.2: The carbon fraction evolved during different temperature cycles and purging gas conditions for the analysis of OC and EC using thermal/optical EC-OC analyzer.

Carbon fraction	Purging gas	Initial Temp. (°C)	Final Temp. (°C)	Ramp Time (s)
	100% He			10
OC1	100% He	35	310	80
OC2	100% He	310	475	60
OC3	100% He	475	615	60
OC4	100% He	615	870	90
Cooling oven	100% He	870	550	40
PC	90% He +10% O ₂	550	625	55
EC1	90% He +10% O ₂	625	700	45
EC2	90% He +10% O ₂	700	775	45
EC3	90% He +10% O ₂	775	850	45
EC4	90% He +10% O ₂	850	850	45
EC5	90% He +10% O ₂	850	870	45
EC6	90% He +10% O ₂	870	870	45
Calibration	100% He			110

In the second stage, the oven is cooled to below 550 °C for 60 s, a mixture of oxygen and helium gas (10% O₂ + 90% He, vol/vol) is then introduced and oven temperature is increased step-wise to 900 °C (550 °C, 625 °C, 700 °C, 775 °C, 850 °C maintained for 45 s, and 900 °C for 120 s). The EC fractions are detected in the same manner as OC fractions. The second heating cycle produces pyrolyzed organic carbon (POC) and six EC fractions (EC₁, EC₂, EC₃, EC₄, EC₅ and EC₆; Table 2.2). The evolved CO₂ is swept out of the MnO₂ oven in the helium stream, mixed with hydrogen gas and passed through a heated nickel catalyst where it is quantitatively reduced to methane (CH₄) and subsequently measured by a flame ionization detector (FID). At the end of every analysis, a fixed volume of methane (5% methane in Helium as an internal standard) is injected to monitor the efficiency of FID whereas solutions of sucrose and potassium hydrogen phthalate (KHP) are used as external standards to ascertain the conversion efficiency of CO₂ to CH₄ in the thermo-optical method.

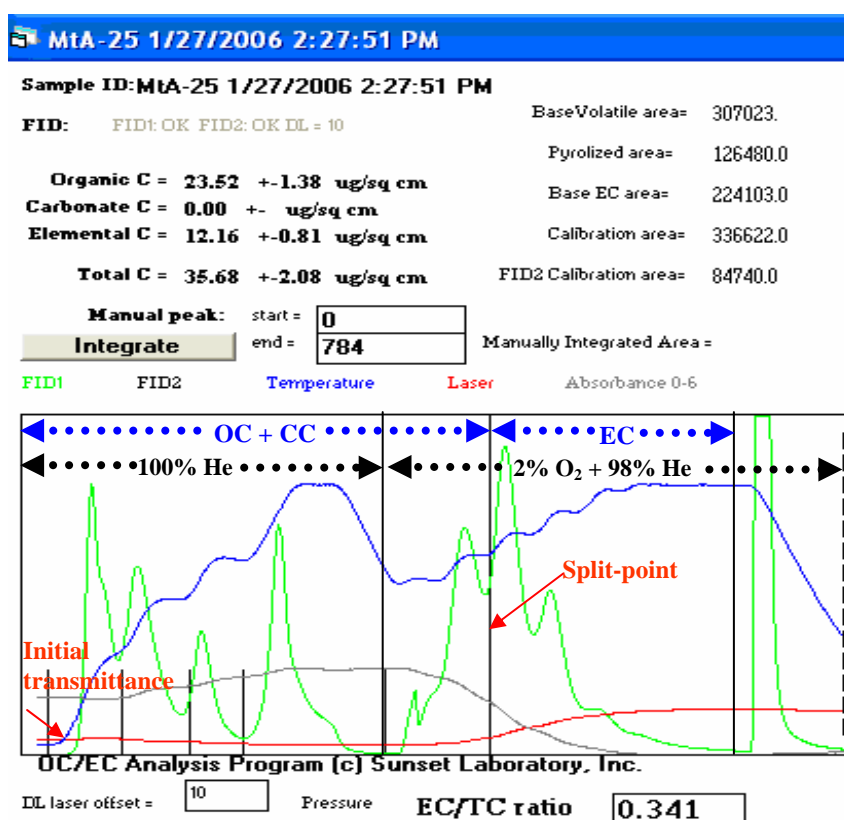


Fig. 2.4: A real-time thermograph of a sample (Mt Abu-25) analyzed on the thermo-optical EC-OC analyzer. The initial transmittance (@678nm) and split-point between OC and EC are also shown.

The thermo-optical method uses the light absorbing characteristics of EC to correct for the pyrolytically formed carbon fraction. The transmittance through the filter samples is continuously monitored with a He-Ne laser of 678 nm wavelength. The initial transmittance of the laser beam is recorded and is attributed to the presence of EC in aerosol samples (Fig 2.4). However, during the heating in inert medium, a part of OC get pyrolyzed (called as pyrolyzed carbon; PC) which can absorb the laser light and reduces the transmittance through the filter and attains the minimum value. When sample is exposed to the oxidizing atmosphere (second thermal heating cycle), PC as well as native EC evolve and the transmittance signal begins to increase during this step. When the transmittance returns to its initial value during heating in an oxidizing medium, it is referred as the split-point between OC and EC. Thus, PC is a part of OC which does not evolve in first heating cycle under inert atmosphere. The carbon fractions that evolve in volatilization step together with PC is defined as OC; and PC subtracted from carbon fraction evolved in oxidizing atmosphere is termed as EC. The OC is operationally defined as $OC = OC_1 + OC_2 + OC_3 + OC_4 + PC$ and EC is defined as $EC = EC_1 + EC_2 + EC_3 - PC$. Thus, OC and EC components are corrected for the charring of hydrocarbons produced in the first step.

Ambient aerosols contain inorganic carbonate carbon (CC) which mainly occurs in the form of calcium carbonate ($CaCO_3$) or other alkali carbonate. Calcium carbonate has a peculiar chemical property and gets oxidized to calcium oxide (CaO) and CO_2 at temperatures greater than 850 °C. Thus, the CO_2 of $CaCO_3$ may interfere with the OC_4 peak in the thermograph. The presence of $CaCO_3$ in the aerosol samples is ascertained by de-carbonizing the sample with 6M HCl fumes (for ~6 hrs) in a desiccator as described by Cachier *et al.* [1989]. The acidified sample is analyzed in the similar fashion as the unacidified sample. If, the OC_4 peak in the thermograph diminishes (completely or partly); it is assumed that carbonate carbon (CC) is present in aerosol samples. The CC and OC_4 peak normally appear at a time interval of 210-220s and 270-285s in the thermograph (at temperature in excess of 850 °C). The concentration of CC is quantitatively estimated by manually integrating the thermogram (signal vs time) by setting Start (~210-220s) and End integration point (~270-285 s). The CC

concentration is automatically subtracted from the OC concentrations. The details of the measurement protocol used such as temperature program, heating cycles are described in our recent publications [*Ram et al.*, 2008; *Rengarajan et al.*, 2007].

The uncertainty in the measurement of OC (OC_{unc}), EC (EC_{unc}) and TC (TC_{unc}) is calculated by summing up the absolute and relative uncertainties. The $0.2 \mu\text{gC cm}^{-2}$ represent the absolute uncertainty in the measurements of OC, EC whereas $0.3 \mu\text{gC cm}^{-2}$ for TC. The relative uncertainty is taken as 5% of the measured concentration (in unit of $\mu\text{gC cm}^{-2}$) of OC, EC and TC. Thus,

$$OC_{unc} = (0.2 + 0.05 * OC) \mu\text{gC cm}^{-2}$$

$$EC_{unc} = (0.2 + 0.05 * EC) \mu\text{gC cm}^{-2}$$

$$TC_{unc} = (0.3 + 0.05 * TC) \mu\text{gC cm}^{-2}$$

Simultaneously, blank filters were run in the same fashion to obtain the blank concentration and detection limit of OC. The average blank concentration was $1.2 \pm 0.4 \mu\text{gC cm}^{-2}$ (Table 2.3) which corresponds to $0.8 \mu\text{gC m}^{-3}$ of OC for an average volume of $\sim 600 \text{ m}^3$ of air filtered. The detection limit for OC was calculated as three times the standard deviation of blank measurements while detection limit for EC was calculated by taking $0.2 \mu\text{gC cm}^{-2}$ as a signal. The corresponding detection limits for OC and EC were calculated to be $0.8 \mu\text{gC m}^{-3}$ and $0.15 \mu\text{gC m}^{-3}$ respectively, for an average volume of $\sim 600 \text{ m}^3$ of air. Scatter plots between the two set of measurements for OC, EC and TC of the same aerosol samples are presented in Fig. 2.5.

It is observed that OC and TC show a very good agreement between the two set of measurements and data points fall very close to 1:1 line. However, significant difference is observed for EC measurements, mainly for concentrations greater than $10.0 \mu\text{gC cm}^{-2}$. This mainly arises due to the problem in the determination of split-point and corrections for pyrolyzed carbon. The replicate analysis of samples provided a good analytical precision; with relative deviation of 3.0, 4.3, and 2.5% for OC, EC and TC respectively (Table 2.3).

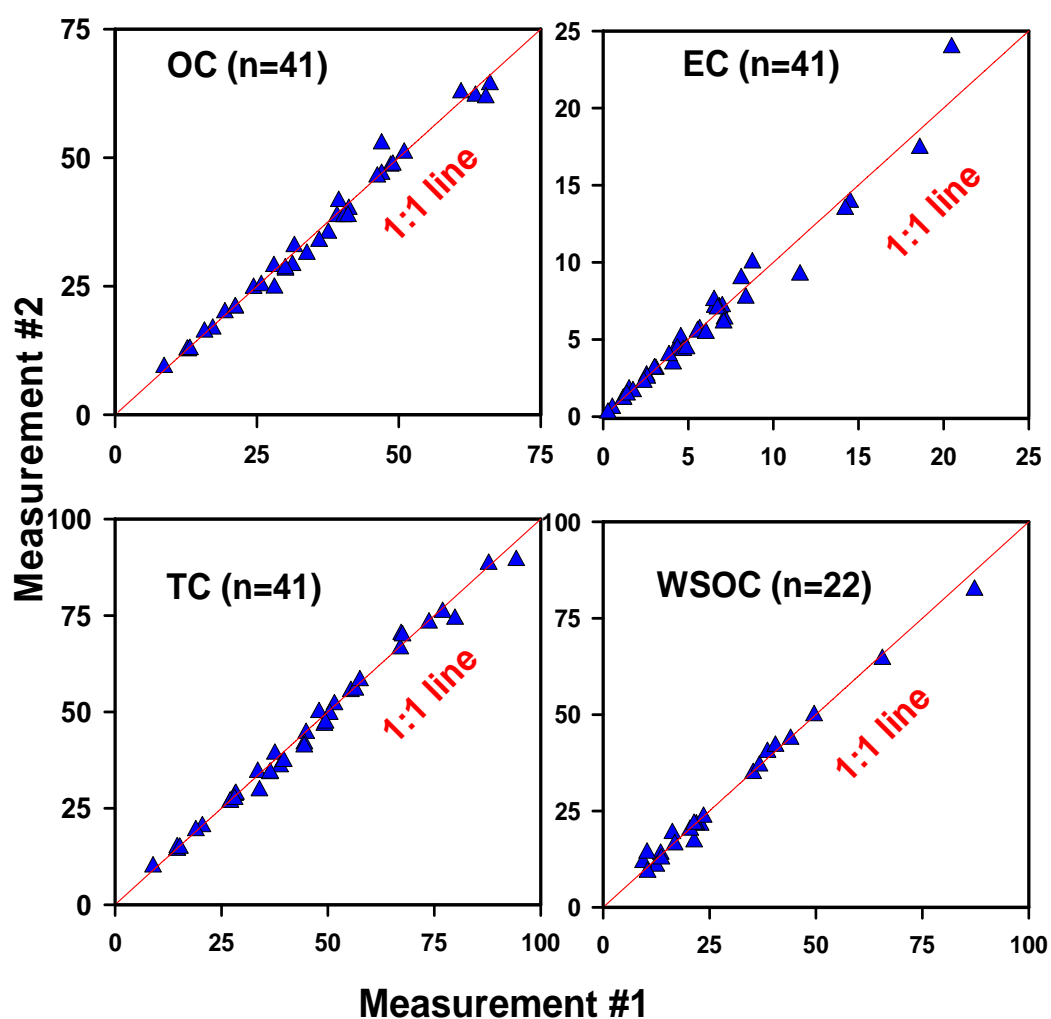


Fig. 2.5. Scatter plots for repeat measurements of OC, EC, TC (concentration unit: $\mu\text{gC cm}^{-2}$) and WSOC (concentration unit: parts per million; ppm) in aerosol samples. The solid line represents the 1:1 line and 'n' represents number of repeat measurements.

Table 2.3: Average blank concentrations, detection limits (DL) and reproducibility of measured chemical species for an effective filter area of $\sim 417 \text{ cm}^2$ and volume of air ($\sim 800 \text{ m}^3$).

Species	n	Blank $\mu\text{gC m}^{-3}$	Detection limit $\mu\text{gC m}^{-3}$	Reproducibility (rpd [#])
OC	41	0.80	0.80	3.0
EC	41	0.00	0.15	4.3
TC	41	0.90	0.80	2.5
WSOC	22	0.10	0.05	3.0

[#]: relative percentage deviation

2.4.3 Analysis of water-soluble organic carbon (WSOC)

For WSOC, one-fourth filter ($\sim 105 \text{ cm}^2$ area) was soaked in 50 ml de-ionized water (resistivity: $18.2 \text{ M}\Omega \text{ cm}$) and ultrasonicated for ~ 8 hrs. The resulting water-extract was filtered through circular PALLFLEXTM membrane filters (size: 47 mm), transferred to pre-cleaned glass vials and analyzed for WSOC on a total organic carbon (TOC) analyzer (Shimadzu, model TOC-5000A). For an optimized analytical procedure, 25 μl of water-extract was injected into the furnace at a temperature of $680 \text{ }^\circ\text{C}$ and oxidized to CO_2 using Platinum catalyst. The evolved CO_2 was measured using a non-dispersive infrared (NDIR) detector to assess total carbon (TC) content. Another aliquot of the solution (100 μl) was acidified with 25% phosphoric acid (25% H_3PO_4 , vol/vol) and evolved CO_2 was measured using a NDIR detector and inferred as inorganic carbon (IC). The difference between the two sets of measurements (i.e. TC and IC) is used as a measure of WSOC in aerosol samples. The NDIR detector response for TC and IC measurements was calibrated using standard solutions of potassium hydrogen phthalate (KHP) and sodium carbonate-bicarbonate mixture ($\text{Na}_2\text{CO}_3 + \text{NaHCO}_3$; 1:1 vol/vol), respectively. Each analysis of TC and IC was performed three times to achieve the coefficient of variation (CV) less than 2%. The replicate analyses of water-extracts provide good reproducibility for TC and IC measurements ($n=22$; average relative standard deviation (r.s.d.) of 3% and 5% for TC and IC respectively). Every batch of water-extraction (total of 10 samples) consists of 9 aerosol samples and one blank filter. The extraction of blank filters was processed simultaneously to obtain the WSOC content in blank filters (WSOC_B). The average blank value obtained by water-extract of blank filters were $1.1 \pm 0.8 \text{ ppm}$ and $350 \pm 40 \text{ ppb}$ ($n=22$; 1σ) for TC and IC, respectively. The average TC and IC blank values correspond to $\sim 3\%$ and 1% of the WSOC concentrations in aerosol samples and all the reported WSOC abundances are corrected for the WSOC_B .

2.4.4 Analysis of water-soluble inorganic species (WSIS)

The analysis of water-soluble cations (Na^+ , K^+ , NH_4^+ , Ca^{2+} and Mg^{2+}) and anions (Cl^- , SO_4^{2-} and NO_3^-) in aerosols were performed on Ion-Chromatograph (Dionex). The clear solution of the water-extracts (the same used for the WSOC analysis) were transferred to pre-cleaned vials and analyzed for their water-soluble inorganic constituents. A mixture of 1.8 mM Na_2CO_3 and 1.7 mM NaHCO_3 was used as an eluent for the analysis of anions and an Anion Self-Regenerating Suppressor (ASRS) was used to suppress the conductivity. For analysis of cations, 20 mM methanesulphonic acid (MSA) was used as an eluent and the conductivity was suppressed by Cation Self-Regenerating Suppressor (CSRS). The anions and cations were separated using analytical columns, Ionpac AS14 column for anion and Ionpac CS12 column for cations respectively, before they were sent to the conductivity detector. Simultaneously processed blank filters were also analyzed to obtain blank concentration of cations and anions. The details of the analytical procedure for water-soluble inorganic constituents are described in our earlier publications [*Rastogi and Sarin, 2006; Rengarajan et al., 2007*]. The replicate analyses for K^+ , Ca^{2+} , Mg^{2+} , Cl^- , SO_4^{2-} and NO_3^- were better than 3% while it was ~6% for NH_4^+ analysis (Table 2.4). Scatter plots for repeat measurements of water-soluble inorganic species in aerosol samples are shown in Fig. 2.6.

2.4.5 Analyses of bicarbonate (HCO_3^-)

An aliquot of the water-extract of aerosol samples was taken and bicarbonate (HCO_3^-) measurement was performed using a fixed end-point acid titration ($\text{pH} = 4.3$) with 0.005 M HCl with the help of an autotitrator (Metrohm, model 702 SM Titrino). The calibration was performed with freshly prepared solutions of sodium carbonate (Na_2CO_3) covering the range of 0 to 1000 μM . Detection limit, based on variability of several blank measurements, was 45 μM . The coefficient of variation (CV) of several repeat measurements ($n=11$) was estimated to be better than 4% (Table 2.4).

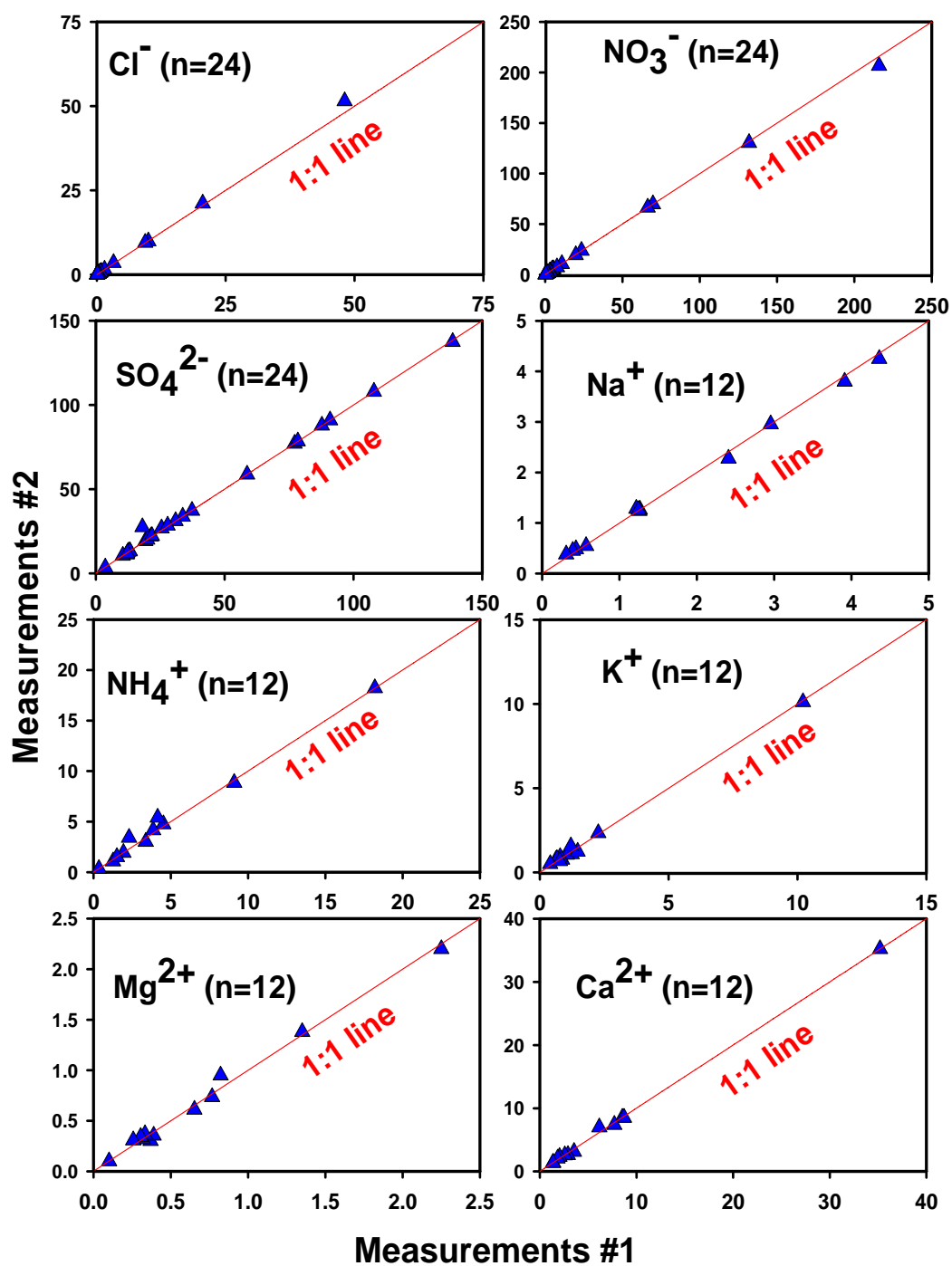


Fig. 2.6. Scatter plots for repeat measurements of water-soluble inorganic species in aerosol samples (concentration unit: parts per million; ppm). The solid line represents the 1:1 line and 'n' represents number of repeat measurements.

Table 2.4: Average blank concentrations, detection limit (DL) and reproducibility of measured chemical species in tissuquartz filters. ‘n’ represents number of repeat measurements for individual species.

Species	n	Blank $\mu\text{g m}^{-3}$	DL $\mu\text{g m}^{-3}$	Reproducibility (rpd [#])
Na⁺	12	0.03	0.02	3.0
NH₄⁺	12	–	0.02	6.0
K⁺	12	0.03	0.02	2.0
Mg⁺²	12	0.01	0.02	2.0
Ca⁺²	12	0.01	0.03	2.0
Cl⁻	24	0.02	0.01	2.1
NO₃⁻	24	0.01	0.3	1.5
SO₄²⁻	24	0.05	0.3	1.1
HCO₃⁻	11	0.03	0.05	4.0

[#]relative percentage deviation

2.4.6 Determination of aerosol absorption coefficient (b_{abs}) and mass absorption efficiency of EC (σ_{abs})

2.4.6 (a) The principle and equations used

The analytical instrument (EC-OC analyzer) provides absorbance (equivalent to initial transmittance) at 678 nm by measuring intensities of incident and transmitted light through the quartz filter loaded with aerosols. The absorption signal is represented by optical-attenuation (ATN, a unit less parameter) and is governed by the Beer-Lambert’s law, according to the following equation:

$$\text{ATN} = -100 \cdot \ln \left(\frac{I}{I_0} \right) \quad (1)$$

where I_0 is the intensity of incident light and I is the transmitted light through the filter substrate and aerosols. The measured ATN signal for blank filters is zero ($n=50$). Thus, the measured ATN through the sample filter is attributed to the presence of light absorbing carbon (LAC) and is equivalent to in-situ EC concentration in aerosols. *Sciare et al.* [2003] had reported that absorption measurements performed on PSAP showed good agreement with those measured from Sunset EC-OC analyser ($R^2=0.93$). Hence, simultaneous measurements of ATN and surface EC loading ($\text{EC}_s, \mu\text{g cm}^{-2}$) can be used to determine the

absorption coefficient (b_{abs}) and mass absorption efficiency of EC (σ_{abs}). The uncertainty in the ATN measurement is no more than 7% (except in few cases where it is as high as 13%) and is expressed as relative percentage deviation from $n=20$ measurements. The relevant parameters used in this study, along with the associated errors, have been summarized in Table 2.5.

The measurement of ATN and methodology used in this study are similar to those employed in filter-based online optical instruments [Weingartner *et al.*, 2003; Yang *et al.*, 2009]. In the latter approach, aerosols are generally collected for a short time on a small filter area at low flow rates and ATN is obtained by measuring the change in transmittance as a function of time. On the contrary, collection of aerosol samples integrated over longer time on a large filter area (as used in this study) minimizes the sample heterogeneity and enhances the ATN signal. The attenuation cross-section (σ_{ATN} , $\text{m}^2 \text{g}^{-1}$) can be directly obtained from above equation (1) by correcting the measured ATN for shadowing effect ($R(\text{ATN})$; as explained in later section) and dividing by EC_s concentration:

$$\sigma_{\text{ATN}} (\text{m}^2 \text{g}^{-1}) = \frac{\text{ATN}}{R(\text{ATN}) \bullet \text{EC}_s} \quad (2)$$

The attenuation coefficient (b_{ATN}) is calculated from the measured ATN with the help of following equation:

$$b_{\text{ATN}} = \frac{\text{ATN} \bullet A (\text{m}^2)}{V (\text{m}^3)} \quad (3)$$

whereas absorption coefficient (b_{abs}) is related to b_{ATN} according to equation (4) as described in literature [Schmid *et al.*, 2006; Weingartner *et al.*, 2003; Yan *et al.*, 2008; Yang *et al.*, 2009]

$$b_{\text{abs}} = \frac{\text{ATN}}{C \bullet R(\text{ATN})} \bullet \frac{A}{V} = \frac{b_{\text{ATN}}}{C \bullet R(\text{ATN})} \quad (4)$$

where, A is the effective filter area ($417 \times 10^{-4} \text{m}^2$ for tissuquartz filter used in this study), V is the volume of air filtered (m^3). C and $R(\text{ATN})$ are the two empirical factors used for correcting the measured absorption due to the multiple scattering and shadowing effects, respectively.

2.4.6 (b) Choices of the empirical parameters: C and f

The value of C depends on the type of absorbing material, the filter substrate and mixing state of BC in aerosols [Bond and Bergstrom, 2006; Weingartner *et al.*, 2003]. A value of 2.14 ± 0.21 has been suggested for correction due to the multiple scattering effect for uncoated and externally mixed soot particles collected on tisuquartz filters (same as used in present study) [Bond and Bergstrom, 2006; Weingartner *et al.*, 2003]. However, much higher values have been reported for internally mixed aerosol particles (e.g. 3.6 ± 0.6 for soot particles coated with organics) [Weingartner *et al.*, 2003]. This introduces large uncertainty in b_{abs} values when filter-based measurements are performed. A value of 2.14 ± 0.21 for C has been used while R(ATN) is calculated using equation (5).

The multiple scattering effect is due to accumulation of particles and leads to an enhancement in absorption while the shadowing effect decreases absorption by reducing the optical path length. Weingartner *et al.* [2003] have provided a wavelength dependent parameter f to estimate R(ATN) by fitting linear empirical curve to the observed data set obtained by Aethalometer:

$$R(ATN) = \left(\frac{1}{f} - 1\right) \left(\frac{\ln ATN - \ln 10}{\ln 50 - \ln 10}\right) + 1 \quad (5)$$

where R(ATN) depends on parameter f and decreases with increasing value of f. It is evident from above equation that for lower values of optical-attenuation (ATN $\leq 10\%$), R(ATN) can be taken as unity. However, for ATN $> 10\%$, R(ATN) values are always less than unity and decreases with increasing ATN. For ATN $> 10\%$, we have used $f=1.103$ during wintertime (Dec-Mar) and $f=1.114$ for rest of the seasons to calculate R(ATN) from equation (5) as per values reported at 660 nm [Sandradewi *et al.*, 2008a]. It is noteworthy that use of f value equal to 1.103 or 1.114 leads to maximum change of 2% in R(ATN). The calculated values of 0.85 ± 0.03 for R(ATN) at the sampling sites (Hisar, Allahabad and Jaduguda) are similar (within errors) to that used by Chou *et al.* [2005] for an urban site in Taipei (0.80) whereas R(ATN) is relatively high (0.92 ± 0.04) for the high-altitude sites. The propagated root-sum-square error (RSSE) for the determination of aerosol absorption coefficient (b_{abs}) is $\sim 23\%$, arising from measurements of ATN, A, V and corrections due to the multiple scattering and shadowing effects.

The attenuation cross-section (σ_{ATN}) and mass absorption efficiency (σ_{abs}) are the two frequently used terms for determination of BC mass concentration via optical methods. Although, both parameters are expressed in same units (m^2g^{-1}); σ_{ATN} accounts for the intrinsic absorption due to BC particles and an additional increase in light absorption due to the multiple scattering effect (C) and is related with σ_{abs} by the following equation:

$$\sigma_{abs} = \frac{\sigma_{ATN} (m^2 g^{-1})}{C} = \frac{b_{abs} (Mm^{-1})}{EC (\mu g m^{-3})} \quad (6)$$

Assuming an uncertainty of ~23% in b_{abs} and 22% in EC measurements [Miyazaki *et al.*, 2008], the propagated RSSE in determination of σ_{abs} is estimated to be of the order of ~32% using our approach.

2.4.6 (c) Assessment of errors in the measured parameters on thermo-optical EC-OC analyzer

The major uncertainties in the estimation of absorption coefficient (b_{abs}) using filter based instrumental techniques mainly results from errors in the measurements of ATN, corrections due to the multiple scattering effect (C) and shadowing effect (R(ATN)) [Weingartner *et al.*, 2003]. The uncertainty in the determination of attenuation coefficient (b_{ATN}) arises from uncertainty in the measurement of ATN (Equation 1); whereas uncertainty in measurements of both A and V are relatively insignificant (better than 1 and 2% respectively, Table 2.5). The overall uncertainty in ATN measurements, arising due to aerosol collection, sample heterogeneity, temperature program and horizontal configuration of sample, is no more than 7% for most of the cases (except in few cases where it can be as high as 13%).

Likewise, uncertainty in the estimation of absorption coefficient (b_{abs} , Equation 4) is relatively high and mainly arises due to uncertainties associated with the corrections applied for the multiple scattering effect (C) and shadowing effect (R(ATN)). The multiple scattering effect (C) is caused due to scattering of same photon more than once within the filter matrix and value of C depends on type of absorbing material (i.e. source of BC) and the filter substrate used for aerosol collection. A value of 2.14 ± 0.21 has been suggested for correction due to

the multiple scattering effect for the uncoated soot particles (externally mixed) collected on tissuquartz filters [Weingartner *et al.*, 2003]. On the contrary, relatively high values have been suggested for internally mixed aerosol particles (e.g. 3.6 ± 0.6 for soot particles coated with organics) [Weingartner *et al.*, 2003]. We have taken 10% uncertainty (relative percentage standard deviation of 2.14 ± 0.21) for the multiple scattering effect in the propagation of the error.

The shadowing effect, $R(ATN)$, is also a major source of uncertainty in the determination of b_{abs} and it is somewhat more complicated to estimate because it not only depends on optical properties of filter substrate and collected material but also depends on the amount of material deposited on to filter substrate. The error in estimation of $R(ATN)$ from equation (5) can arise from the two independent variables, namely f and ATN . The error in estimation of $R(ATN)$ can also arise from the use of the reference ATN value of 50 in equation (5). A value of 50 for reference ATN has been used in most of the optical methods for correction due to the shadowing effect where ATN does not exceed 75. The sensitivity analyses by changing the reference ATN from 50 to 100 (for four different ATN values; 50, 75, 90 and 100) reveals a maximum change of 8-10% in $R(ATN)$ values.

For aged aerosols, the value of $R(ATN)$ is unity [Weingartner *et al.*, 2003]. However, it decreases with increasing f values and keeping ATN constant. There are two values of f ($f=1.013$ in winter and $f=1.114$ in summer) reported in the literature at 660 nm (close to wavelength used by us i.e. 678 nm) [Sandradewi *et al.*, 2008a]. We have made sensitivity analyses by interchanging f values in (Equation 5) and observed that this can result in a maximum error of 2% in the estimation of $R(ATN)$. However, determination of $R(ATN)$ using equation (5) critically depends on the choice of the parameter ' f ' and hence, the use of ' f ' needs to be examined in details otherwise this can lead to large errors (>2%). Using a maximum value of 1.2 for f and varying ATN values from a minimum of 11 to 180% (the maximum ATN value used in present study for which Beer-Lambert's law is valid); $R(ATN)$ values can vary from 0.99 to 0.701, respectively. This indicates that b_{abs} values would be underestimated by $\sim 30\%$ at maximum ATN value (i.e. 180), if not corrected for the shadowing effect. Furthermore,

R(ATN) values are 0.808 and 0.895 respectively, for the average ATN value (i.e. ~64) obtained in this study and for f values of 1.2. and 1.1 (an average of 1.0 and 1.2), respectively. As stated earlier, the estimation of R(ATN) using equation (5) depends on value of f used and measured ATN, which can vary sample to sample and sampling locations. Taking an average ATN value of 64 and an average value of 1.1 for f , R(ATN) is 0.895 while it is 0.837 for the maximum ATN value of 180. This indicates an underestimation of ~16% for b_{abs} measurements for an average value of 1.1 for ' f ' and maximum ATN (i.e. 180) used in this study. Hence, we have assigned an uncertainty of 19% (root-sum-square error; RSSE) for the shadowing effect correction (after adding the error for the use of reference ATN value of 50) in the error propagation of absorption coefficient (b_{abs}) measurements. The maximum propagated error in b_{abs} measurements, arising from corrections due to the multiple scattering (10%) and shadowing effects (19%), is estimated to be of the order of 23% in present study.

Finally, errors in the estimation of mass absorption efficiency (σ_{abs}) are due to errors in b_{abs} (23%) and EC concentration measurements (22%) [Miyazaki *et al.*, 2008]. Assuming above mentioned errors in b_{abs} and EC measurements, σ_{abs} values can have an RSSE of 32% in present study. The nomenclature of various parameters using thermo-optical EC-OC analyzer and associated uncertainties are given below in Table 2.5.

Table 2.5: Measured optical parameters and related uncertainties.

Parameter	Symbol	Unit	Error (RSSE)*
Area	A	m ²	1%
Volume of air sampled	V	m ³	2%
Optical-attenuation	ATN	unit less	7%
Surface EC concentration	EC _s	µgC cm ⁻²	7%
EC mass concentration	EC	µgC m ⁻³	22% [Miyazaki <i>et al.</i> , 2008]
Attenuation coefficient	b _{ATN}	Mm ⁻¹	8%
Multiple scattering effect	C	unit less	10%
Shadowing effect	R(ATN)	unit less	19%
Absorption coefficient	b _{abs}	Mm ⁻¹	23%
Mass absorption efficiency	σ _{abs}	m ² g ⁻¹	32%

* Root-sum-square error

AEROSOL CHARACTERISTICS OVER URBAN AND HIGH-ALTITUDE SITES

3.1 Introduction

The rapid urbanization, growth of industries and emissions from biomass burning (wood-fuel and agricultural waste) and vehicular exhaust have led to a substantial increase in the atmospheric aerosol loading in south and south-east Asia [Adhikary *et al.*, 2007; Jethva *et al.*, 2005; Rengarajan *et al.*, 2007]. The high aerosol loading, persistent throughout the year, can induce significant dimming of the solar radiation at the surface and can counter the influence of warming caused by greenhouse gases [Carmichael *et al.*, 2009]. A few studies conducted over Indian regions suggest that fine-mode ($<1 \mu\text{m}$) aerosols contribute as much as 83% of the total aerosol mass at Kanpur during wintertime (Dec 2004) [Tare *et al.*, 2006] whereas naturally derived aerosols (mainly mineral dust) contribute significantly to the aerosol loading and aerosol optical depth (AOD) during summer months (April-June) [Chinnam *et al.*, 2006; Hegde *et al.*, 2007; Jethva *et al.*, 2005].

The formation of secondary aerosols, in conjunction with the airborne particles of primary origin, has been recently recognized as a dominant process contributing to air pollution over urban areas and mega-cities [Dall'Osto *et al.*, 2009; Guo *et al.*, 2010; Lee and Sequeira, 2002; Zhang *et al.*, 2010]. Secondary inorganic aerosols (SO_4^{2-} , NO_3^- and NH_4^+), along with organic carbon (OC), scatter the solar radiation and their hygroscopic growth enhances the scattering property of aerosols [Malm *et al.*, 1996]. For example, Lee and Sequeira [2002] have suggested that SO_4^{2-} aerosols are the prominent species in reducing the visibility over Hong Kong. On the

contrary, black carbon (BC) is a major absorbing particulate species in the atmosphere with a warming potential of ~55% in comparison to that of CO₂ [Carmichael *et al.*, 2009]. Although, BC is a minor component of atmospheric aerosols and contributes only 5-10% of the total aerosol optical depth (AOD) [Pant *et al.*, 2006; Ramana *et al.*, 2004]; it plays an important role in modulating Earth's radiation budget, regional climate and hydrological cycle [Jacobson, 2001; Lelieveld *et al.*, 2001; Menon *et al.*, 2002; Ramanathan and Carmichael, 2008]. Thus, the knowledge of chemical composition, size-distribution and optical properties of aerosols (absorption and scattering coefficients, single scattering albedo and aerosol optical depth) is crucial for the estimation of aerosol radiative forcing on a regional scale.

In this chapter, temporal and spatial variability in the total aerosol mass and AOD values, acquired through a long-term monitoring of ambient aerosols collected from different environmental conditions representing urban (Kanpur: Jan 2007-March 2008) and high-altitude sites (Mt Abu: May 2005-Feb 2006 and Manora Peak: Feb 2005-July 2008) in India, are presented. The mass concentrations and ratios of selected chemical tracers (K⁺, K⁺/OC and OC/EC ratios) has been used for the characterization of carbonaceous aerosols. On the other hand, concentrations of water-soluble Ca (Ca²⁺; a tracer of mineral aerosols) and back trajectory analyses has been made to understand the long-range atmospheric transport of mineral aerosols.

3.2 Results and Discussion

3.2.1 Characterization of sources of aerosols using the tracer approach

It is well recognized that K⁺ is an ideal tracer for the source characterization of carbonaceous aerosols from biomass burning emissions [Andreae, 1983; Andreae and Merlet, 2001]. However, appropriate corrections for aerosol K⁺ derived from sea-salt and mineral dust are rather essential [Chester, 1990]. In the absence of biomass burning source, one would expect the contribution from mineral dust to be more in the summer (April-June) due to the long-range transport from arid regions. During summer months, K⁺ content in the majority of the samples is relatively low (0.33 to

$0.93 \mu\text{g m}^{-3}$) compared to that during the winter and post-monsoon ($\sim 2.0 \mu\text{g m}^{-3}$). The mineral dust content in the aerosols (inferred based on the measured concentration of Ca^{2+}) during summer and winter seasons is significantly different; the relatively low dust content during post-monsoon and winter would result in lower contribution to aerosol K^+ . Based on the average Na^+ concentration of $0.42 \pm 0.32 \mu\text{g m}^{-3}$ and assuming K^+/Na^+ molar ratio of 0.037 in sea-water [Chester, 1990], the contribution of K^+ derived from sea-salt is insignificant ($\sim 0.01 \mu\text{g m}^{-3}$). Thus, K^+ from sea-salt contributes no more than 3% and 1% of the total K^+ during summer and winter seasons, respectively. Furthermore, the mass concentration of OC exhibits a linear correlation with K^+ for the samples collected during winter and post-monsoon ($R^2=0.79$ and 0.50 , respectively; Fig. 3.1a); suggesting that K^+ and OC have been derived from the same emission source (biomass burning). Furthermore, correlation between K^+ and OC is poor for the samples collected during March and summer months (Fig. 3.1b).

Dust storms are very common over the IGP during summer months (April-June). The PM_{10} mass concentration can increase to as high as $1000 \mu\text{g m}^{-3}$ during dust storm events at Kanpur [Chinnam *et al.*, 2006]. For a semi-arid urban location in western India, Rastogi and Sarin [2006] have reported that mineral dust contributes ~ 70 - 80% of the total suspended particulate matter throughout the year. A significant fraction of calcium (Ca) is soluble in water and measured Ca^{2+} is generally used as an indicator of mineral aerosol [Lin *et al.*, 2007; Rastogi and Sarin, 2006]. The measured Ca^{2+} concentration shows a significant linear trend with PM_{10} mass for the samples collected during spring and summer seasons ($R^2=0.67$; Fig. 3.1c). However, a large scatter is observed for the samples collected during winter and post-monsoon months (Fig. 3.1d). The dominance of mineral aerosol is further affirmed by low total carbonaceous aerosol (TCA)-to- Ca^{2+} mass ratio in summer months ($\text{TCA}/\text{Ca}^{2+} = 15 \pm 8$) while ratios are much higher during winter season (62 ± 37).

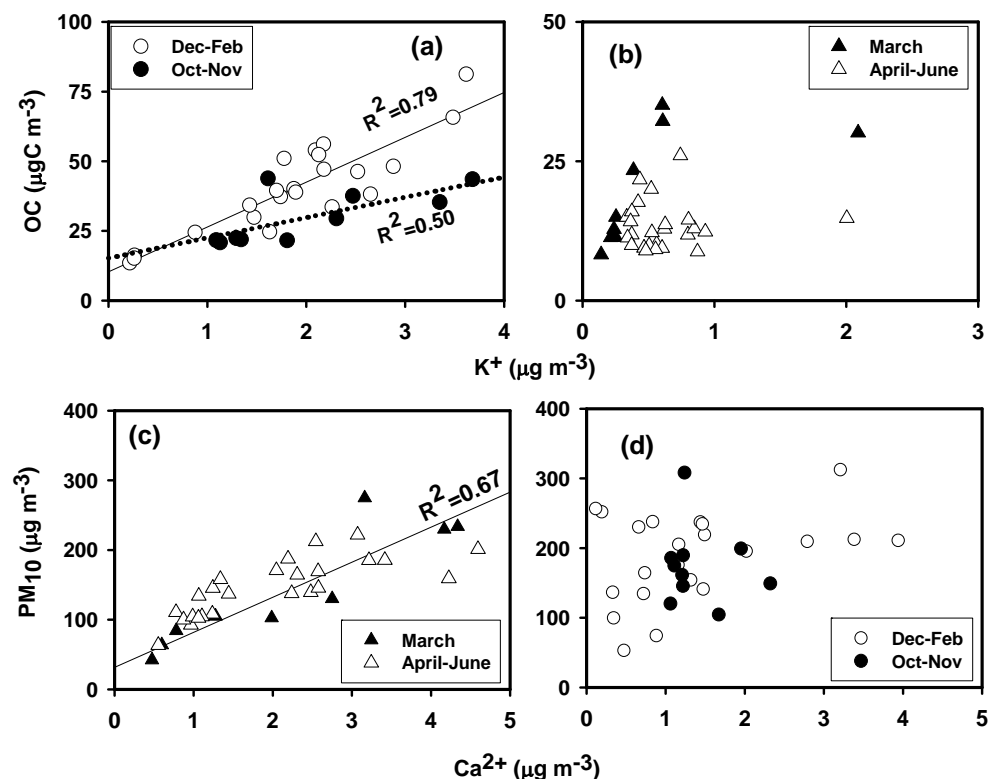


Fig. 3.1: Scatter plots between (a) OC and K^+ for Oct-Nov and Dec-Feb and (b) OC and K^+ for March and April – June; (c) PM_{10} and Ca^{2+} for March and April – June and (d) PM_{10} and Ca^{2+} for Dec-Feb and Oct-Nov at Kanpur.

3.2.2 Seasonal variability in PM_{10} mass at Kanpur

Based on satellite retrievals and ground-based measurements of optical properties, earlier studies have documented relatively high aerosol optical depth (AOD) values over the IGP throughout the year [Chinnam *et al.*, 2006; Dey and Tripathi, 2008; Jethva *et al.*, 2005]. For example, Jethva *et al.* [2005] reported that AOD values over the IGP ranged from 0.6-1.2 (at 550 nm) during summer with relatively low fine-mode aerosol fraction (FMAF) values (<0.4) suggesting the dominance of coarse-mode particles. However, fine-mode aerosols (derived from anthropogenic emissions) dominate PM_{10} mass and AOD values during wintertime at Kanpur [Jethva *et al.*, 2005].

The monthly average PM_{10} concentration at Kanpur is presented in Fig. 3.2a and the fractional contribution of total carbonaceous aerosols ($\text{TCA} = 1.6 \times \text{OC} +$

EC) and water-soluble ionic species (WSIS: sum of the mass concentrations of ionic species) to PM_{10} mass are shown in Fig. 3.2b. In general, higher PM_{10} mass is associated with the samples collected during the post-monsoon (Oct-Nov) and wintertime (Dec-Feb); whereas relatively low concentrations are characteristic of the samples collected during March and summer months (April-June) (Fig. 3.2a). Carbonaceous and water-soluble inorganic species (WSIS) contribute significantly to the PM_{10} mass concentration during winter and post-monsoon seasons (Fig. 3.2b).

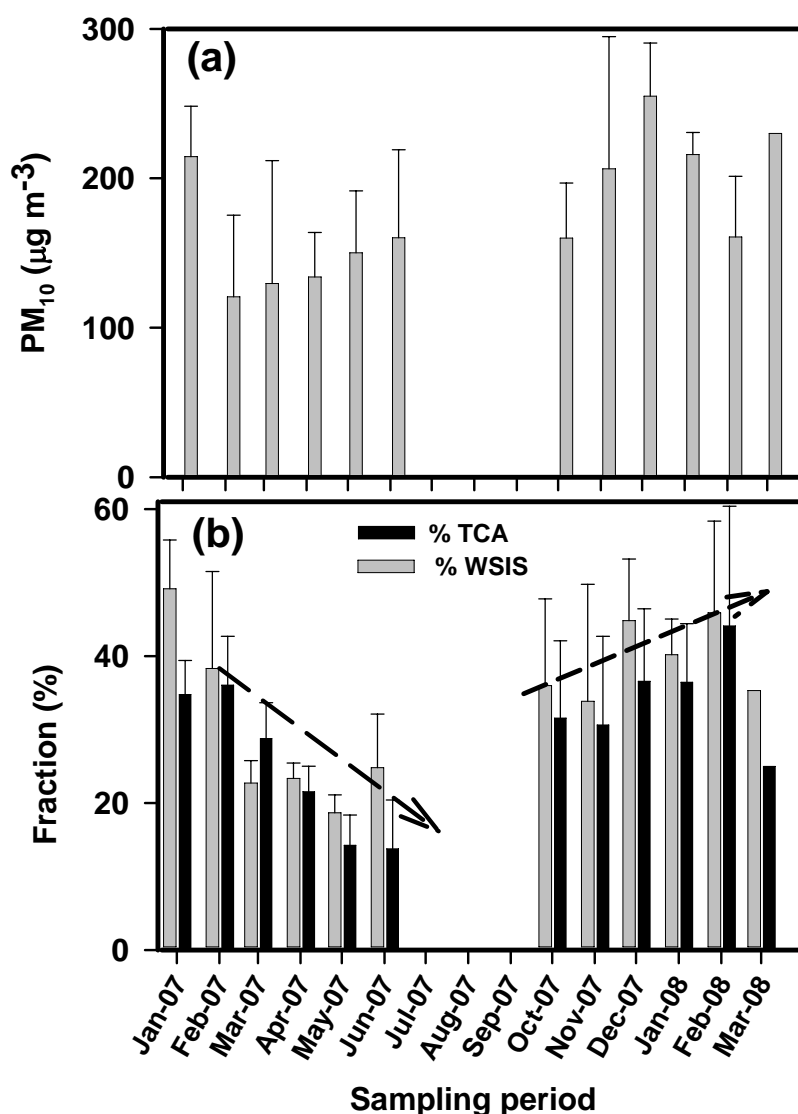


Fig. 3.2: Monthly-average concentrations of (a) PM_{10} and (b) mass fractions of TCA and WSIS at Kanpur. No samples were collected during the period of south-west monsoon (July – Sep).

The seasonal variability in PM_{10} mass can be explained as a combined effect of local emission sources and the prevailing meteorological conditions (wind regimes and boundary layer dynamics). Although, PM_{10} mass concentration is relatively low during summer compared to that in winter, it shows an increasing trend from Feb to June (Fig. 3.2a). The increasing trend in the PM_{10} mass is attributed to the dominant contribution from mineral aerosols during summer months. As evident from Fig. 3.2b, the contribution of TCA and WSIS decreased by a factor of two during summer months compared to that in winter months. Thus, the decrease in contribution of TCA and WSIS during summer months is compensated by the increased contribution from mineral aerosols.

3.2.3 Total suspended particulate (TSP) mass and long-range transport of aerosols at high-altitude sites

The total suspended particulate (TSP) mass, at Manora Peak, exhibit a large temporal variability during the sampling period (Feb 2005-July 2008) and ranges from 13 to 272 $\mu\text{g m}^{-3}$ (Fig. 3.3a). A characteristic feature of the TSP mass relates to the dominance of carbonaceous aerosols during wintertime resulting from local biomass burning (used for cooking and heating purposes) and vehicular emissions whereas long-range atmospheric transport of mineral dust, originating from the Thar Desert (in western India) and middle-East, dominate aerosol chemical composition during summer months. Mineral dust is primarily composed of calcite (CaCO_3), magnesite (MgCO_3), dolomite [$\text{CaMg}(\text{CO}_3)_2$], calcium sulphate (or Gypsum) and alumino-silicates [Cong *et al.*, 2008]. Although, carbonate carbon (CC) is only a minor component of TSP, it co-varies with TSP mass throughout the sampling period at Manora Peak (Figs. 3.3a and c) and serves as an useful index for documenting high dust events. Carbonate carbon (CC) mass concentrations show an order of magnitude increase (compared to the average CC concentration) during dust events (Fig. 3.3c).

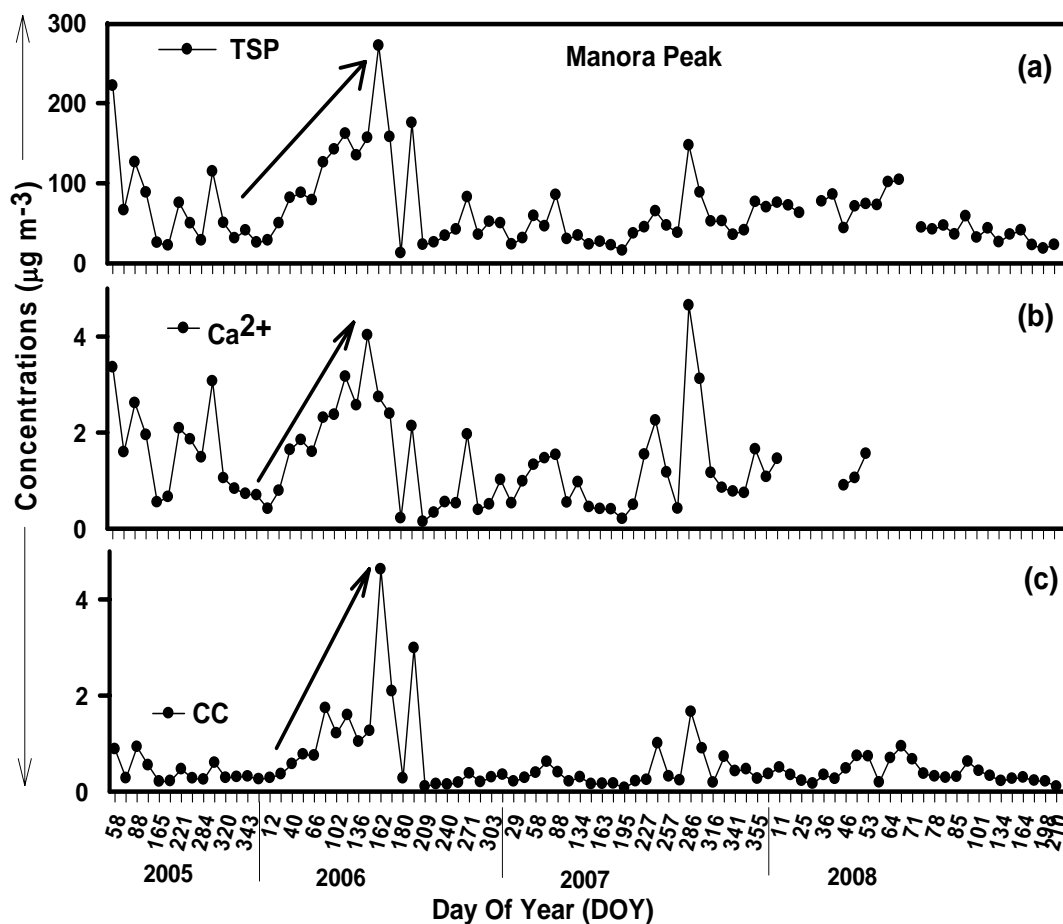


Fig. 3.3: Temporal variability in the mass concentrations of (a) TSP, (b) water-soluble Ca (Ca^{2+}) and (c) carbonate carbon (CC) at Manora Peak during the sampling period (Feb 2005-July 2008).

The carbonate carbon (CC) and TSP linear regression analysis yield a significant correlation coefficient ($R^2=0.95$, $n = 15$, $p < 0.05$; Fig. 3.4a) at Mt Abu and ($R^2=0.87$, $n = 20$, $p < 0.05$; Fig. 3.4b) at Manora Peak for the samples collected during summer months. Thus, a relative increase in the mass concentration of Ca^{2+} and carbonate carbon (CC) concentrations in aerosols can be used as an indicator of high dust events (Figs. 3.3 b & c).

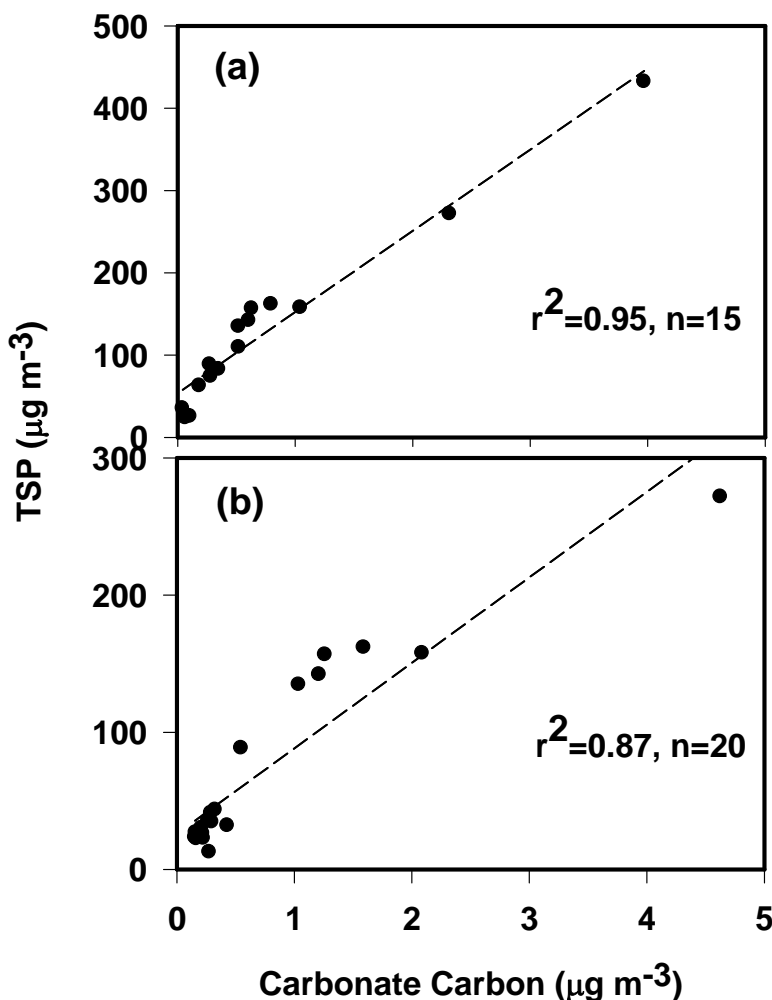


Fig. 3.4: Scatter plots between TSP and carbonate carbon at (a) Mt Abu and (b) Manora Peak, the two high-altitude sites in India.

The total suspended particulate (TSP) mass varies from 13.4 to 432.3 $\mu\text{g m}^{-3}$ at Mt Abu (Av: $47.2 \pm 22.3 \mu\text{g m}^{-3}$, $n=40$, excluding one data point with TSP value of 432.3 $\mu\text{g m}^{-3}$; Fig. 3.5). The higher TSP mass concentrations at Mt Abu, during summer, are dominated by mineral dust due to its location in a semi-arid region of western India and proximity to the Thar Desert. Dust storms are a common phenomenon in the western as well as northern parts of India during summer [Chinnam *et al.*, 2006; Hegde *et al.*, 2007; Rastogi and Sarin, 2006]. The highest TSP (432.3 $\mu\text{g m}^{-3}$) at Mt Abu, along with the highest carbonate carbon (7.95 $\mu\text{g m}^{-3}$),

recorded on 11th June 2005 is attributed to the dust storm event (Fig. 3.5). The back trajectory analysis based on NOAA Hysplit Model (<http://www.arl.noaa.gov/ready>) also indicates the transport of mineral dust from Pakistan and Afghanistan through the Thar Desert in western India (Fig. 3.6a). During wintertime, TSP mass concentrations at Mt Abu are predominantly governed by the transport of air-masses from northern India under favorable meteorological conditions. This is further supported by the air-mass back trajectory analysis (Fig. 3.6b) indicating localized air-mass and the highest OC and EC concentrations observed on 21st Dec, 2005 (12.3 and 2.3 $\mu\text{gC m}^{-3}$, respectively; Fig. 3.5).

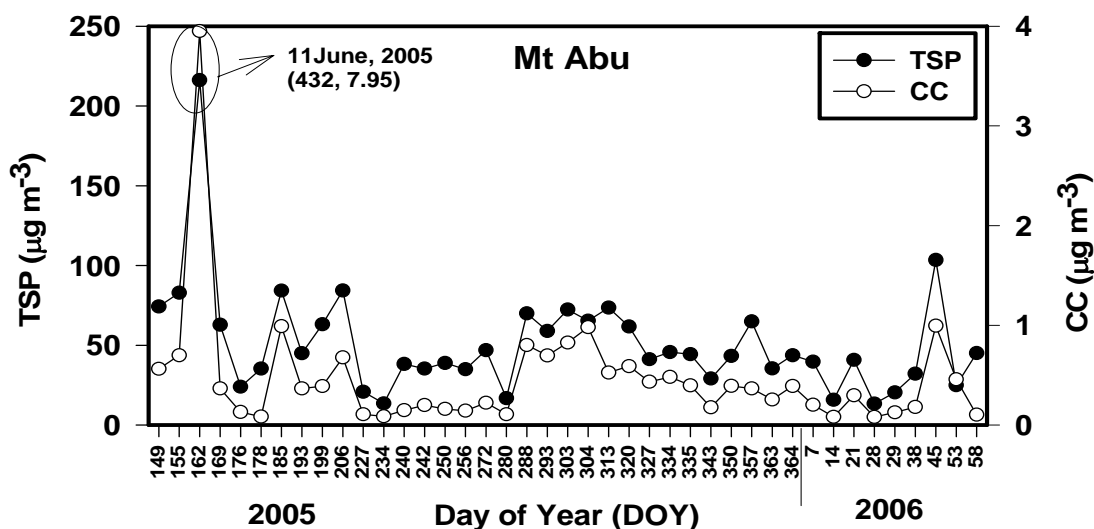


Fig. 3.5: Temporal variability in the mass concentrations of TSP and carbonate carbon (CC) at Mt Abu during the sampling period (May 2005-Feb 2006).

The relatively high TSP mass at Manora Peak, during summer, are also supported by back trajectories (NOAA Hysplit model, <http://www.arl.noaa.gov/ready>) indicating the long-range transport of mineral dust from Pakistan and as far as from Saharan Desert (Fig. 3.6c). Carrico *et al.* [2003a] have also reported the impact of long-range transport of desert dust in the aerosol

chemical composition at Kathmandu Valley and Langtong sites, located in the Himalayan regions.

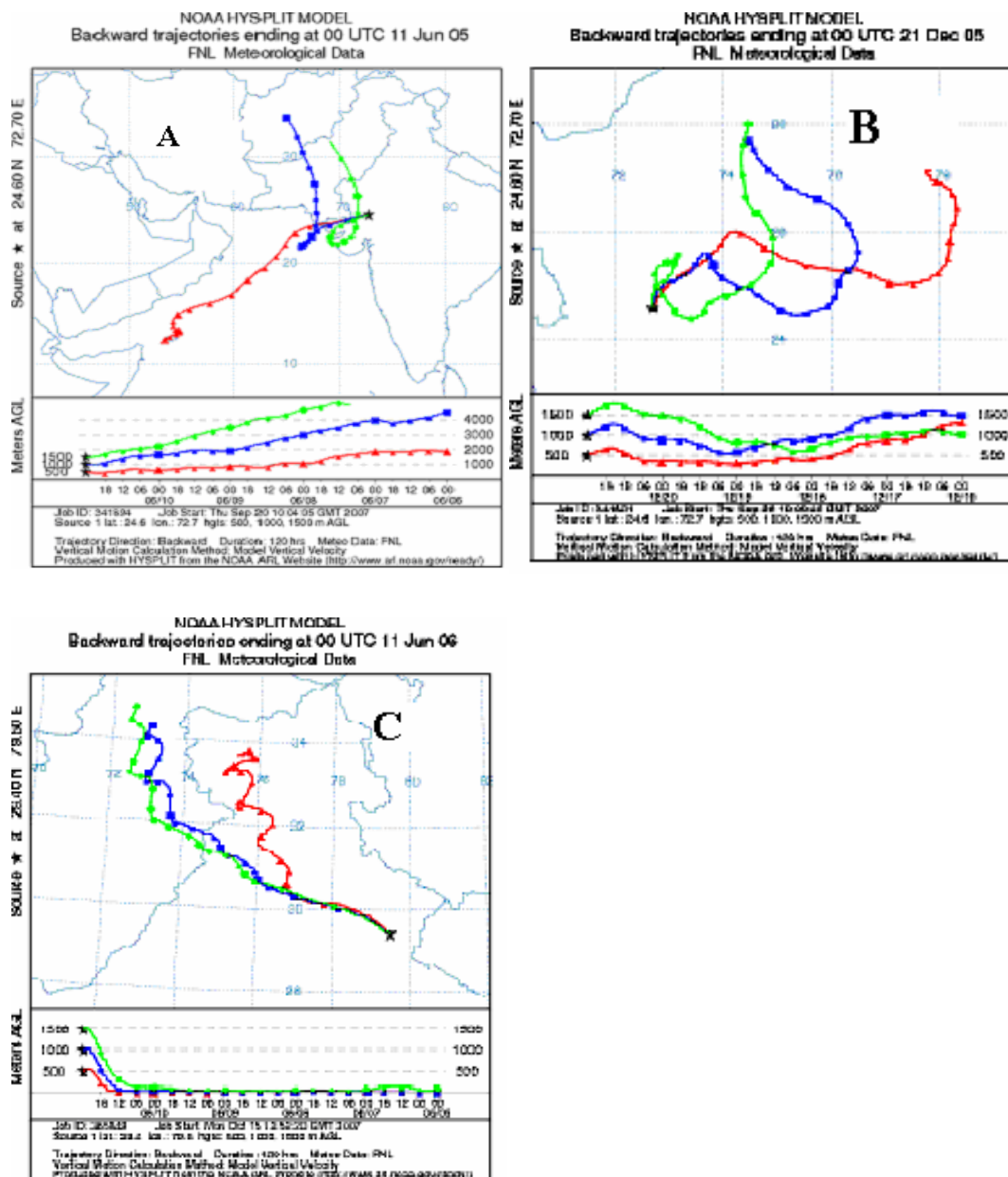


Fig. 3.6: Five-day back trajectory analyses of air masses reaching at Mt Abu and Manora Peak, the two high-altitude sites in India.

The highest TSP value of $272 \mu\text{g m}^{-3}$ at Manora Peak, that occurred on 11th June 2006 (DOY: 162; Fig. 3.4a), was associated with a dust storm event [Hegde *et al.*, 2007]. The fractional contribution of water-soluble ionic species (WSIS; sum of the mass concentrations of cations and anions) decreased to 7% on 11th June 2006. It is noteworthy that not only the contribution of WSIS decreased during dust events; the contribution of TCA was reduced to 6.6% on 11th June 2006. These results suggest that the contribution from mineral aerosols can be as high as ~85% during some dust storm events (as observed on 11th June 2006). On the contrary, aerosol chemical composition shows relatively higher mass concentrations of carbonaceous species during normal days. On average, TCA contributes ~25% of the TSP during normal days. However, the fractional contribution of TCA increases to as high as 65% during winter and post-monsoon seasons at Manora Peak.

3.2.4 Aerosol optical depth at Manora Peak

The long-term data (~42 months) of TSP and aerosol optical depth (AOD) at Manora Peak has been compared in order to understand the impact of long-rang transport of mineral aerosols. A compilation of AOD values, reported in the literature (2002 onward) and those measured during 2006-2008 at Manora Peak, are presented in Fig. 3.7. It is noticeable that AOD values at Manora Peak show a significant increase (factor of two to six) during summer months (April-June) compared to those during winter months (Fig. 3.7). The dust storm does not only affect the aerosol chemical composition, they also change physical and optical properties (e.g. AOD and fine-mode aerosol fraction, FMAF) of aerosols [Jethva *et al.*, 2005]. The aerosol size-distribution during storm days shows an increase in the coarse-mode particles [Hegde *et al.*, 2007] and a decrease in the FMAF values [Jethva *et al.*, 2005]. During the dust-storm event in the year of 2006 at Manora Peak, Hegde *et al.* [2007] have reported that the number concentration of coarse-mode particles and AOD values increased by a factor of five as compared to the respective monthly mean values. Furthermore, Hegde *et al.* [2007] have reported a relative increase in the Angstrom turbidity coefficients (β) and a significant reduction in wavelength exponent (α).

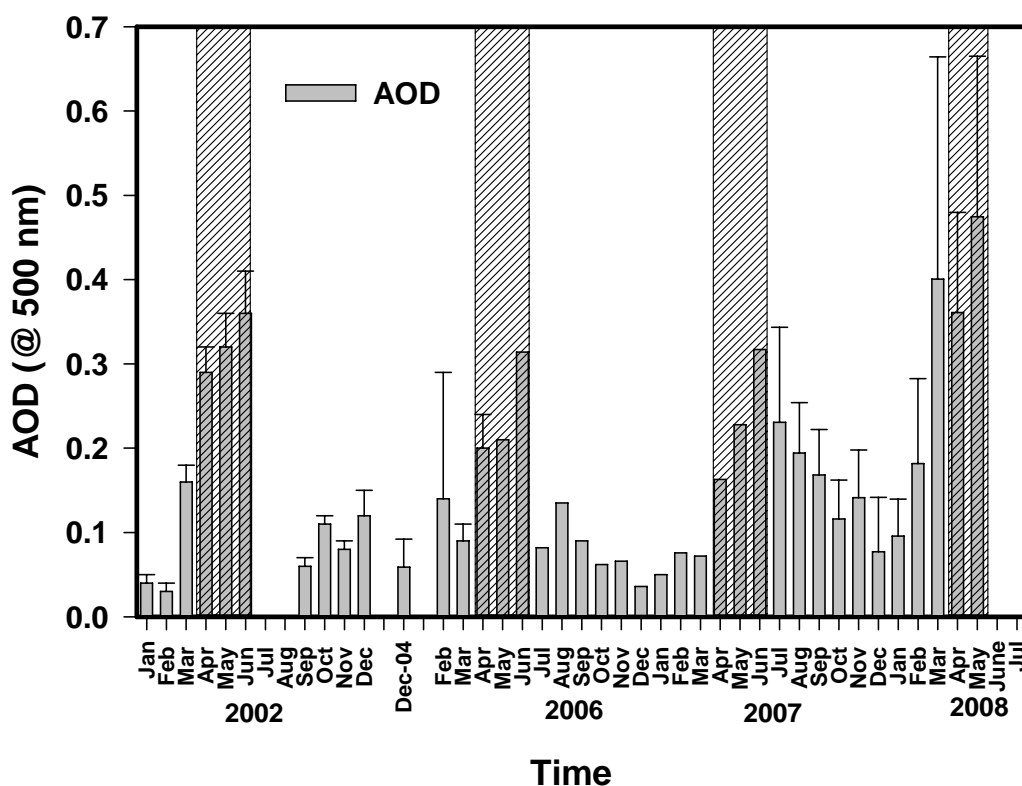


Fig. 3.7: The monthly mean aerosol optical depth (AOD @ 500 nm) at Manora Peak. The AOD data for the years 2002 and Dec 2004 are taken from Sagar *et al.* [2004] and Pant *et al.* [2006] respectively. The vertical strips indicate the high AOD values during pre-monsoon season of the respective years.

Based on a one-year measurement of aerosol optical depth with a Sunphotometer at the Nepal Climate Observatory-Pyramid (NCO-P) in the Himalaya, Gobbi *et al.* [2010] have also found higher AOD values during summer and lower during winter. The monthly averaged AOD values and TSP mass concentrations at Manora Peak for the sampling period are presented in Fig. 3.8. The TSP mass and AOD show a similar pattern and the higher AOD during summer are attributed to the increase in the concentration of mineral aerosols. In contrast, the lower AOD values during monsoon months (July-Sep) are attributed to an efficient wash-out of atmospheric aerosols by rain.

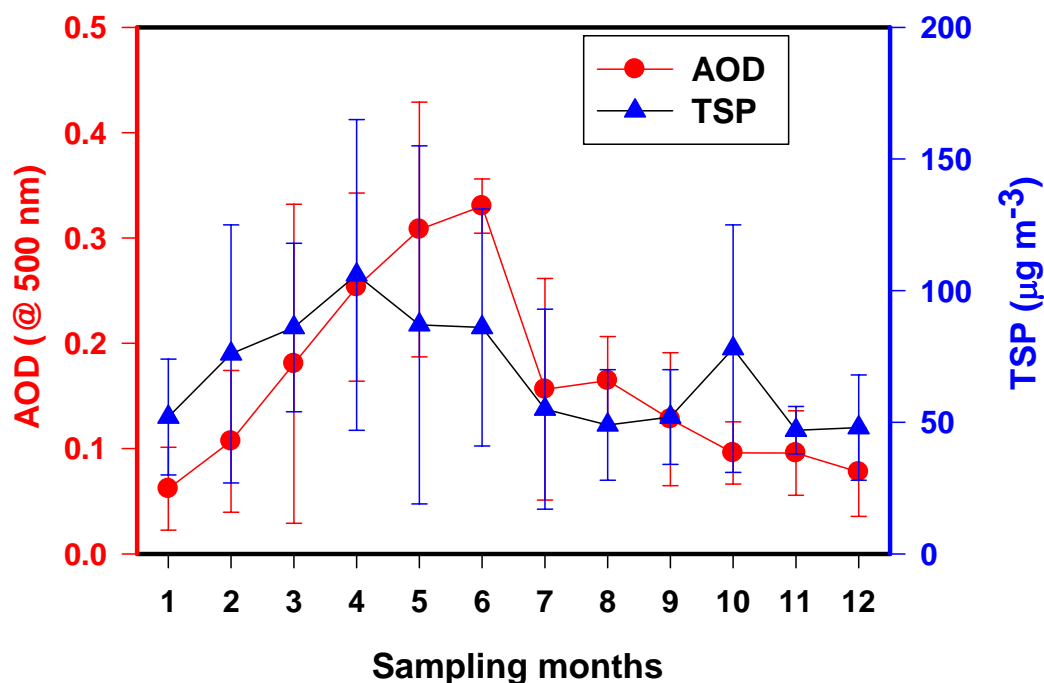


Fig. 3.8: Temporal variability of monthly averaged AOD and TSP mass concentrations at Manora Peak during the sampling period (Feb 2005-July 2008).

3.3 Summary

A long-term study from an urban (Kanpur) and two high-altitude sites (Manora Peak and Mt Abu) has provided important information on temporal variability in the abundance pattern of total aerosol mass, their sources and long-range transport of aerosols. The major observations and conclusions drawn from this chapter are listed below:

- The PM_{10} mass concentrations exhibit relatively higher values during wintertime at an urban location (Kanpur) in the Indo-Gangetic Plain. However, seasonal variability in total suspended particulate (TSP) mass is insignificant at Manora Peak, except for the sampling year 2006 marked by dust storm events.
- The aerosol chemical composition at Kanpur suggests that total carbonaceous aerosols (TCA) and water-soluble inorganic species (WSIS) contribute nearly

35% and 25% (of the PM_{10} mass) during wintertime. In contrast, their contribution at Manora Peak is only 25% and 10% of the TSP mass. The contribution of TCA and WSIS reduces by ~50% during summer months at all the sampling sites.

- The monthly mean AOD varied from 0.03 to 0.47 at Manora Peak with higher values during summer months. The relatively high TSP and AOD values, during summer, are attributed to the transport of mineral dust originating from desert regions in middle-East and Thar Desert (in western India).
- A significant increase in the mass concentrations of Ca^{2+} and carbonate carbon (CC) is observed during the dust storm events at urban and high-altitude sites.
- A three- to four-fold increase in the OC and K^+ concentrations during wintertime and significant linear relation between them suggest biomass burning (wood-fuel and agricultural-waste) emissions as the dominant source.
- The relatively high OC/EC (Av: 7.4 ± 3.5) and K^+/OC ratios (0.006 ± 0.002) at Kanpur also supports that emissions from biomass burning are overwhelming for the particulate OC.

CABONACEOUS AEROSOLS AT AN URBAN SITE (KANPUR) IN THE INDO-GANGETIC PLAIN

4.1 Introduction

Carbonaceous aerosols, consisting of organic carbon (OC) and elemental carbon (EC), are the major components of atmospheric particulate matter (PM) and constitute ~30 – 70% of the fine (<1 μm) mass over an urban atmosphere [Cao *et al.*, 2003; Fuzzi *et al.*, 2006; Ram and Sarin, 2010; Rengarajan *et al.*, 2007]. Carbonaceous species (EC and OC) emitted from anthropogenic emission sources (biomass burning, vehicular exhausts and fossil-fuel combustion) have direct impact on air quality, aerosol radiative forcing and climate on a regional to global scale [Dey and Tripathi, 2008; Gustafsson *et al.*, 2009; Menon *et al.*, 2002; Venkataraman *et al.*, 2005; Yang *et al.*, 2005]. In addition, they have indirect effects on cloud-droplet formation processes and precipitation efficiency by acting as cloud condensation nuclei (CCN) [Haywood and Boucher, 2000].

In recent years, several studies have been carried out to study the optical properties of aerosols in the IGP and to understand their impact on radiation budget [Badarinath *et al.*, 2007; Dey and Tripathi, 2008; Dumka *et al.*, 2006; Nair *et al.*, 2007; Pant *et al.*, 2006; Tripathi *et al.*, 2005a, b]. However, chemical characterization of aerosols, in particular that of carbonaceous species over the IGP is lacking in the literature [Miyazaki *et al.*, 2009; Rengarajan *et al.*, 2007; Sheesley *et al.*, 2003]. Thus, there is a need for long-term measurements of carbonaceous aerosols from the Indo-Gangetic Plain for better understanding the temporal and spatial variability and their impact on radiative forcing of climate. Furthermore, satellite and optical observations do not provide information with

regard to OC/EC, WSOC/OC ratio and secondary organic aerosol (SOA) formation.

In this chapter, temporal and spatial variability in the mass concentrations of OC, EC and water-soluble OC (WSOC) in ambient aerosols (PM_{10}), collected during Jan 2007-March 2008, from an urban location (Kanpur) in the Indo-Gangetic Plain (IGP) will be presented. These observations have been compared with a short-term aerosol sampling conducted during Dec 2004, from urban (Hisar, Allahabad) and rural (Jaduguda) sites in the Indo-Gangetic Plain. The principal objective is to assess the temporal/seasonal variability in the mass concentrations of carbonaceous species associated with the changes in meteorological conditions, emissions and their source strengths; and to document the representative OC/EC and WSOC/OC ratios from the Indo-Gangetic Plain.

4.2 Results and Discussion

4.2.1 Meteorological details and back trajectory analysis

The regional meteorology, topography and emission sources (natural and anthropogenic) play an important role in determining the spatio-temporal variability in the aerosol mass concentration and chemical composition. The flat topography of the Indo-Gangetic Plain (extending from north-east to north-west and parallel to the Himalayan range), the moderate winds and a shallow boundary layer height during wintertime favour an efficient trapping of aerosols in the lower atmosphere. The rainfall during south-west monsoon (late June – Sep) accounts for ~70% of annual precipitation over India whereas very little rainfall occurs during winter (Dec – Feb). Based on the regional meteorology, the temporal variability in the aerosol composition has been discussed in terms of four different seasonal patterns referred as winter (Dec – Feb), summer/pre-monsoon (April – June), monsoon (late June – Sep) and post-monsoon (Oct – Nov). It is relevant to state that the annual seasonal cycle, as defined in this study, represents the tropical climate of the Gangetic Plain. The month of March represents a transition phase between the winter and summer. In general, the major wind regime observed in all

seasons during the sampling period was northwesterly (NW) with additional components from the northeast (NE) and southwest (SW) directions (Fig. 4.1).

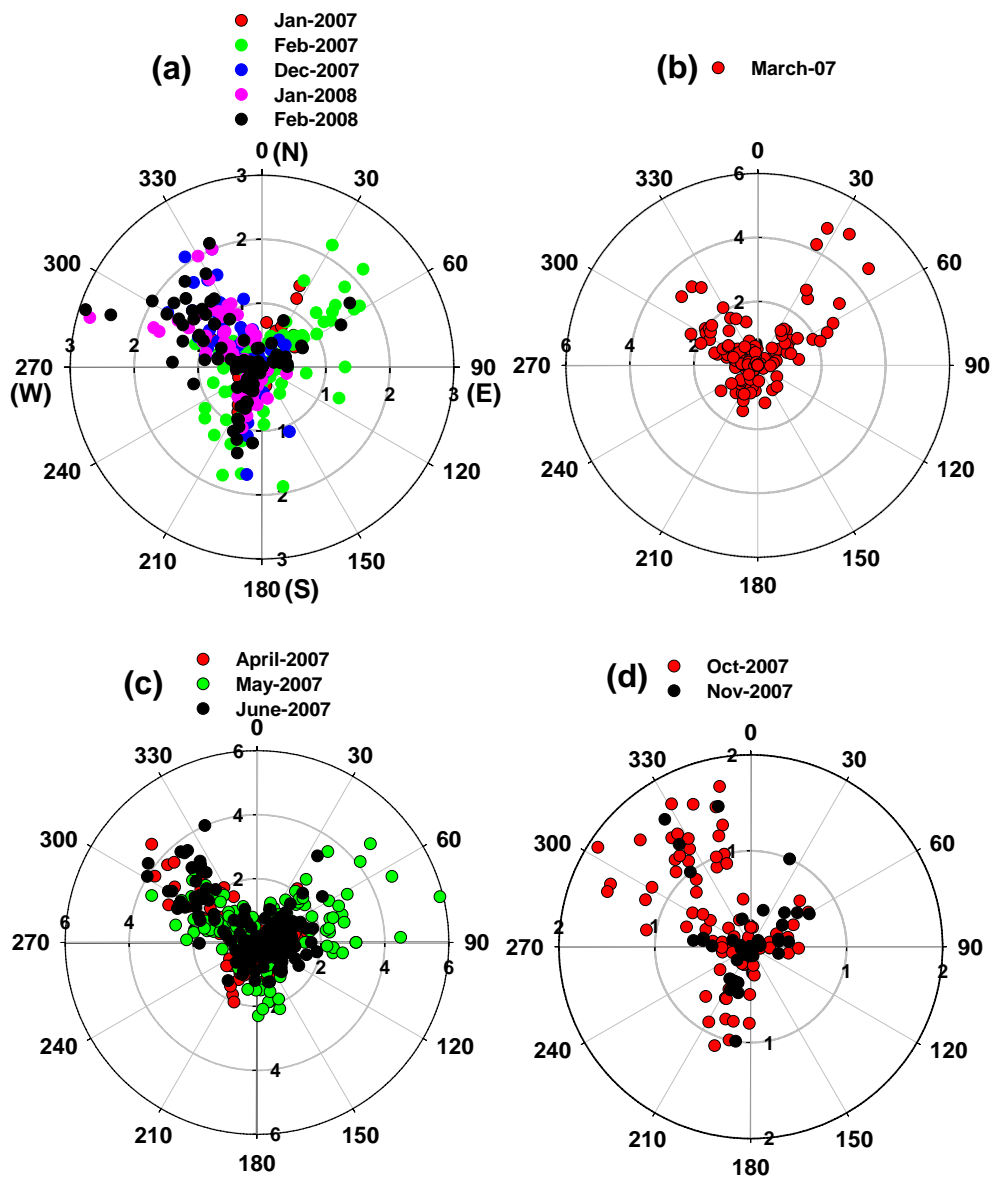


Fig. 4.1: Wind-rose plot for the sampling period from Jan 2007 to March 2008: (a) winter (Dec – Feb), (b) spring (March), (c) summer (April – June) and (d) post – monsoon (Oct – Nov). The letters N, E, S and W refers to north, east, south and west-directions, respectively.

The seasonally averaged ($\pm 1\sigma$) data of temperature, wind-speed, wind-direction and relative humidity (RH) are presented in Table 4.1. The temperature and wind-speed was generally low during winter and post-monsoon seasons compared to those during summer seasons. The relative humidity goes as high as

100% with average RH close to 70% during winter and post-monsoon seasons (Table 4.1). The stagnant atmosphere and the relatively higher concentrations of anthropogenic aerosols and their hygroscopic growth lead to reduction in the visibility and fog-haze formation during wintertime over the IGP [Gautam *et al.*, 2007; Ramachandran *et al.*, 2006; Ramanathan and Ramana, 2005; Tare *et al.*, 2006]. The relative humidity is generally lower (~25–60%) but temperature rises to 44 °C and wind speed is relatively higher during summer months (Table 4.1). The surface level low pressure in north-western India, aided by the westerly and north-westerly winds and high ambient temperatures, is mainly responsible for the long-range transport of mineral aerosols during summer months [Mishra and Tripathi, 2008; Singh *et al.*, 2005]. The change in wind regimes and an increase in ambient temperature favour vertical convective mixing and lead to a rapid decrease in the concentrations of chemical species during summer months.

Table 4.1: Meteorological data during the sampling period (Jan 2007-March 2008) at Kanpur. Numbers within parenthesis represent the range of values.

Months	Temperature (°C)	Wind-speed (m s ⁻¹)	Wind-direction	Relative humidity (%)
Dec-Feb	15.7 ± 5.6 (5.2-29.6)	0.5 ± 0.5 (0.0-2.9)	192 ± 97 (6-355)	70 ± 24 (17-100)
March	22.9 ± 5.2 (15.4-30.6)	0.8 ± 0.5 (0.1-5.1)	196 ± 37 (134-286)	56 ± 19 (28-84)
April-June	31.5 ± 5.4 (17.3-44.1)	1.0 ± 1.0 (0.1-6.1)	177 ± 99 (15-355)	43 ± 13 (25-60)
Oct-Nov	22.9 ± 6.3 (9.3-35.5)	0.3 ± 0.5 (0.0-3.5)	170 ± 100 (1-359)	67 ± 24 (17-100)

The five-day back trajectory analysis was performed (at three different heights 500, 1000 and 1500 m above ground level) to track the origin and transport of air masses arriving at the sampling site. The air mass trajectories were obtained from the final run data archive of GDAS model using NOAA Air Resource Laboratory (ARL) Hybrid Single-Particle Lagrangian Integrated Trajectory (HYSPLIT) model [Draxler and Rolph, 2003; Rolph, 2010]. The back trajectories computed for the specific sampling dates (28th March, 2nd June, 16 and 20th Nov, 1st and 16th Dec, Fig. 4.2) indicate localized as well as long-range transport of aerosols. The long-range transport of aerosols originating from Iran,

Afghanistan and Pakistan and the Thar Desert (western India) is a characteristic feature during the summer months whereas localized air masses during wintertime and post-monsoon indicate the dominance of anthropogenic emission sources.

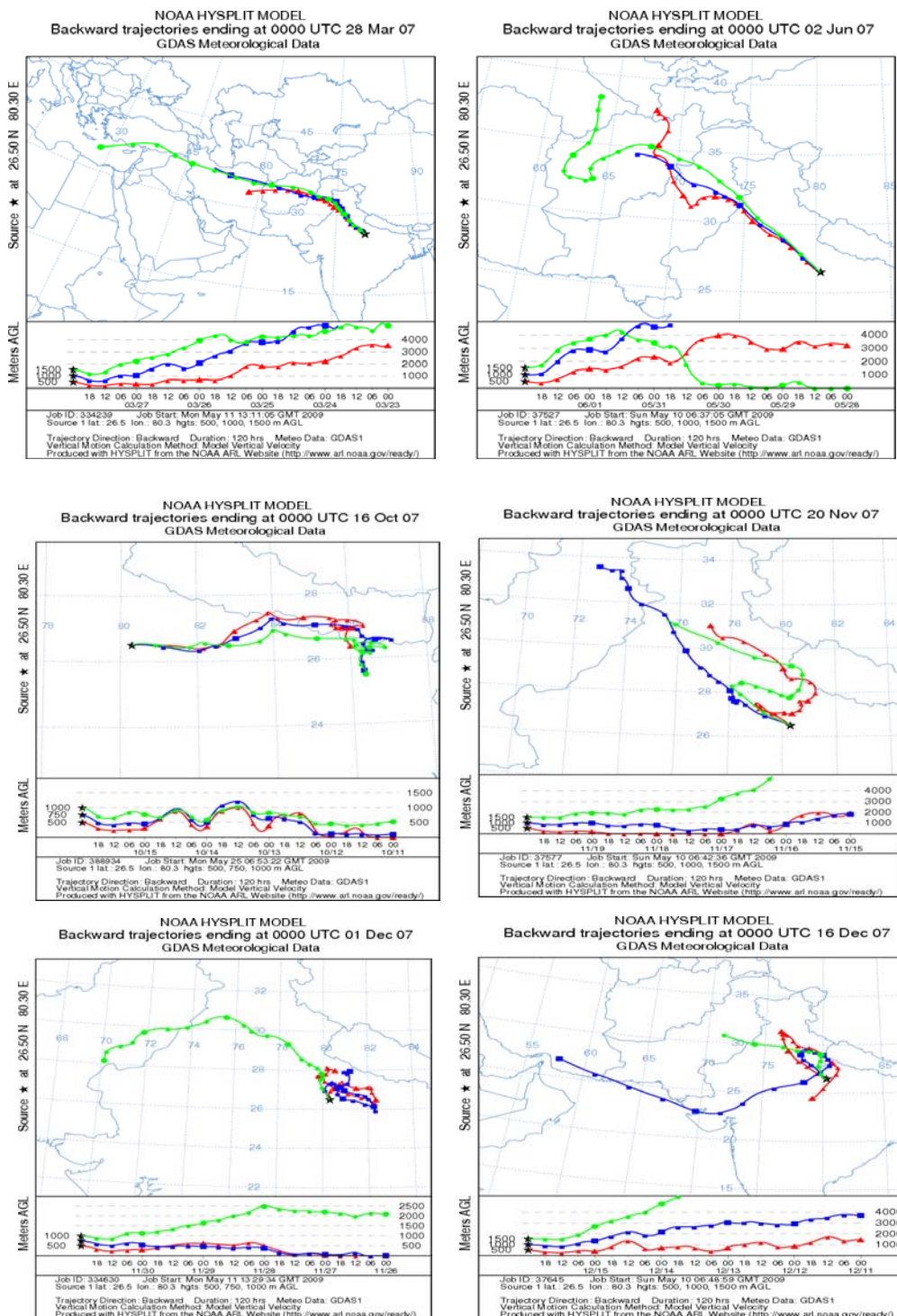


Fig. 4.2: Five-day back trajectory analyses for the selected sampling dates in order to ascertain the localized and/or long-range transport of air-mass.

4.2.2 Mass concentrations of carbonaceous species (OC and EC): Spatio-temporal variability

The OC and EC mass concentrations, at Kanpur, exhibit large temporal variability during the sampling period (Jan 2007-March 2008) and varied from 8.3 to 81.2 $\mu\text{gC m}^{-3}$ (Fig. 4.3a) and 0.7 to 14.4 $\mu\text{gC m}^{-3}$ (Fig. 4.3b), respectively. The annual average OC and EC mass concentrations, 25.8 ± 16.1 and 3.8 ± 2.3 $\mu\text{gC m}^{-3}$ respectively, accounts for $\sim 16\%$ and 2.5% of the PM_{10} mass at Kanpur. The highest OC concentration (81.2 $\mu\text{gC m}^{-3}$) was observed for the sample collected during winter month (Dec) while the highest EC (14.4 $\mu\text{gC m}^{-3}$) was obtained in the month of March.

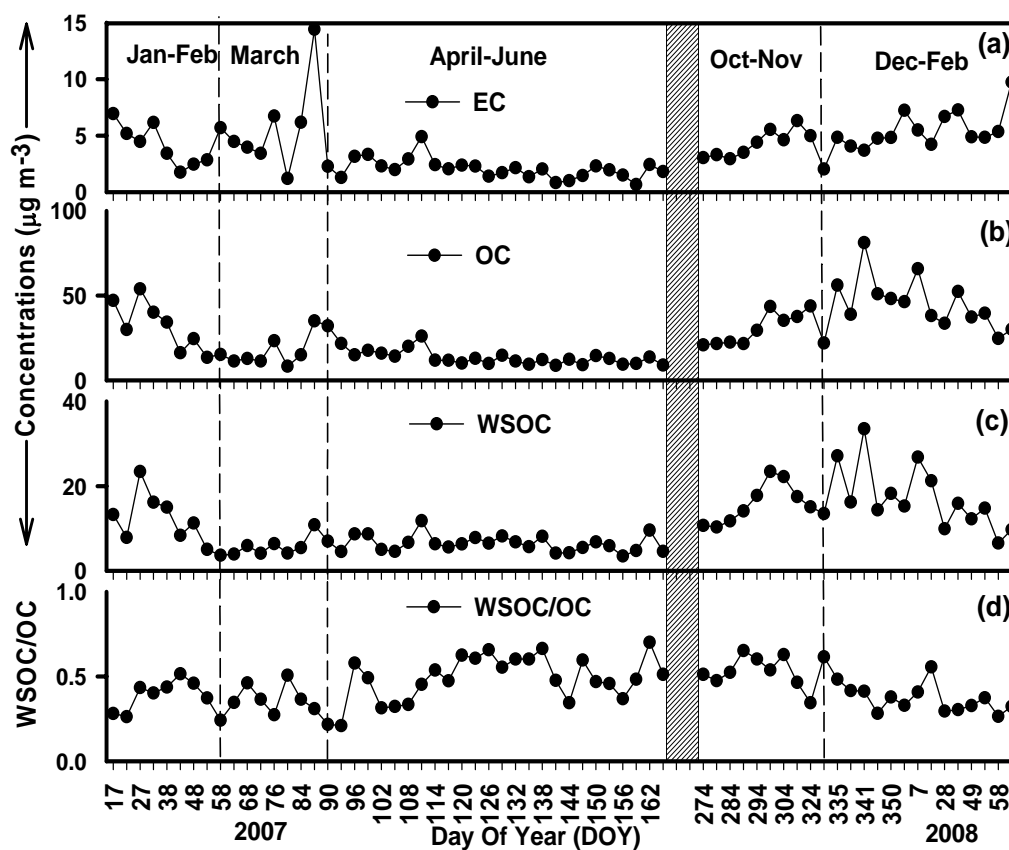


Fig. 4.3: Temporal variability of the concentrations of carbonaceous species: (a) EC, (b) OC, (c) WSOC and (d) WSOC/OC ratios at Kanpur. The time-period between June and Sep, shown by a vertical bar, represents the monsoon period and no samples were collected.

The abundance patterns of carbonaceous species (OC, EC and WSOC) show a seasonal variability with higher values during winter and post-monsoon and lower during summer months (Figs. 4.3a, b & c respectively). The monthly average mass concentrations of OC, EC, TCA, WSOC and OC/EC and WSOC/OC ratios are presented in Table 4.2. The average OC and EC concentrations during winter and post-monsoon are two-to-three times higher than in summer (Table 4.2).

Table 4.2: Monthly-averaged mass concentrations of OC, EC, TCA, WSOC and their ratios ($\pm 1 \sigma$) at Kanpur. Numbers within parenthesis are median values.

Month	n	PM ₁₀	OC	EC	TCA	WSOC	OC/EC	WSOC/OC
		$\mu\text{g m}^{-3}$					ratio	
Jan-07	3	215 ± 34 (213)	43.7 ± 12.4 (42.4)	5.5 ± 1.3 (5.4)	75.4 ± 19.8 (73.5)	15.0 ± 7.9 (13.6)	8.2 ± 3.4 (7.8)	0.33 ± 0.09 (0.32)
Feb-07	6	121 ± 55 (110)	24.0 ± 11.1 (22.0)	3.7 ± 1.8 (3.4)	42.1 ± 18.6 (38.9)	10.0 ± 5.1 (8.8)	7.2 ± 3.1 (6.5)	0.41 ± 0.9 (0.39)
Mar-07	8	130 ± 82 (109)	18.7 ± 10.3 (16.5)	5.3 ± 4.1 (4.2)	35.2 ± 19.2 (31.1)	6.2 ± 2.3 (5.9)	4.8 ± 4.0 (3.9)	0.36 ± 0.09 (0.34)
Apr-07	10	134 ± 30 (131)	16.4 ± 5.0 (15.8)	2.7 ± 1.0 (2.5)	29.0 ± 8.5 (27.9)	6.7 ± 2.3 (6.4)	6.8 ± 2.3 (6.3)	0.43 ± 0.13 (0.41)
May-07	10	150 ± 41 (145)	11.5 ± 2.2 (11.4)	1.7 ± 0.5 (1.6)	20.1 ± 3.8 (19.8)	6.2 ± 1.5 (6.0)	7.5 ± 2.3 (7.2)	0.56 ± 0.10 (0.55)
Jun-07	5	160 ± 59 (148)	11.0 ± 2.1 (10.8)	1.7 ± 0.7 (1.5)	19.2 ± 3.9 (18.9)	5.5 ± 2.3 (5.2)	7.7 ± 4.1 (7.0)	0.50 ± 0.12 (0.49)
Oct-07	7	160 ± 37 (156)	27.9 ± 8.8 (26.8)	3.9 ± 1.0 (3.8)	48.5 ± 14.9 (46.7)	15.5 ± 5.5 (14.7)	7.1 ± 0.6 (7.0)	0.56 ± 0.07 (0.56)
Nov-07	3	206 ± 88 (195)	34.5 ± 11.3 (33.1)	4.4 ± 2.2 (4.0)	59.6 ± 19.9 (57.0)	15.2 ± 2.0 (15.1)	8.5 ± 2.4 (8.3)	0.47 ± 0.14 (0.46)
Dec-07	5	255 ± 35 (253)	55.5 ± 15.9 (53.5)	4.4 ± 0.5 (4.4)	92.6 ± 25.2 (90.1)	21.7 ± 8.2 (20.6)	12.8 ± 5.2 (12.1)	0.39 ± 0.07 (0.39)
Jan-08	4	216 ± 15 (216)	46.0 ± 14.2 (44.5)	5.9 ± 1.3 (5.8)	79.4 ± 22.7 (77.2)	18.2 ± 7.3 (17.0)	8.1 ± 3.1 (7.7)	0.40 ± 0.12 (0.39)
Feb-08	4	160 ± 41 (158)	38.5 ± 13.4 (37.2)	5.6 ± 1.3 (5.5)	67.1 ± 18.9 (65.1)	12.3 ± 4.2 (11.6)	6.9 ± 2.6 (6.7)	0.32 ± 0.05 (0.32)
Mar-08	1	230	30.1	9.7	58.0	25	3.1	0.32
Annual	66	164 ± 66 (160)	25.8 ± 16.1 (21.7)	3.8 ± 2.3 (3.4)	45.0 ± 27.1 (36.8)	10.8 ± 6.6 (8.5)	7.4 ± 3.5 (6.7)	0.44 ± 0.12 (0.46)

Total carbonaceous aerosol (TCA) was estimated by summing up the organic matter (OM) and elemental carbon (EC) concentrations. The OM concentration was taken as 1.6 times that of organic carbon measured in aerosols

(i.e. $OM = 1.6 \times OC$). Although, a wide range of values for OM/OC ratios (1.2 to 2.1) have been reported in the literature [Turpin and Lim, 2001]; a value of 1.6 for OM/OC ratio have been suggested for urban aerosols [Cao *et al.*, 2003; Rengarajan *et al.*, 2007]. The conversion factor is used to account for the elements, present in aerosols, other than carbon (such as oxygen, nitrogen and sulfur etc). The seasonal average mass concentrations of OC, EC, TCA and respective ratios are presented in Table 4.3. On a seasonal basis, TCA accounts for ~38, 17 and 31% of the PM_{10} mass during winter, summer and post-monsoon seasons, respectively.

Table 4.3: Seasonal-average mass concentrations of PM_{10} , OC, EC, TCA, WSOC and their ratios ($\pm 1\sigma$) at Kanpur. Numbers within parenthesis are median values.

Seasons	n	PM_{10}	OC	EC	TCA	WSOC	OC/EC	WSOC/O C
$\mu g m^{-3}$							ratio	
Dec-Feb	22	189 ± 64 (172)	40.4 ± 16.6 (34.0)	4.9 ± 1.5 (4.4)	69.5 ± 27.0 (59.0)	15.3 ± 7.6 (13.4)	8.7 ± 3.9 (7.8)	0.37 ± 0.09 (0.37)
March	9	141 ± 84 (119)	19.9 ± 10.3 (17.6)	5.8 ± 4.1 (4.6)	37.7 ± 19.5 (33.3)	6.4 ± 2.5 (6.0)	4.6 ± 3.8 (3.8)	0.39 ± 0.11 (0.37)
April-June	25	146 ± 41 (140)	13.4 ± 4.3 (12.8)	2.1 ± 0.9 (1.9)	23.5 ± 7.5 (22.5)	6.6 ± 2.0 (6.2)	7.3 ± 3.2 (6.8)	0.51 ± 0.13 (0.48)
Oct-Nov	10	174 ± 56 (167)	29.8 ± 9.5 (28.6)	4.1 ± 1.3 (3.9)	51.8 ± 16.3 (49.6)	15.6 ± 4.6 (15.1)	7.5 ± 1.4 (7.4)	0.54 ± 0.09 (0.53)

The temporal variability of the mass concentrations PM_{10} , TCA and WSIS are presented in Figs. 4.4a, b and c, respectively and the fractional contribution of TCA and WSIS (to PM_{10} mass) are shown in Fig. 4.4d. The higher concentrations of carbonaceous species during winter and post-monsoon seasons are related to an increase in biomass burning emission from residential heating purposes. However, the increase in mass concentrations of carbonaceous species (EC and OC) cannot be fully explained in terms of increase in their source strength. The role of meteorological conditions (wind patterns and boundary layer dynamics) is necessary to explain these variabilities. The wind speed is generally low ($<2 \text{ ms}^{-1}$) and air masses are localized during wintertime (Table 4.1 and Fig. 4.1). Nair *et al.* [2007] have reported that the boundary layer height at the urban site (Kanpur)

varied between 500-800 m during the observations made in Dec 2004. An increase in the source strength of carbonaceous aerosols and a lower boundary layer height during the wintertime are the main causes for the high mass concentrations of EC and OC. The water-soluble ionic species (WSIS; sum of the mass concentrations of cations and anions) also exhibit a similar seasonal variability (Fig. 4.4c). The seasonally averaged WSIS concentrations account for ~24, 9 and 19% of PM_{10} mass during winter, summer and post-monsoon, respectively. The variability in TCA and WSIS abundances is also reflected in the variability in PM_{10} mass concentrations at Kanpur during the sampling period (Fig. 4.4a).

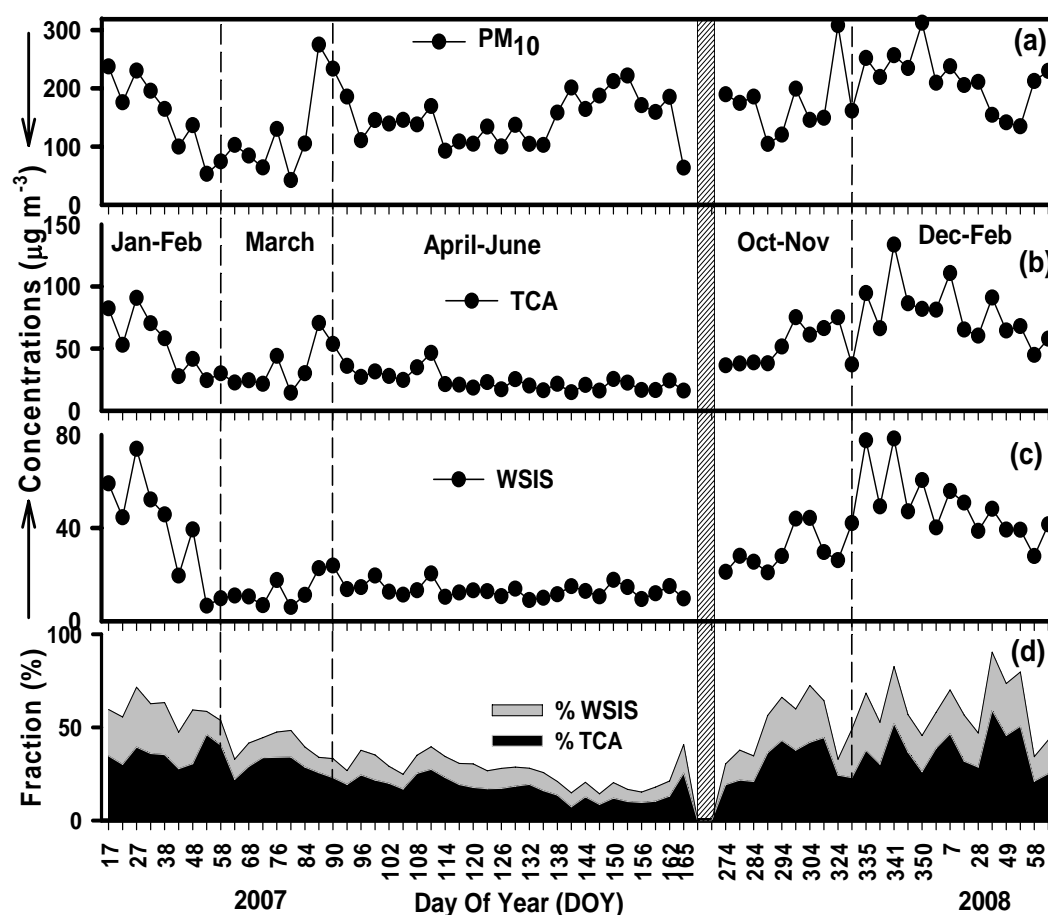


Fig. 4.4: Temporal variability of: (a) PM_{10} ; mass concentrations of (b) TCA, (c) WSIS and (d) fractional contribution of TCA and WSIS to PM_{10} during the sampling period. The time-period between June and Sep, shown by a vertical bar, represents the monsoon period and no samples were collected.

4.2.3 The OC/EC ratios and characterization of sources of carbonaceous aerosols

The OC/EC ratio at Kanpur also shows a large temporal variability and varies from 2.4 to 22.0 during Jan 2007 – March 2008 (Av. 7.4 ± 3.5 , n=66). Similarly, the OC/EC ratios at Allahabad varied from 5.7 to 11.4 (Av: 8.1 ± 1.7 , n=19) and those at Hisar varied from 5.4 to 17.8 (Av: 8.5 ± 2.2 , n=41) during Dec 2004. In contrast, the OC/EC ratios at Jaduguda are relatively lower and ranged from 2.1 to 4.0 (Av: 3.1 ± 0.6 , n =7) during Dec 2004. The OC/EC ratios in urban aerosols, except for few of the samples collected during March at Kanpur, are significantly higher compared to those reported in the literature for urban areas of the world (typical OC/EC ~2 to 3) [Duan *et al.*, 2006; He *et al.*, 2001]. The OC/EC ratios in ambient aerosols at urban sites (Hisar, Allahabad and Kanpur) are characteristically different than those at a rural site (Jaduguda) in the IGP. The observed variability in abundance patterns of carbonaceous species and OC/EC ratio can be attributed to the variability in the emission sources and their emission strength.

Biomass burning and fossil-fuel emissions have characteristically different end member OC/EC ratios. Several investigators have used OC/EC ratio to identify the sources of carbonaceous aerosols [Andreae and Merlet, 2001; Ram *et al.*, 2008; Sandradewi *et al.*, 2008b; Sudheer and Sarin, 2008]. These studies have suggested relatively high OC/EC ratios for biomass burning emission and low ratios for vehicular (traffic) emissions. The OC/EC ratio, obtained in this study, covers the range of ratios documented for vehicular exhaust and biomass burning emissions. For example, Saarikoski *et al.* [2008] have reported OC/EC ratio of 6.6 for biomass burning emission and 0.71 for vehicular emission whereas Sandradewi *et al.* [2008b] obtained values of 7.3 and 1.1 for the two sources, respectively.

The seasonally averaged OC/EC ratios at Kanpur are given in Table 4.3; indicating higher OC/EC ratios from biomass burning emissions. However, it is noteworthy that the average OC/EC ratio of 2.9 ± 0.5 (range: 2.4 to 3.5; n=7, excluding two high values of 6.9 and 14.1) is much lower than those for winter and post-monsoon season (Table 4.3) and most of the lower OC/EC ratio are

observed for the samples collected during March. The month of March is characterized as a transition period between the winter and summer in India; the strength of biomass burning emission decreases significantly because residential heating is switched off. The coal-based (from brick-kiln and thermal power plants) and vehicular emission becomes prominent. *Reddy and Venkataraman* [2002] have estimated that ~3% and 1% of particulate matter (PM) can be identified as OC and EC respectively; thus producing OC/EC ratios of about three during the emissions from coal-fired industries. Jaduguda is located in the eastern part of India where coal-based emissions are predominant [*Prasad et al.*, 2006]. The OC/EC ratio at Jaduguda is quite similar to emissions from coal-fired industries and thus, indicates coal-based emission as a major source of carbonaceous species at Jaduguda.

Biomass burning emissions, including savanna burning, forest fires and agricultural waste burning, produce a significant amount of K^+ and carbonaceous species (OC and EC). In contrast, fossil-fuel and vehicular emissions also produce high concentrations of OC and EC but low K^+ concentration. Thus, K^+/OC and K^+/EC ratios can be used to characterize aerosols produced from biomass burning and/or fossil fuel emissions. The K^+/OC ratios exhibit a narrow range of 0.08 – 0.10 for savanna burning [*Echalar et al.*, 1995] and 0.04 – 0.13 for agricultural waste burning [*Andreae and Merlet*, 2001]. Similarly, relatively high K^+/EC ratios have been reported for biomass burning (range: 0.21– 0.46) and low ratios for fossil-fuel emissions (range: 0.025 – 0.09) [*Andreae*, 1983 and references therein]. The K^+/EC ratio at Allahabad varied from 0.30 to 0.69 (Av: 0.44 ± 0.11), similar to that reported for biomass burning emissions. However, K^+/EC ratios at Jaduguda (Av: 0.13 ± 0.04 ; range: 0.08 – 0.19) are somewhat lower and indicative of fossil-fuel emissions. The K^+/OC and K^+/EC ratios in aerosols from the Indian and Chinese sites, along with ratios for savanna burning and agricultural waste burning, are presented in Table 4.4.

However, a fraction of K^+ can be derived from the fertilizers (used for agricultural purposes), sea-salt and mineral dust [*Chester*, 1990] and can increase K^+/OC and K^+/EC ratios. For example, *Duan et al.* [2004] have reported that K^+/OC can be as high as 0.20 during the wheat straw burning episode and possible

contribution from fertilizer sources. Nevertheless, based on OC/EC and K⁺/EC ratios, biomass burning (agricultural waste and wood-fuel) emission has been inferred as a major source of carbonaceous species at Hisar, Kanpur (except in March), and Allahabad during the wintertime while fossil-fuel (coal-based) emission dominates at Jaduguda.

Table 4.4: The average ($\pm 1 \sigma$) and range (in parenthesis) of K⁺/OC and K⁺/EC ratios in aerosols from the Indian and Chinese sites. The range of ratios for savanna burning and agricultural waste burning is also given.

Sampling site	Time-period	K ⁺ /OC	K ⁺ /EC	Emission sources	References
Kanpur	Oct-2008	0.06 \pm 0.02 (0.02 – 0.09)	0.28 \pm 0.10 (0.15 – 0.55)	Biomass burning	Present study
Kanpur	Jan-Feb 2007	0.04 \pm 0.01 (0.02 – 0.07)	0.42 \pm 0.18 (0.15 – 0.98)	Biomass burning	Present study
Allahabad [#]	Dec-2004	0.05 \pm 0.01 (0.04 – 0.06)	0.44 \pm 0.11 (0.30 – 0.69)	Biomass burning	Present study
Hisar [#]	Dec-2004	0.08 \pm 0.02 (0.04 – 0.14)	0.64 \pm 0.19 (0.28 – 1.21)	Biomass burning	<i>Rengarajan et al.</i> [2007]
		0.08 – 0.10		Savanna burning	<i>Echalar et al.</i> [1995]
		0.04 – 0.13		Agricultural waste burning	<i>Andreae and Merlet</i> [2001]
Beijing	Nov-Oct-1997-98	0.19 – 0.21		Straw burning/ Fertilizer	<i>Duan et al.</i> [2004]

[#]: Aerosol samples were collected during Dec 2004 land-campaign

4.2.4 Mass concentrations of WSOC

Water-soluble organic carbon (WSOC) is one of the major contributors to the total water-soluble constituents in atmospheric aerosols. The WSOC mass concentrations, in aerosol samples collected during Jan 2007 – March 2008, varied from 3.3 to 33.5 $\mu\text{gC m}^{-3}$ (Fig. 4.3c). The WSOC concentrations are two-to-four times higher during the wintertime compared to those in summer months. However, the measured WSOC concentrations at Kanpur (during the wintertime) are similar to those obtained at urban and rural sites in the IGP (during Dec 2004 land-campaign) [*Ram and Sarin*, 2010; *Rengarajan et al.*, 2007]. For example, the WSOC concentrations ranged from 5.6 to 27.8 $\mu\text{gC m}^{-3}$ (Av: 17.7 \pm 5.9 $\mu\text{gC m}^{-3}$) at Allahabad and 3.5 to 22.1 $\mu\text{gC m}^{-3}$ (Av: 10.7 \pm 4.5 μgCm^{-3}) at Hisar, the two urban locations in the IGP. Furthermore, the WSOC mass concentrations at urban

in the IGP are similar to those obtained at a rural site (Jaduguda), located in the eastern part of India (range: 10.5 to 21.6; Av: $16.2 \pm 3.5 \mu\text{gC m}^{-3}$).

The WSOC concentrations in the day- and night-samples, collected during 19-30th Oct 2008 at Kanpur, varied from 12.2 to 71.6 $\mu\text{gC m}^{-3}$ (average: $31.6 \pm 15.3 \mu\text{gC m}^{-3}$) and 14.4 to 73.5 $\mu\text{gC m}^{-3}$ (average: $32.9 \pm 13.8 \mu\text{gC m}^{-3}$) in $\text{PM}_{2.5}$ and PM_{10} , respectively. Thus, on average, more than 95% of the WSOC mass is found in the fine-mode aerosols (i.e. aerosols with aerodynamic diameter less than 2.5 μm). Scatter plots between WSOC and OC, for the samples collected at urban sites in the IGP, are shown in Fig. 4.5.

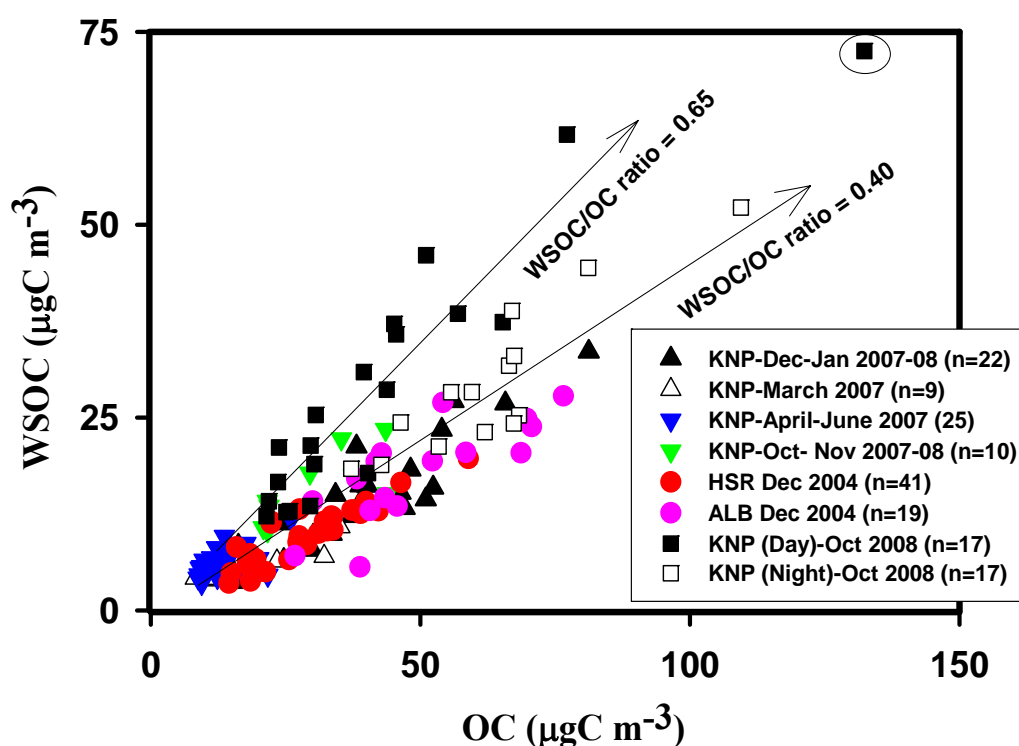


Fig. 4.5: Scatter plots between WSOC and OC in aerosol samples collected during Jan 2007-March 2008 and Oct 2008 from an urban location (KNP; Kanpur). The data from other urban sites (ALB; Allahabad and HSR; Hisar) in the IGP are also shown. One encircled data point is excluded from the regression analysis. “n” represents the number of aerosol samples collected during each sampling period.

The WSOC shows a linear dependence on the OC with all the data points, collected during the wintertime, falling on a line with a slope of 0.40 (Fig. 4.5). However, the samples collected during daytime (Oct 2008) and summer (April-June 2007) fall on a different line (slope=0.65; Fig 4.5).

4.2.5 The WSOC/OC ratio and secondary organic aerosol (SOA) formation

The WSOC/OC ratios ranged from 0.21 to 0.70 at Kanpur for the samples collected during Jan 2007-March 2008 (Fig. 4.3d). The monthly average WSOC/OC ratios at Kanpur are presented in Fig. 4.6. The WSOC/OC ratios, during wintertime, are similar to those at Allahabad and Hisar (obtained during Dec 2004 land-campaign [Ram and Sarin, 2010]). However, relatively higher WSOC/OC ratios are observed for the samples collected during summer and post-monsoon (Fig. 4.6).

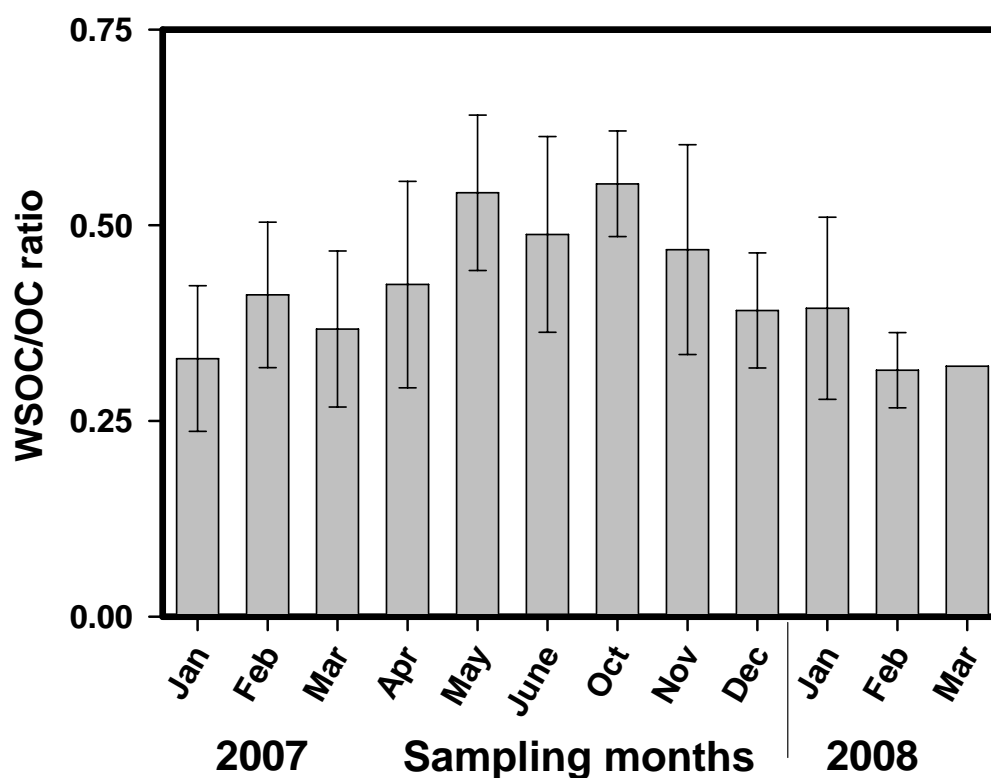
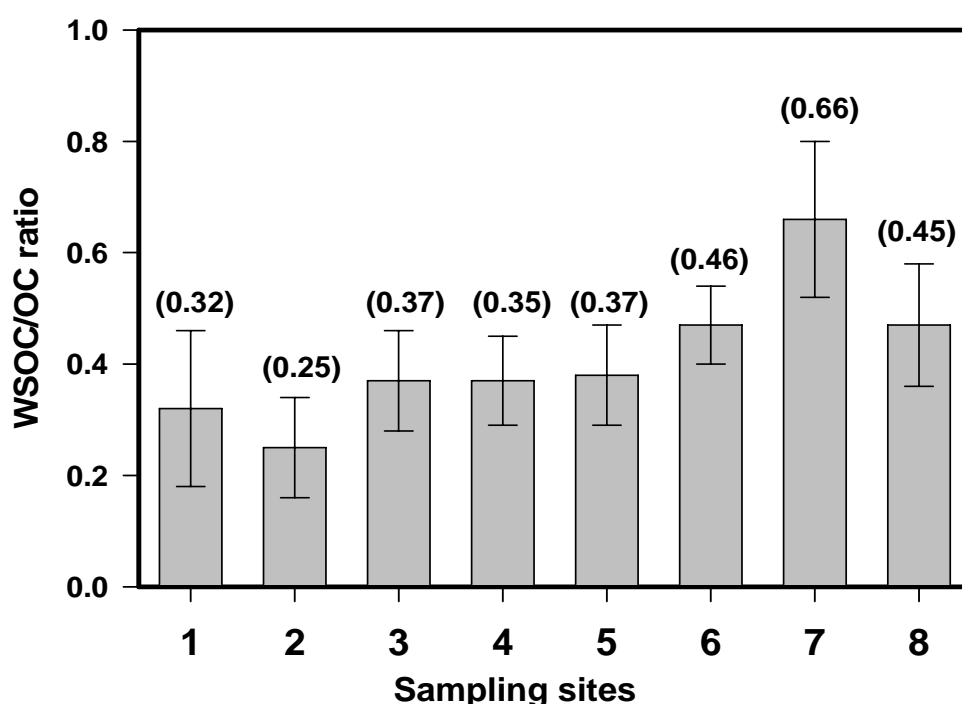


Fig. 4.6: Monthly-averaged WSOC/OC ratios at Kanpur during Jan 2007- March 2008.

The higher WSOC/OC ratios, during summer (Fig. 4.6), can be attributed to the enhanced secondary organic aerosol (SOA) formation. In order to get an insight of the SOA formation, WSOC/OC ratios are compared with the day- and night-samples collected during Oct 2008 at Kanpur. The WSOC/OC ratios range from 0.44 to 0.90 for the samples collected during daytime whereas WSOC/OC

ratios, for the night-samples, are relatively lower and vary from 0.36 to 0.58 during Oct 2008. The average WSOC/OC ratios for samples collected during daytime (0.67 ± 0.14 , $n=17$) are significantly higher than that for the night-samples (0.47 ± 0.07 , $n=17$). For inter-comparison, the average WSOC/OC ratios at urban sampling sites (Delhi, Hisar, Kanpur, and Allahabad) and a rural site (Jaduguda) in the IGP are presented in Fig 4.7.



1. Hisar; 2. Delhi (nighttime); 3. Delhi (daytime); 4. Allahabad; 5. Kanpur^a;
6. Kanpur (nighttime), 7. Kanpur (daytime) and 8. Jaduguda

Fig. 4.7: The average WSOC/OC ratios at urban sampling sites (1-5) and rural site (8) in the Indo-Gangetic Plain during wintertime. The data for day and night-samples are also shown (6-7). Delhi: Miyazaki *et al.* [2009], Hisar: Rengarajan *et al.* [2007], Allahabad: Ram and Sarin [2010], Kanpur^a (Jan-Feb 2007). Number within parenthesis represents median values.

The WSOC/OC ratios have been used to infer the secondary organic aerosol (SOA) formation because most of the SOAs have polar functional groups and thus, are soluble in water [Miyazaki *et al.*, 2007; Pio *et al.*, 2007; Weber *et al.*, 2007]. The SOA formation depends on the photochemical activity (the solar radiation and particularly the ultraviolet region of the spectrum), concentrations of volatile organic compounds (VOCs) and oxidizing agents such as O₃, OH,

peroxide and nitrate radicals. Several experimental and modeling studies suggest that SOA formation increases with increasing O₃ concentration and the photochemical activity, thus, resulting in a diurnal pattern in the SOA abundances. For example, *Chang and Lee* [2007] have reported that SOA formation shows a diurnal pattern and SOA concentration reaches to the maximum when O₃ concentration exceeds 120 ppb. Furthermore, SOA formation also shows a seasonal pattern (higher SOA formation during the summer and low during the winter) and the seasonal variability has been explained in terms of the lower photochemical activity during the wintertime [*Castro et al.*, 1999].

Along with the SOA formation, a significant fraction of WSOC results from the particulate OC produced during direct emissions from biomass burning and vehicular exhaust. Thus, primary emissions of particulate OC can contribute to the WSOC/OC ratios measured in the aerosol samples. Furthermore, it has also been suggested that biomass burning emissions produce relatively high amount of water-soluble organic compounds and higher WSOC/OC ratios [*Kundu et al.*, 2010; *Mayol-Bracero et al.*, 2002; *Saarikoski et al.*, 2008]. For example, *Saarikoski et al.* [2008] have reported a ratio of 0.40 for biomass burning and a low of 0.27 for traffic (vehicular) emissions. In the context of regional emissions, relatively lower oxygenated organic aerosols and WSOC/OC ratios have been observed at urban locations (near the source region of emissions) and the WSOC/OC ratio increases at remote locations [*Pio et al.*, 2007; *Zhang et al.*, 2007]. In the present study, aerosol samples collected from Kanpur represent their collection within the source region of biomass burning emission, especially those collected during wintertime. In addition, the ambient temperature and photochemical activity is lower during wintertime resulting in lower WSOC/OC ratios. Earlier studies have also suggested that WSOC/OC ratios, during wintertime, are relatively lower (range: 0.30 to 0.45) over urban sites in northern India [*Miyazaki et al.*, 2009; *Ram and Sarin*, 2010; *Rengarajan et al.*, 2007]. Thus, higher WSOC/OC ratios (in the samples collected during daytime and summer months) provide an evidence for the enhanced SOA formation. However, the role of oxidizing species and VOCs needs to be further investigated for the

better understanding of the SOA formation and its influence on the hygroscopicity of ambient aerosols and fog-haze weather formation over the IGP.

4.2.6 Estimation of Secondary Organic Carbon (SOC)

Secondary organic aerosols (SOA) are one of the major components of organic aerosol (OA); however, the estimation of SOA is not straight forward and requires the knowledge of chemical and physical transformation processes (e.g. their formation and partitioning into the particulate phase). The secondary organic carbon (SOC) in aerosol is either estimated using the EC tracer method [*Cabada et al.*, 2004; *Turpin and Huntzicker*, 1995] or by adding up all the oxidation products measured in aerosols [*Schauer et al.*, 1996]. The EC tracer method has been applied to estimate the SOC content in aerosols using following equations:

$$(OC)_{tot} = (OC)_{prim} + SOC \quad (1)$$

which can be rewritten as

$$(OC)_{tot} = \left(\frac{OC}{EC} \right)_{prim} \cdot (EC)_{tot} + SOC \quad (2)$$

The estimation of secondary organic carbon (SOC), using the EC tracer method [*Castro et al.*, 1999; *Ram et al.*, 2008], is very difficult because of the vast primary emission sources over Indian subcontinents. All the primary emission sources such as biomass burning, fossil-fuel and vehicular exhaust (with characteristically different end member OC/EC ratios) will contribute to OC/EC ratio and thus, the approximation of minimum OC/EC ratio (i.e. $(OC/EC)_{min}$) in aerosol samples is rather disputable. The use of lower $(OC/EC)_{min}$ ratio can provide an overestimation of SOC while higher $(OC/EC)_{min}$ ratio will result in an underestimation. However, for smaller sampling period (such as on a seasonal basis), primary emission sources can be assumed to be invariable, although emission strength may vary over the sampling period. Thus, for the first order approximation, the minimum OC/EC ratio obtained during the sampling period can be taken as a representative of $(OC/EC)_{min}$.

Using the EC as a tracer for primary emission of carbonaceous aerosols, estimated SOC concentrations contribute to ~40, 50 and 20% in winter, summer and post-monsoon seasons, respectively for the samples collected during Jan

2007-March 2008 from Kanpur. Based on the similar approach, SOC was estimated for other sampling locations in the IGP during the wintertime and it was observed that SOC contribution is nearly same at all sites in the IGP (~30% of OC) which is similar to those reported in literature. For example, *Cabada et al.* [2004] have shown that SOA formation shows a similar pattern with ozone concentration and photochemical activity, and about 35% of OC at western Pennsylvania was estimated to be of secondary origin in nature. *Castro et al.* [1999] reported the SOC contribution to OC was as low as 17% during winter. The low SOC abundance at Allahabad is further supported by the low ozone concentration and photochemical activity during wintertime. *Badarinath et al.* [2007] have reported that daily mean ozone concentrations ranges from 14 to 35 ppbv (average: 20 ppbv) and photochemical activity was lower during wintertime (Dec 2004) at Allahabad, suggesting low SOA formation.

4.2.7 Fractional contribution of the absorbing EC to aerosol mass

Although EC constitutes only a minor fraction of PM₁₀ mass, it is one of the major absorbing particulate species of the solar radiation. The EC/PM₁₀ mass ratio can thus, provide a qualitative assessment of the absorbing nature of aerosols and helps to understand the radiative impact of EC. In general, EC/PM₁₀ ratio varies from 3-10% over the urban locations in India [*Babu and Moorthy*, 2002; *Babu et al.*, 2002], but it can be as high as 15% during wintertime in some parts of the IGP [*Ganguly et al.*, 2009; *Tripathi et al.*, 2005a]. The EC/PM₁₀ mass ratio at Kanpur exhibit a large temporal variability (range: 0.4 to 7.7% of PM₁₀; average: $2.5 \pm 1.5\%$ of PM₁₀) during the study period. The EC/PM₁₀ mass ratios are slightly higher during winter (range: 1.4 to 7.7%; average: $2.9 \pm 1.5\%$ of PM₁₀) and post-monsoon season (range: 1.4 to 7.7%; average: $2.5 \pm 1.1\%$ of PM₁₀) and lower during summer (range: 0.4 to 2.9%; average: $1.6 \pm 0.8\%$ of PM₁₀). However, the highest EC/PM₁₀ ratio is obtained for the samples collected during March (range: 1.0 to 5.9%; average: $4.3 \pm 1.5\%$ of the PM₁₀). Such a large variability in the EC/PM₁₀ ratio at Kanpur results from the change in the sources and emission strength of carbonaceous and mineral aerosols and meteorological conditions. Earlier studies, reported in the literature, have suggested relatively low EC/PM₁₀

ratios over semi-arid and high-altitude locations compared to those over urban environments [Hegde *et al.*, 2007; Hyvärinen *et al.*, 2009; Pant *et al.*, 2006; Ram and Sarin, 2010]. The seasonal variability in mass concentrations of absorbing EC and EC/PM₁₀ ratios, observed in this study, can have a significant influence on the estimation of SSA and direct aerosol radiative forcing on a regional scale.

4.2.8 Inter-comparison of mass concentrations of OC and EC over Indian regions

A land-campaign was carried out during wintertime (Dec 2004) over the Indo-Gangetic Plain (IGP) wherein measurements of BC mass concentrations along with several other chemical and optical properties were performed [Nair *et al.*, 2007; Ramachandran and Rajesh, 2007; Ramachandran *et al.*, 2006; Rengarajan *et al.*, 2007; Tare *et al.*, 2006; Tripathi *et al.*, 2005a]. These studies have reported a large scale heterogeneity and spatio-temporal variability in aerosol chemical and optical properties over the IGP. The OC and EC mass concentrations at Kanpur, during winter and post-monsoon seasons, are similar to those at Hisar (Table 4.5). Although, filter-based measurements of OC and EC are limited over Indian regions [Rengarajan *et al.*, 2007; Venkataraman *et al.*, 2002]; BC measurements using an Aethalometer have been extensively performed to document the spatio-temporal variability. However, OC and EC concentrations are two to three times lower in summer months. A comparison of measured OC and EC concentrations at Kanpur during 2007-2008 and those reported in the literature from different sampling locations in India are given in Table 4.5.

Over urban locations, BC mass concentrations are generally less than 15 $\mu\text{gC m}^{-3}$ (Table 4.5), however, it can be as high as 60 $\mu\text{gC m}^{-3}$ at some locations [Ganguly *et al.*, 2006; Latha and Badarinath, 2003]. Tripathi *et al.* [2005a] have reported that BC mass concentration at Kanpur varied from 6 to 20 $\mu\text{gC m}^{-3}$ during the field-campaign (Dec 2004) and resulted in a low value of 0.76 for single scattering albedo (SSA). During the same field-campaign, Ganguly *et al.* [2006] have reported that BC mass concentration was as high as 60 $\mu\text{gC m}^{-3}$ at Delhi (an urban location) with an average value of $29 \pm 14 \mu\text{gC m}^{-3}$ resulting in further lower value of 0.68 for SSA.

Table 4.5: Comparison of OC, EC (or BC) mass concentrations and OC/EC ratios over Indian regions.

Sampling Time	Location	Type	Lon ° N	Lat ° E	Elevation m amsl ^s	OC µgC m ⁻³	EC or BC µgC m ⁻³	OC/EC	References
Jan-Feb 07+ Dec 07-Feb 08			26.5	80.3	142	40.4 ± 16.6	4.9 ± 1.5	8.7 ± 3.9	This study
Mar-07 & 08	Kanpur	urban	26.5	80.3	142	19.9 ± 10.3	5.8 ± 4.1	4.6 ± 3.8	This study
Apr-June 07			26.5	80.3	142	13.4 ± 4.3	2.1 ± 0.9	7.3 ± 3.2	This study
Oct-Nov 07			26.5	80.3	142	29.8 ± 9.5	4.1 ± 1.3	7.5 ± 1.4	This study
Dec-04	Allahabad	urban	25.4	81.9	123	49 ± 14.1	6.2 ± 2.0	8.1 ± 1.7	Ram and Sarin [2010]
Dec-04	Jaduguda	rural	22.5	85.7	150	35.3 ± 7.1	11.6 ± 2.0	3.1 ± 0.6	Ram and Sarin [2010]
Dec-04	Hisar	urban	29.2	75.7	219	33.0 ± 17.9	3.8 ± 1.4	8.5 ± 2.2	Rengarajan et al. [2007]
Dec-04	Manora Peak	high-altitude	29.4	79.5	1950	4.8 ± 1.1	0.9 ± 0.3	6.0 ± 1.9	Rengarajan et al. [2007]
Feb 05-June 07	Manora Peak	high-altitude	29.4	79.5	1950	8.7 ± 4.5	1.1 ± 0.7	8.4 ± 2.8	Ram et al. [2008]
June 05 - Feb 06	Mt Abu	high-altitude	24.6	72.7	1700	3.7 ± 2.4	0.5 ± 0.5	6.1 ± 2.0	Ram et al. [2008]
Jan- Mar 1999	Mumbai [#]	urban	18.9	72.9	0	37.3 ± 10.5	12.4 ± 5.1	3.1 ± 0.5	Venkataraman et al. [2002]
Jan- Mar 2000	Mumbai [#]	urban	18.9	72.9	0	25.3 ± 9.9	12.6 ± 3.0	2.0 ± 0.3	Venkataraman et al. [2002]
Dec-04	Manora Peak [#]	high-altitude	29.4	79.5	1950		1.4 ± 0.9		Pant et al. [2006]
Sep 05- Sep 07	Mukteshwar	high-altitude	29.44	79.62	2180		0.80		Hyvärinen et al. [2009]
Dec-04	Kanpur [#]	urban	26.5	80.3	142		6.0 - 20.0		Tripathi et al. [2005a]
Aug 2000-Oct 2001	Trivandrum [#]	urban	8.57	77.0	1		4.0-8.0		Babu and Moorthy, [2002]
Jan-July	Hyderabad [#]	urban	17.2	78.3	500		0.5-68		Latha and Badarinath, [2003]
Oct-Dec 2001	Bangalore [#]	urban	13.0	77.6	960		0.4-10.2		Babu et al. [2002]
Sep 03 - June 05	Ahmedabad [#]	urban	23.0	72.5	55		0.2-10.0		Ramachandran and Rajesh, [2007]
Dec-04	Delhi [#]	urban	28.6	77.2	239		29.0 ± 14.0		Ganguly et al. [2006]
Dec-04	Kharaghpur [#]	urban	22.3	87.3	30		8.0-28.0		Nair et al. [2007]

^sAbove mean sea level; [#]Aethalometer BC data

4.3 Summary

The major observations and conclusions drawn from this chapter are listed below:

- A comprehensive one-year (Jan 2007- March 2008) set on the chemical composition of ambient aerosols (PM₁₀), collected from an urban location (Kanpur) in the Indo-Gangetic Plain (IGP) suggests that the varying strength of the regional emission sources, boundary layer dynamics and formation of secondary aerosols all contribute significantly to the temporal variability in the mass concentrations of carbonaceous and inorganic species.
- Carbonaceous aerosols contribute nearly one-third of the PM₁₀ mass during wintertime whereas their contribution is only ~10% during summer. The long-range transport of mineral aerosols from Iran, Afghanistan and the Thar Desert (western India) is significantly pronounced during summer months.
- A three-to-four fold increase in K⁺ and OC concentrations during wintertime and significant correlation ($R^2=0.79$) between them suggest the dominance of biomass burning emission (wood-fuel and agricultural waste) at Kanpur.
- The fractional mass of absorbing EC varies from less than a percent (during summer) to as high as 8% (during winter).
- The WSOC/OC ratios are fairly uniform (~0.35 – 0.40) in aerosols over urban and rural sites in the IGP for the samples collected during wintertime. However, elevated WSOC/OC ratios were observed for the samples collected during daytime and summer. The relatively higher WSOC/OC ratios during daytime and summer suggest significant contribution from secondary organic aerosols.
- The efficient neutralization of H₂SO₄ by NH₃ in the winter and NH₄⁺/SO₄²⁻ molar ratio greater than two suggest the formation of (NH₄)₂SO₄ and NH₄HSO₄ salts; whereas their molar ratio is less than one during summer. The formation of secondary particulate species over urban regions has implications to the degradation in the air-quality and reduction in visibility.

CABONACEOUS AEROSOLS AT HIGH-ALTITUDE SITES IN INDIA

5.1 Introduction

Atmospheric carbonaceous aerosols over south Asian region, originating from anthropogenic activities, forest fires and biomass burning emissions, are gaining significant importance in terms of their impact on regional air quality and climate system [Cao *et al.*, 2004; Charlson *et al.*, 1992; Lelieveld *et al.*, 2001; Menon *et al.*, 2002]. These aerosols contribute nearly 20 to 50% of the total suspended particulate (TSP) matter in the ambient atmosphere over continental mid-latitude regions [Jacobson *et al.*, 2000; Sillanpaa *et al.*, 2005] and as high as 90% over tropical forested areas [Kanakidou *et al.*, 2005]. The carbonaceous aerosols are mainly composed of organic carbon (OC) as a major component, contributing up to 90% of the total carbon and relatively low contribution (5-10%) from elemental carbon (EC). The direct emissions from biomass burning and fossil fuel combustion produce primary organic carbon (POC) and occur in the form of particulate organic matter (POM). On the other hand, secondary organic carbon (SOC) is formed via the oxidation of volatile organic reactive compounds in the atmosphere through the formation of secondary organic aerosols (SOA).

Both, OC and EC have different optical and chemical properties. For example, OC (the fraction associated with condensed organic compounds) scatters the solar radiation while EC act as an efficient absorber [Ackerman *et al.*, 2000; Jacobson, 2001]. Organic aerosols, predominantly found in fine-mode (<1 μm), represent a large variety of organic compounds (aliphatic, aromatic compounds and acids). Some of these organic compounds can act as cloud condensation nuclei (CCN) [Sun and Ariya, 2006] and, thus, have indirect climatic effects

through changes in cloud albedo and precipitation efficiency [Haywood and Boucher, 2000].

Elemental carbon is produced during incomplete combustion of fossil fuel/biomass burning and pyrolysis of high molecular weight hydrocarbons. EC exists in the atmosphere as a basic constituent of “soot” particles, is highly refractory in nature and its chemical structure is somewhat similar to graphitic carbon. Although, EC is a minor component of carbonaceous aerosols, it plays an important role in the estimation of radiative forcing as an efficient absorbing species in the atmosphere after CO₂ [Horvath, 1993]. It has positive radiative forcing (warming) at top of the atmosphere (TOA) and negative radiative forcing (cooling) at the surface [Ramanathan *et al.*, 2001]. EC is considered to be inert and does not directly take part in atmospheric chemical reactions but it can provide active surfaces for heterogeneous reactions [Ammann *et al.*, 1998]. It is, thus, important to study physical as well as chemical characteristics of carbonaceous species in order to understand their impact on air quality, atmospheric chemistry and the climate on a regional scale. In this chapter, time-series measurements on the mass concentrations of EC, OC, water-soluble OC (WSOC) and secondary organic carbon (SOC), as studied from the two high-altitude sites in India, are presented. The temporal and spatial variability in the mass concentrations of carbonaceous species and the role of emission sources and their emission strength are discussed.

5.2 Results and Discussion

5.2.1 Meteorological Details at Manora Peak

The meteorological parameters, namely rainfall, wind-patterns, boundary layer height, and the emission strength of natural/anthropogenic aerosols govern the atmospheric loading, chemical composition and optical properties of aerosols. The total aerosol mass and concentrations of chemical species are inversely related to rainfall and thus, the amount of rainfall during a particular season of the year determines the seasonal and intra-annual variability. The monthly mean

values of wind-direction, wind-speed, temperature and rainfall at Manora Peak are shown in Figs. 5.1a, b, c and d, respectively during the sampling period.

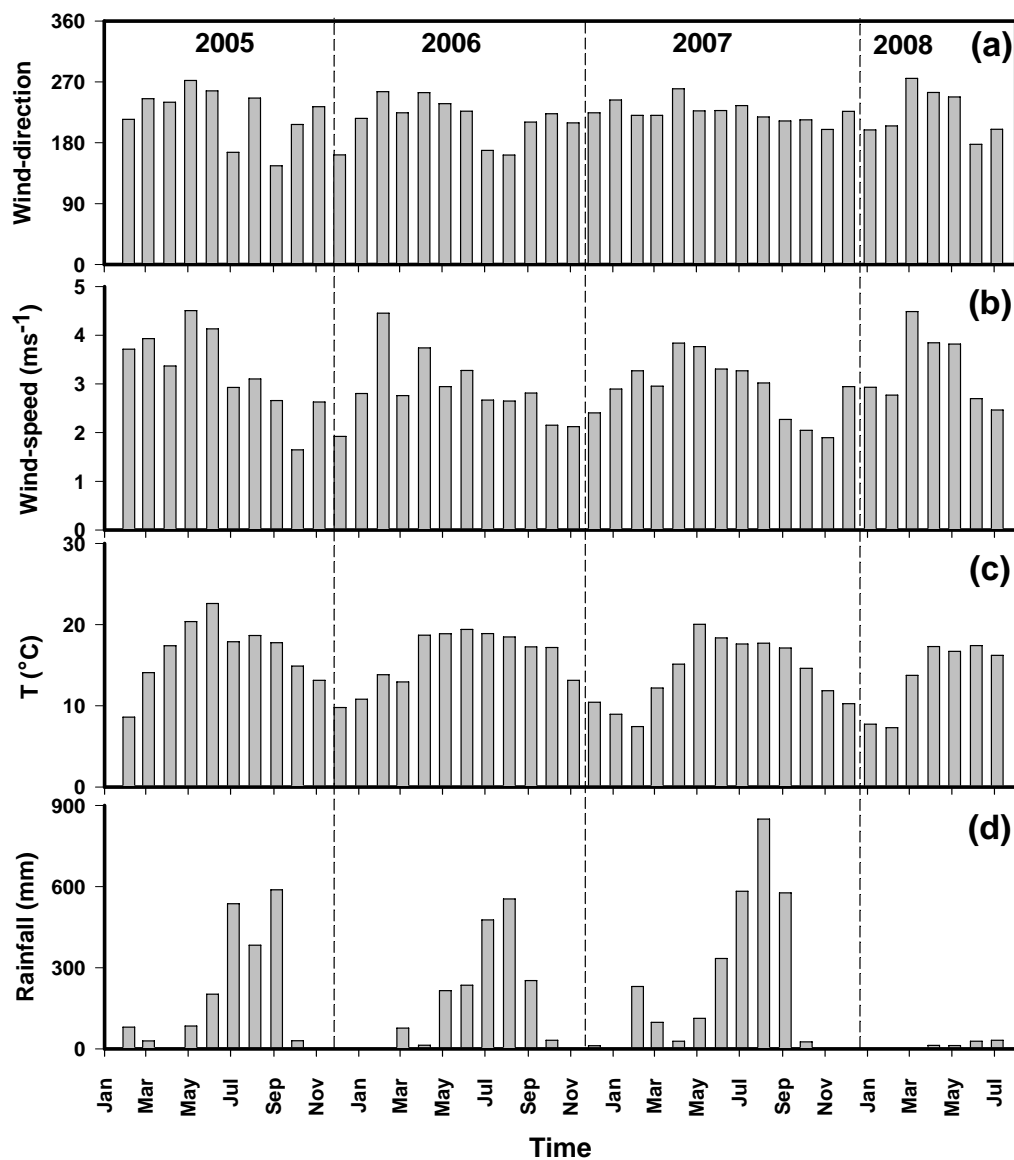


Fig. 5.1: The monthly-average meteorological data of (a) rainfall, (b) temperature, (c) wind-speed and (d) wind-direction during the sampling period (Feb 2005-July 2008) at Manora Peak.

The precipitation over Indian subcontinent is mainly (>80% of the total annual rainfall) observed during the south-west monsoon (late June to Sep) (Fig. 5.1d) and leads to an efficient washout of atmospheric aerosols. Based on the local meteorological data (mainly temperature and rainfall), the seasons are generally

classified as: winter (Dec-Feb), pre-monsoon or summer (March-June), monsoon (late June-Sep) and post-monsoon (Oct-Nov). The major wind regime (south-westerly) passing through the Deserts in middle-East and the Thar Desert (in western India) transport aerosols to north-eastern parts of India and over the Himalayan mountains [Hegde *et al.*, 2007; Prasad and Singh, 2007; Ram *et al.*, 2008]. The surface level low pressure in north-western India, aided by the westerly and north-westerly winds and high ambient temperatures, is mainly responsible for the long-range transport of mineral aerosols during summer months [Mishra and Tripathi, 2008; Singh *et al.*, 2005].

The boundary layer dynamics also play an important role in determining the ambient concentrations of chemical species. Hegde *et al.* [2008] have reported that boundary layer height (BLH) is shallower during the post-monsoon compared to that in pre-monsoon season. The BLH for the four seasons for the year 2006-07 are 1300, 1450, 1000 and 600 m for winter, pre-monsoon, monsoon and post-monsoon, respectively [Hegde *et al.*, 2008]. Relatively lower temperature, poor thermal convection and a shallower boundary layer height lead to an increase in the mass concentrations of chemical species during wintertime.

5.2.2 Temporal and spatial variability in the mass concentrations of carbonaceous species

The mass concentrations of OC and EC at the two high-altitude sites, Manora Peak and Mt Abu, exhibit a large temporal and seasonal variability during the sampling periods. The mass concentrations of OC and EC at Manora Peak varied from 0.4 to 22.3 $\mu\text{gC m}^{-3}$ (1.9 to 39.3% of TSP) and 0.14 to 7.6 $\mu\text{gC m}^{-3}$ (0.1 to 7.6% of TSP), respectively (Figs. 5.2a, b). The observed OC and EC mass concentrations at Manora Peak, in the present study, during April 2005 (9.6 and 1.5 $\mu\text{gC m}^{-3}$, respectively) are lower than the values of 51.0 and 4.0 $\mu\text{gC m}^{-3}$, respectively reported by Adhikary *et al.* [2007] for the same time period. In fact, OC concentrations never went beyond 25 $\mu\text{gC m}^{-3}$ and the highest OC (22.3 $\mu\text{gC m}^{-3}$) was observed on 26th Oct 2005 (DOY 299; Fig. 5.2a). However, EC concentrations on some occasions can be as high as 7.6 $\mu\text{gC m}^{-3}$ (e.g. on 4th March 2008; DOY 64; Fig. 5.2b).

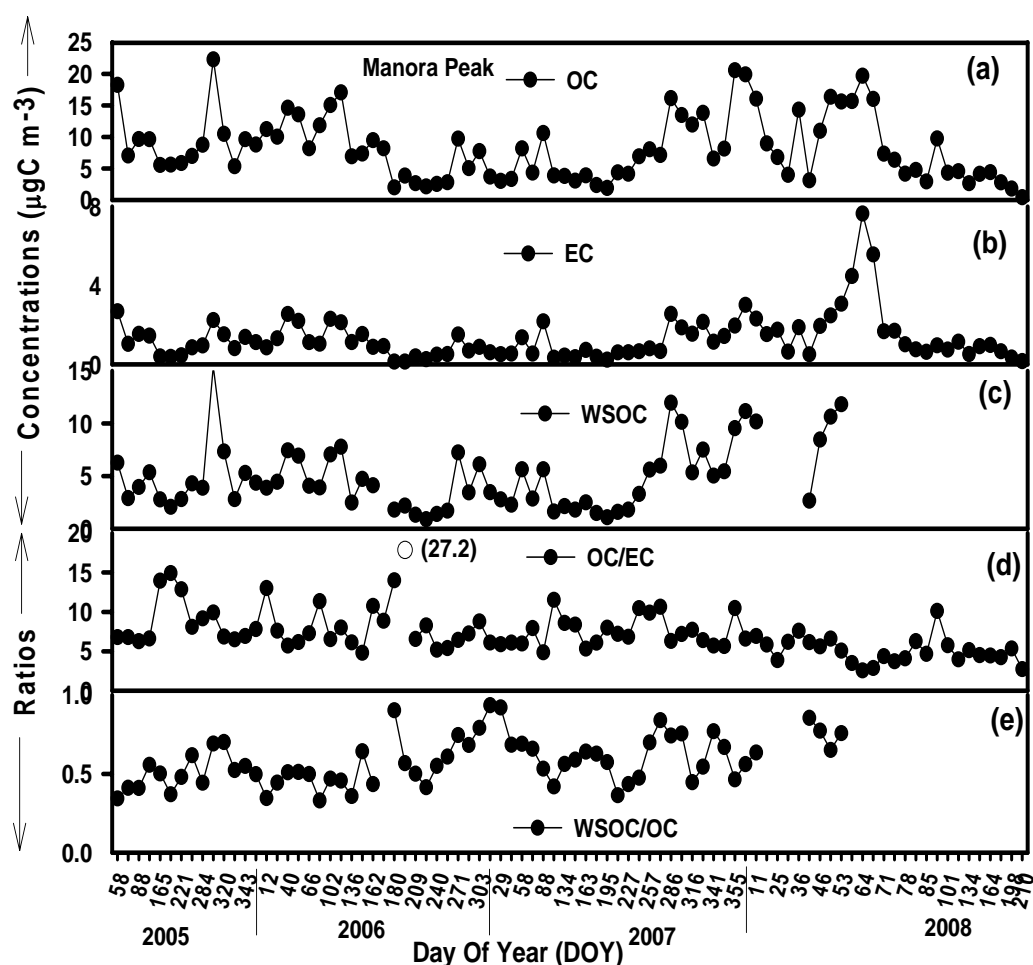


Fig. 5.2: Temporal variability in the concentrations of (a) OC, (b) EC, (c) WSOC, (d) OC/EC and (e) WSOC/OC ratio during the sampling period.

The mass concentration of OC and EC ranged from 0.9 to 12.3 $\mu\text{gC m}^{-3}$ and 0.05 to 2.3 $\mu\text{gC m}^{-3}$, respectively at Mt Abu (Fig. 5.3). The lower OC and EC concentrations, at both high-altitude sites, are typical of monsoon (due to efficient wash-out of aerosols) and summer months (due to lower biomass burning emission) whereas relatively higher values were observed for the samples collected during post-monsoon and winter months (Figs. 5.2 and 5.3).

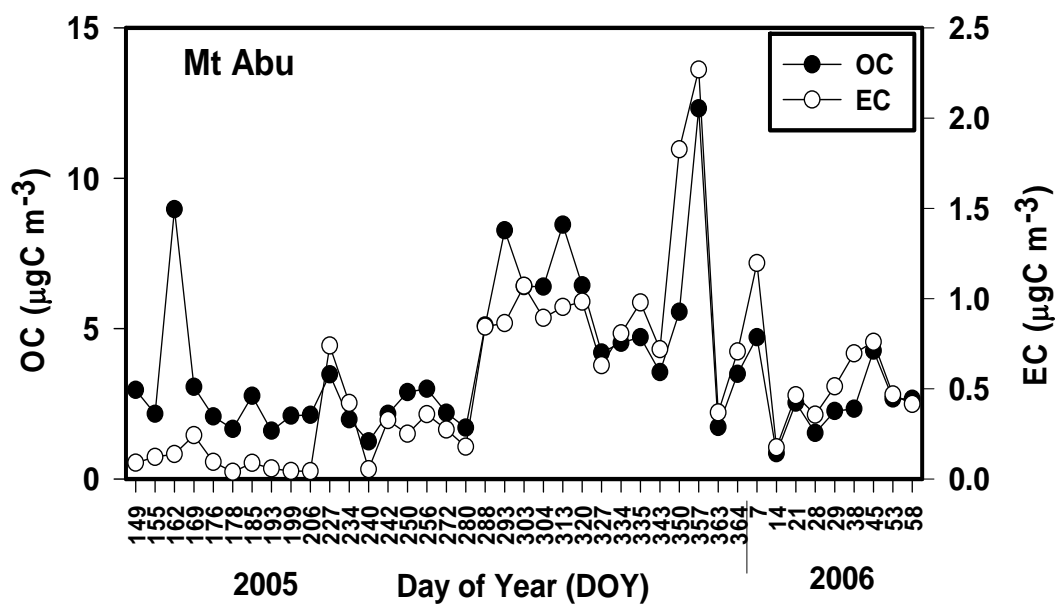


Fig. 5.3: Temporal variability of OC and EC mass concentrations at Mt Abu during May 2005-Feb 2006.

Both, OC and EC mass concentrations are relatively higher at Manora peak compared to those at Mt Abu. The annual average mass concentrations of TSP, OC, EC and OC/EC ratio at Manora Peak and Mt Abu are shown in Figs. 5.4 a, b, c and d respectively. On annual basis, OC ($3.7 \pm 2.4 \mu\text{gC m}^{-3}$, $n = 41$, 1σ) and EC ($0.5 \pm 0.5 \mu\text{gC m}^{-3}$) at Mt Abu account for about 10% and 2% of TSP, respectively. In contrast, annual average concentrations of OC and EC at Manora Peak are ($8.2 \pm 5.2 \mu\text{gC m}^{-3}$, $n = 86$, 1σ) and ($1.3 \pm 1.2 \mu\text{gC m}^{-3}$, $n = 86$, 1σ), respectively which are about 14% and 2% of TSP mass.

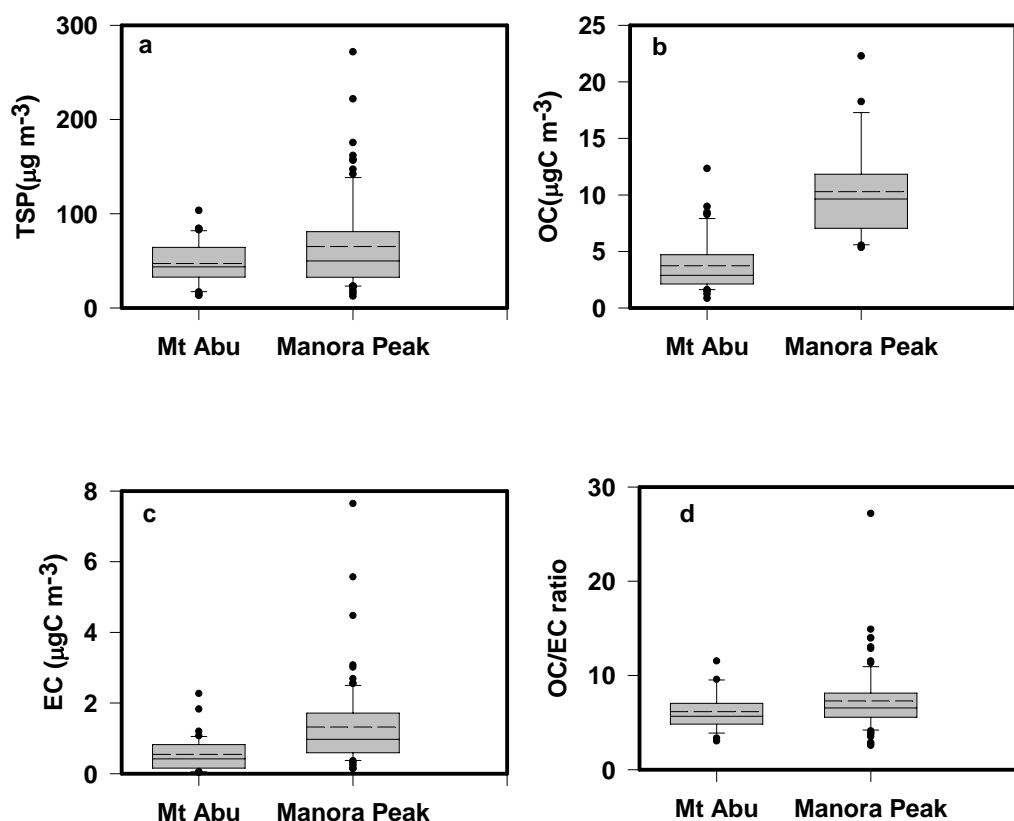


Fig. 5.4: Box plots of TSP, OC, EC and OC/EC ratio at Mt Abu ($n=41$) and Manora Peak ($n=86$). The boundary of the box closest to zero indicates the 25th percentile, a line within the box marks the median, and the boundary of the box farthest from zero indicates the 75th percentile. Whiskers (error bars) above and below the box indicate the 90th and 10th percentiles. The mean is represented by dashed line and points lying outside the whiskers denote outliers.

Total carbonaceous aerosols (TCA), at Manora Peak, constitute ~25-30% of TSP during winter (Dec-March) and post-monsoon (Oct-Nov) and ~15-20% during summer (April-June) and monsoon (July-Sep). A value of 1.8 has been taken for converting the measured OC to organic matter (OM) [Cozic *et al.*, 2008] and TCA is estimated as the sum of OM and EC (i.e. $TCA=1.8*OC + EC$). The conversion factor taken in this study is relatively higher than those used for urban locations [Rengarajan *et al.*, 2007; Turpin and Lim, 2001] because aerosols at high-altitude sites are aged and contain oxygenated organic compounds [Pio *et al.*, 2007; Zhang *et al.*, 2007]. This is further supported by relatively high WSOC/OC ratios (0.55 ± 0.05) at Manora Peak compared to those at urban locations of the IGP [Ram and Sarin, 2010].

The monthly average mass concentrations of TSP, OC, EC, TCA, WSOC, OC/EC and WSOC/OC ratios at Manora Peak are presented in Table 5.1. A clear seasonal variability could be noticed for the mass concentrations of carbonaceous species with relatively high concentrations during post-monsoon and winter months. The mass concentrations of OC and EC are almost a factor of two lower in July 2006 to Sep 2007 compared to those in other sampling years (Fig. 5.2a and b). The lower concentrations of carbonaceous species during these time-periods are attributed to the high rainfall during monsoon season (July-Sep). A similar variability in BC mass concentrations (measured using the Aethalometer) have been recently reported at a nearby high-altitude station, Mukteshwar, in northern India [Hyvärinen *et al.*, 2009]. The average BC mass concentration was $0.8 \mu\text{gC m}^{-3}$ for the sampling period (Sep 2005- Sep 2007) with an average single scattering albedo (SSA) value of 0.81 at Mukteshwar [Hyvärinen *et al.*, 2009].

Table 5.1. Monthly average concentrations (Average $\pm 1\sigma$) of TSP, OC, EC, TCA and WSOC along with the OC/EC and WSOC/OC ratios at Manora Peak during the sampling period (Feb 2005-July 2008).

Month	n	TSP	EC	OC	TCA	WSOC	OC/EC	WSOC/OC
$\mu\text{g m}^{-3}$							ratios	
Jan	6	52 ± 22	1.3 ± 0.8	9.3 ± 4.4	16.3 ± 7.5	5.2 ± 3.3	7.2 ± 2.4	0.57 ± 0.24
Feb	12	76 ± 49	1.9 ± 0.9	10.6 ± 5.5	18.8 ± 9.8	6.1 ± 3.2	5.6 ± 1.5	0.56 ± 0.15
March	14	86 ± 32	1.5 ± 0.5	8.8 ± 3.1	15.4 ± 5.3	3.8 ± 1.0	5.9 ± 3.1	0.46 ± 0.11
April	6	106 ± 59	1.4 ± 0.8	9.1 ± 5.8	15.9 ± 10.0	5.3 ± 2.7	6.5 ± 2.8	0.46 ± 0.06
May	6	87 ± 68	0.8 ± 0.5	4.7 ± 2.0	8.3 ± 3.6	2.7 ± 1.3	5.9 ± 2.0	0.51 ± 0.12
June	8	86 ± 111	0.6 ± 0.2	4.8 ± 2.7	8.4 ± 4.4	2.4 ± 1.1	8.0 ± 2.7	0.58 ± 0.09
July	7	55 ± 68	0.3 ± 0.2	2.9 ± 1.8	5.0 ± 2.9	1.5 ± 0.5	9.7 ± 1.8	0.44 ± 0.10
Aug	5	49 ± 21	0.5 ± 0.2	4.3 ± 2.1	7.4 ± 3.4	1.9 ± 1.0	8.6 ± 1.1	0.44 ± 0.05
Sep	5	52 ± 18	0.9 ± 0.4	6.9 ± 2.6	12.0 ± 4.4	4.8 ± 2.1	6.9 ± 2.6	0.68 ± 0.11
Oct	6	78 ± 47	1.5 ± 0.8	12.2 ± 6.3	21.1 ± 10.9	8.4 ± 4.8	8.1 ± 1.3	0.67 ± 0.13
Nov	5	47 ± 9	1.3 ± 0.6	9.1 ± 4.3	15.8 ± 7.5	5.2 ± 2.2	7.0 ± 2.3	0.61 ± 0.19
Dec	6	48 ± 20	1.7 ± 0.7	12.3 ± 6.3	21.3 ± 10.6	6.7 ± 2.8	7.2 ± 1.3	0.57 ± 0.11

5.2.3 The OC/EC ratio

The OC/EC ratios at Manora Peak varied from 4.0 to 27.2 during the sampling period (Fig. 5.4d; Av: 7.7 ± 3.4 , 1σ). The relatively high OC/EC ratios at Manora Peak indicate the dominance of scattering OC over the absorbing EC. The elevated OC/EC ratios also suggest that either these species have been

derived from a primary emission source which is enriched in OC or there is a significant contribution of secondary organic aerosol (SOA) at Manora Peak. The biomass burning emissions produces relatively high fraction of OC compared to EC and thus, results in an enriched OC/EC ratios [Andreae and Merlet, 2001]. Manora Peak is located at an altitude of ~ 2000 m and emissions from vehicular and industrial activities are lower compared to those at the sampling locations in the Indian Plains. Furthermore, a good linear relationship between OC and EC ($R^2=0.83$, $n=86$, Fig. 5.5a) suggest that emission sources of carbonaceous species have remained the same during the sampling period.

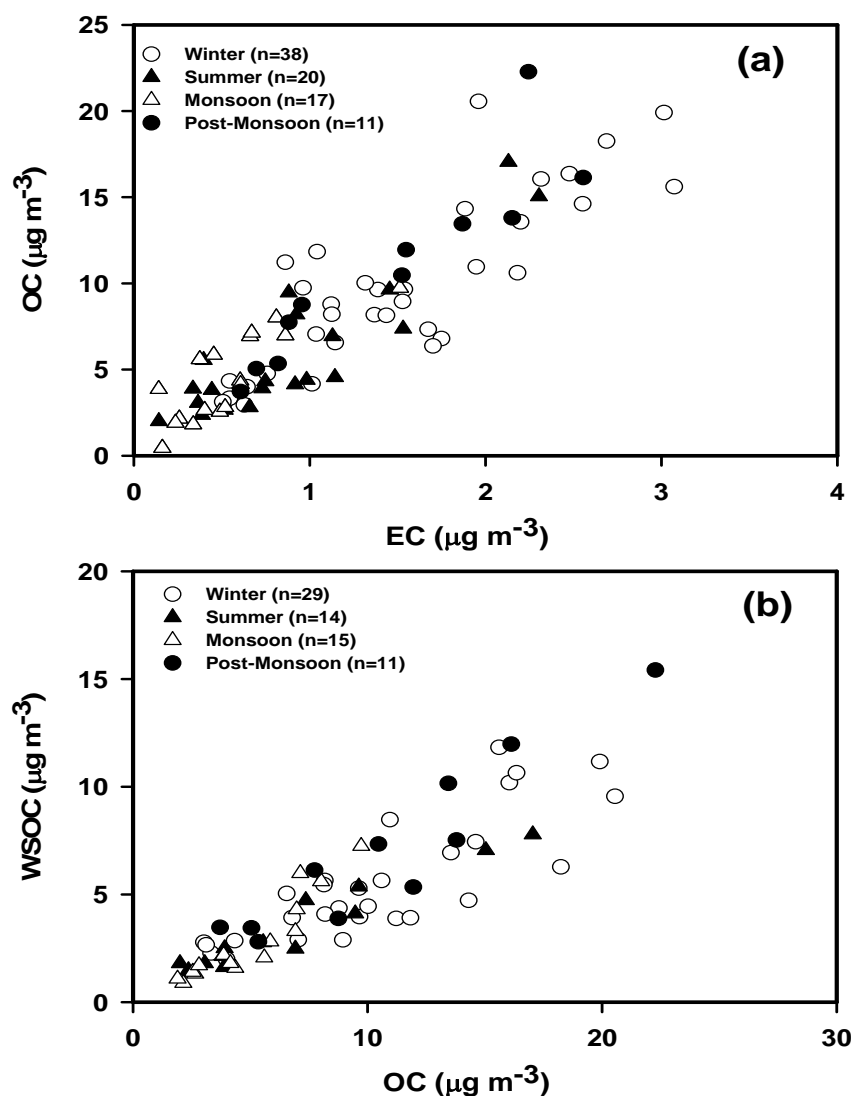


Fig. 5.5: Scatter plots between (a) OC and EC; and (b) WSOC and OC at Manora Peak.

The changes in the emission strength of carbonaceous aerosols and meteorological conditions (e.g. boundary layer height and wind-patterns) have lead to observed variabilities in the abundance patterns of OC and EC at Manora Peak. The majority of carbonaceous aerosols in India originate from the emissions from biomass burning (used for cooking and residential heating purposes) and agricultural-wastes [Gustafsson *et al.*, 2009; Venkataraman *et al.*, 2005]. The emission from the former source increases during wintertime (Dec-Feb) when ambient temperatures are relatively lower. Furthermore, relatively low boundary layer height and poor thermal convection, during wintertime, confine the aerosols. The increase in ambient concentrations of measured carbonaceous species during the wintertime are, thus, attributed to the enhanced biomass burning emissions from residential heating/cooking and a shallower boundary layer height.

5.2.4 Water-soluble organic carbon (WSOC) and WSOC/OC ratio

The WSOC mass concentration at Manora Peak varied from 0.9 to 15.4 $\mu\text{gC m}^{-3}$ during the study period (Feb 2005 to July 2008). The scatter plot between measured WSOC and OC concentration shows a good correlation with a slope of 0.55 ($R^2=0.79$, $n=69$, $p<0.05$, Fig. 5.5b). Although, a significant linear relationship is observed between WSOC and OC for the entire sampling period, some of the data points show different WSOC/OC ratios. For example, the lower WSOC/OC ratios (0.35) in the aerosol samples collected during winter season probably indicate fresh emission from the Indo-Gangetic Plain (IGP) and less chemical processing during transport. This observation is also corroborated by the lower WSOC/OC ratios observed at urban locations (range: 0.32 to 0.40) in the IGP during wintertime [Ram and Sarin, 2010]. Furthermore, a good correlation between WSOC and SO_4^{2-} during wintertime ($R^2=0.57$, $n=29$), compared to that during summer months ($R^2=0.25$, $n=14$), suggest their anthropogenic emissions and transport from the Valley. However, the average WSOC/OC ratio observed at Manora Peak (0.55 ± 0.15 ; median = 0.53) is lower than that reported at the Himalayan Nepal Climate Observatory-Pyramid (0.65 ± 0.15), situated at an altitude of $\sim 5079\text{m amsl}$ [Decesari *et al.*, 2010]. Thus, an increasing trend in the WSOC/OC ratio is observed as we move from sampling sites in the IGP toward

the high-altitude sites. It has been suggested that WSOC/OC ratios can be used as an indicator for the secondary organic aerosol (SOA) formation [Kondo *et al.*, 2007; Weber *et al.*, 2007]. Therefore, the increasing trend in the WSOC/OC ratios suggest the aging, chemically processed aerosols and/or possible contribution from secondary organic aerosols [Zhang *et al.*, 2007].

However, a recent study have reported that a significant fraction of freshly formed SOAs in a semi-arid region can be water-insoluble in nature [Favez *et al.*, 2008b]. The water-insoluble OC (WIOC; defined as the difference between OC and WSOC) could also be derived from primary emissions such as biomass burning and vehicular exhausts [Favez *et al.*, 2008a]. The WIOC concentration shows a linear relationship with EC concentrations ($R^2=0.48$, $n=69$) and the slope (2.6) is similar to WIOC/EC ratios in the IGP for the primary emission sources [Ram and Sarin, 2010]. The median WIOC/EC ratios at Manora Peak during four seasons are: 3.0 (winter), 3.8 (summer), 3.9 (monsoon) and 2.6 (post-monsoon). The resemblance of the WIOC/EC ratios at Manora Peak to those in the IGP further substantiates the advective transport of primary emitted aerosols from Indian Plains.

5.2.5 Estimation of secondary organic carbon (SOC)

Secondary organic aerosols are produced in the atmosphere via various chemical and physical transformation processes involving the oxidation of volatile organic reactive gases (VORGs) with reactive species like; ozone, hydroxyl and NO_x radicals followed by coagulation/condensation onto the pre-existing aerosol particles and ultimately becoming a part of atmospheric aerosols. The direct measurement of SOAs and secondary organic carbon (SOC), is not possible as they are being derived from the various physical and chemical transformation processes. Rather, they are estimated either by accounting the primary organic carbon (POC) using the EC tracer method and then subtracting it from the total organic carbon (OC) measured in aerosol samples [Castro *et al.*, 1999; Turpin and Huntzicker, 1995] or by summing up the concentrations of all such oxidation products [Schauer *et al.*, 1996].

The major uncertainty in the estimation of SOC by the EC tracer method arises due to underlying assumption and assessment of $(OC/EC)_{\min}$ ratio. The estimation of SOC is based on the assumption that the samples with minimum OC/EC ratio have negligible amount of SOC; and the composition of primary carbonaceous aerosols, their sources are spatially and temporally constant. However, the latter assumption is not strictly valid as the source composition of OC and EC is highly variable. The slope of the regression line between OC and EC is usually used to assess the minimum OC/EC ratio. However, the use of slope of regression line may provide under-estimation of SOC because of the use of higher OC/EC ratio resulting from already formed secondary organic aerosols. We have used the minimum OC/EC ratio from different seasons for the data set as a representative value for those particular seasons in calculation of SOC.

The estimated secondary organic carbon (SOC), using the EC tracer method, exhibit a seasonal pattern at both the high-altitude sampling sites. The average concentrations of SOC at Manora Peak during winter (Dec-March) and summer 2005 are $1.6 \mu\text{g m}^{-3}$ and $4.3 \mu\text{g m}^{-3}$, accounting for 14% and 52% of total OC, respectively, while that in winter and summer 2006 are $2.7 \mu\text{g m}^{-3}$ and $3.2 \mu\text{g m}^{-3}$; contributing 26% and 36% of total OC, respectively. For the entire sampling period, average SOC concentrations contribute to ~30, 48, 37 and 20% (of OC) during winter, summer, monsoon and post-monsoon seasons, respectively. The average SOC mass concentrations at Mt Abu during post-monsoon (Oct-Nov) and winter are $1.1 \mu\text{g m}^{-3}$ and $1.3 \mu\text{g m}^{-3}$, accounting 23% and 35% of OC, respectively. Furthermore, the average SOC concentrations are higher at Manora Peak compared to that at Mt Abu for the sample collected during the same time-period of years 2005-2006. The SOC concentrations show seasonal variation at Manora Peak with maximum observed during summer (April-June). *Castro et al.* [1999] have reported that SOC contribute to minimum of about 17% in winter and maximum 78% during the summer in Portugal based on the minimum OC/EC ratio method. A similar study by *Cabada et al.* [2004] had reported that nearly 35% of the OC concentration in western Pennsylvania, during summer of July 2001, is estimated to be secondary in origin. Likewise, *Na et al.* [2004] have also suggested that the contribution of SOC to the total organic carbon tends to be

higher during the season with enhanced photochemical activity (63%) than that during the time of lower photochemical activity (44%). More recently, study by *Gelencser et al.* [2007] suggests that SOA from non-fossil fuel sources becomes predominant in summer and contribute about 63-76 % of the total organic carbon.

5.2.6 Inter-comparison of mass concentrations of OC and EC with other high-altitude sites

The mass concentrations of EC and OC at Manora Peak are similar to the concentrations at other high-altitude sites in the world. For example, *Puxbaum et al.* [2000] have reported that average EC and OC mass concentrations at Nylsvley Natural reserve (altitude: 1100 m) were 0.85 and 14.1 $\mu\text{gC m}^{-3}$ during May 1997. *Hitzenberger et al.* [1999] have reported values of 3.8 and 16.2 $\mu\text{gC m}^{-3}$ for EC and OC at a European background site (Mt Sonnblick, altitude: 3100 m Austria). *Han et al.* [2008] have found a similar EC and OC concentrations (3.1 and 19.9 $\mu\text{gC m}^{-3}$ respectively) at a rural-high mountain site (Daihai) in northern China. However, EC concentrations at Manora Peak are relatively higher compared to the average BC mass concentrations of 0.15 and 0.45 $\mu\text{gC m}^{-3}$ at Mt Krvavec [*Bizjak et al.*, 1999] and 0.22 $\mu\text{gC m}^{-3}$ at Mt Mitchell [*Bahrmann and Saxena*, 1998]. *Cozic et al.* [2008] have reported that maximum EC and OC concentrations at Jungfrauoch (altitude: 3580 m) were 0.5 and 2.2 $\mu\text{gC m}^{-3}$, respectively. In a recent study, *Cao et al.* [2009] have reported an average values of 0.055 and 0.48 $\mu\text{gC m}^{-3}$, respectively for EC and OC at Muztagh Ata, a remote mountain in China for the sampling period Dec 2003-Feb 2005. However, the mass concentrations of EC and OC at Manora Peak are an order of magnitude lower compared to those at sampling sites in the Indo-Gangetic Plain [*Ram and Sarin*, 2010].

5.3 Summary

The major conclusions drawn from this chapter are listed below:

- The study suggests relatively high TSP mass at the two high-altitude sites and is associated with high mass fraction of mineral dust throughout the

sampling period. Total carbonaceous aerosols (TCA) contribute ~15% and 25% of TSP at Mt Abu and Manora Peak, respectively.

- The mass concentrations of carbonaceous species are three-to-four times higher during wintertime (Dec to Mar). On an annual basis, absorbing EC mass contributes ~2% of TSP mass at high-altitude sites.
- The relatively high OC/EC ratios, 8.4 and 6.1 at Manora Peak and Mt Abu respectively, compared to those for urban areas (2.0-3.0), are attributed to the dominance of organic carbon (associated with poor practices of burning of wood-fuel and agricultural waste and secondary organic carbon). This is also reflected in the seasonal variability of secondary organic carbon concentrations, estimated based on minimum OC/EC ratio method, with maximum in summer and contributing as much as 50% of OC.
- The WSOC/OC ratios center around 0.55 ± 0.15 at Manora Peak. The WSOC/OC ratios are much higher than those over urban and rural sites in the Indo-Gangetic Plain.
- The higher WSOC/OC ratios suggest a significant contribution from the secondary organic aerosols (SOA) produced during the transport and aging of aerosols.

AEROSOL ABSORPTION PROPERTIES OVER INDIAN REGIONS

6.1 Introduction

Black carbon (BC), produced during incomplete fossil-fuel and biomass combustion processes, is one of the major absorbing particulate species in the atmosphere and is being considered as a driver of the global warming [*Andreae and Gelencser, 2006; Jacobson, 2001*]. The absorption and scattering properties of aerosols are the key parameters to assess direct aerosol radiative forcing and their climatic impact on a regional to global scale [*Menon et al., 2002; Pant et al., 2006; Venkataraman et al., 2005*]. The absorption coefficient (b_{abs}) is either measured using photoacoustic instruments [*Arnott et al., 1999; Barnard et al., 2005*] or more commonly used online filter-based absorption methods [*Bond and Bergstrom, 2006; Sharma et al., 2002; Weingartner et al., 2003; Yan et al., 2008; Yang et al., 2009*]; whereas scattering coefficient (b_{scat}) is mainly inferred from Nephelometer based measurements [*Yan et al., 2008; Yang et al., 2009*]. Nevertheless, the assessment of radiative forcing is associated with large uncertainty arising due to the lack of reliable measurements of these optical parameters [*Schmid et al., 2006*]. The filter-based online absorption measurements are affected by the shadowing and multiple scattering effects [*Bond and Bergstrom, 2006; Schmid et al., 2006; Weingartner et al., 2003; Yan et al., 2008; Yang et al., 2009*]. Also, relevant information on the mixing state of aerosols is essential as the internal mixing leads to further increase in absorption signal [*Jacobson, 2001; Martins et al., 1998; Schwarz et al., 2008*].

The measurement of BC mass concentration via optical methods is relatively convenient and rapid but requires knowledge of ‘site-specific’ mass absorption efficiency (MAE or σ_{abs}). A wide range of values for σ_{abs} (2 to 25 m^2g^{-1}) have been reported in the literature, derived based on independent and simultaneous measurements of EC concentration (by thermal method) and absorption coefficient by optical methods [Bond and Bergstrom, 2006; Lioussé et al., 1993; Sharma et al., 2002]. The variability in MAE has been interpreted in terms of source regions, analytical measurement protocols, chemical and optical properties of aerosols at a sampling site [Martins et al., 1998; Schwarz et al., 2008; Sharma et al., 2002]. Furthermore, aging and atmospheric chemical processing can lead to an internal mixing and, thus, increases the MAE through enhancement in absorption signal for the same amount of BC [Schmid et al., 2006; Schwarz et al., 2008]. The use of site-specific σ_{abs} for the determination of BC mass concentration by optical methods has been suggested [Sharma et al., 2002]. However, it is common practise to use a constant value of σ_{abs} at a given wavelength. For example, the Aethalometer uses a value of 16.6 m^2g^{-1} (at 880 nm) while Particle Soot Absorption Photometer (PSAP) uses a value of 10 m^2g^{-1} to convert measured absorption into BC mass concentration [Sharma et al., 2002]. A recent review by Bond and Bergstrom [2006] has suggested a value of $7.5 \pm 1.2 \text{ m}^2\text{g}^{-1}$ at 550 nm for σ_{abs} for uncoated soot particles.

Carbonaceous aerosols in south-Asian regions, originating from a variety of anthropogenic emission sources, are gaining considerable importance because of their potential impact on regional climate [Menon et al., 2002; Pant et al., 2006; Venkataraman et al., 2005]. In this context, systematic measurements of relevant optical parameters (BC mass, b_{abs} , b_{scat} and site-specific σ_{abs}) from Indian regions are essential. In this chapter, the measurement of these parameters at 678nm, made on a thermo-optical EC-OC analyzer, are reported from northern India. The temporal and spatial variability in absorption coefficient (b_{abs}) and mass absorption efficiency (σ_{abs}) from urban, rural and high-altitude sites are discussed in terms of the varying

emission sources (vehicular exhaust, biomass burning and fossil-fuel emissions) and probable mixing states of aerosols.

6.2 Results and Discussion

6.2.1 Optical -attenuation and surface EC concentration

The measured optical-attenuation (ATN) and surface EC concentrations (EC_s ; $\mu\text{gC cm}^{-2}$) at Manora Peak varied from 8 to 134 and 0.3 to 9.3 $\mu\text{gC cm}^{-2}$ over the entire sampling period (Feb 2005-July 2008); whereas the two parameters varied from 15 to 95 and 0.5 to 3.5 $\mu\text{gC cm}^{-2}$, respectively for the daily samples collected during wintertime (Dec 2004). The measured ATN and EC_s concentration exhibit a significant linear relationship at Manora Peak ($R^2= 0.96$ and 0.86 respectively in Figs. 6.1a, b), indicating the validity of Beer-Lambert's law and EC as a principal absorbing component in aerosols. However, this linearity does not extend for EC_s exceeding 4.5 $\mu\text{gC cm}^{-2}$. Recently, *Junker et al.* [2006] have reported that ATN measured by Aethalometer (range: 22 to 178) varied linearly with BC surface mass loading (in unit of $\mu\text{gC cm}^{-2}$). In a related study, it has been shown that about 90% of data fall in the linear range for $b_{\text{abs}} < 50 \text{ Mm}^{-1}$ ($1 \text{ Mm}^{-1} = 10^{-6} \text{ m}^{-1}$) and $EC < 5 \mu\text{gC m}^{-3}$; but the relationship becomes non-linear for higher EC concentrations [*Watson and Chow, 2002*]. In this study, the maximum ATN value of 134 (Fig. 6.1b) and corresponding b_{abs} values (33.6 Mm^{-1}) at Manora Peak are lower compared to those reported in the literature [*Junker et al., 2006; Watson and Chow, 2002*].

The linear regression analysis between ATN and EC_s concentration at Manora Peak yields a slope of $22.4 \text{ m}^2\text{g}^{-1}$ and an intercept of 6.6 ($R^2=0.86$, for $n=39$, excluding 7 data points with $EC_s > 4.5 \mu\text{gC cm}^{-2}$, Fig. 6.1b). During a field campaign conducted in Taipei (Taiwan), *Chou et al.* [2003] had reported a value of $23.7 \text{ m}^2\text{g}^{-1}$ for the slope and 12.0 for the intercept with a correlation coefficient (R^2) of 0.69. Based on the absorption measurements from PSAP and Aethalometer, and thermal EC concentration using Sunset Lab EC-OC analyser, *Snyder and Schauer* [2007]

have reported σ_{ATN} values of $23.7 \pm 0.4 \text{ m}^2\text{g}^{-1}$ at 660 nm (for the Aethalometer) and $18.3 \pm 0.5 \text{ m}^2\text{g}^{-1}$ at 565 nm (for PSAP). The slope of the regression lines (Fig. 6.1) provides a valuable parameter -attenuation cross-section (σ_{ATN})- which in turn has been used to infer 'site-specific' mass absorption efficiency of EC (σ_{abs}).

It is noteworthy that intercepts in the linear regression plots for the two high-altitude sites, Manora Peak (Figs. 6.1a, b) and Mt Abu (Figs. 6.1c, d), are very small ($\sim 1/10^{\text{th}}$ of the average ATN) and can be neglected. The near-zero intercept for the data set from these high-altitude sampling sites suggest EC as principal absorbing component in aerosols. In contrast, intercepts of regression plots for two urban locations, Allahabad and Hisar (Figs. 6.1e, f), are 60 and 50 (compared to average ATN: 140 and 130, respectively); statistically very different from zero. The relatively high intercept in linear regression analyses observed in case of data from urban sites could be attributed to high ATN values and high EC_s concentration. We suggest that sampling time can be cut down for collection of aerosol samples from the highly polluted urban sites. The non-zero intercept could also be attributed to the presence of absorbing species other than EC. Mineral dust is another absorbing species present in aerosols, however, absorption due to mineral dust is very low compared to that of BC [Bodhaine, 1995]. The aerosol chemical composition at an urban location, Hisar, indicates equal dominance of both mineral dust and total carbonaceous aerosols ($\sim 40\%$ of total suspended particulate (TSP) matter) [Rengarajan *et al.*, 2007]. Assuming that contribution of mineral dust to TSP is $\sim 40\%$ and externally mixed with BC; and by using a value of $0.009 \text{ m}^2\text{g}^{-1}$ for mass absorption efficiency of dust [Clarke *et al.*, 2004], its contribution to total absorption is no more than 2% at Hisar. However, a recent study has documented a value of $0.03 \text{ m}^2\text{g}^{-1}$ for mass absorption efficiency of dust [Yang *et al.*, 2009] which indicate that absorption from dust can be $\sim 7\%$ of total absorption at Hisar.

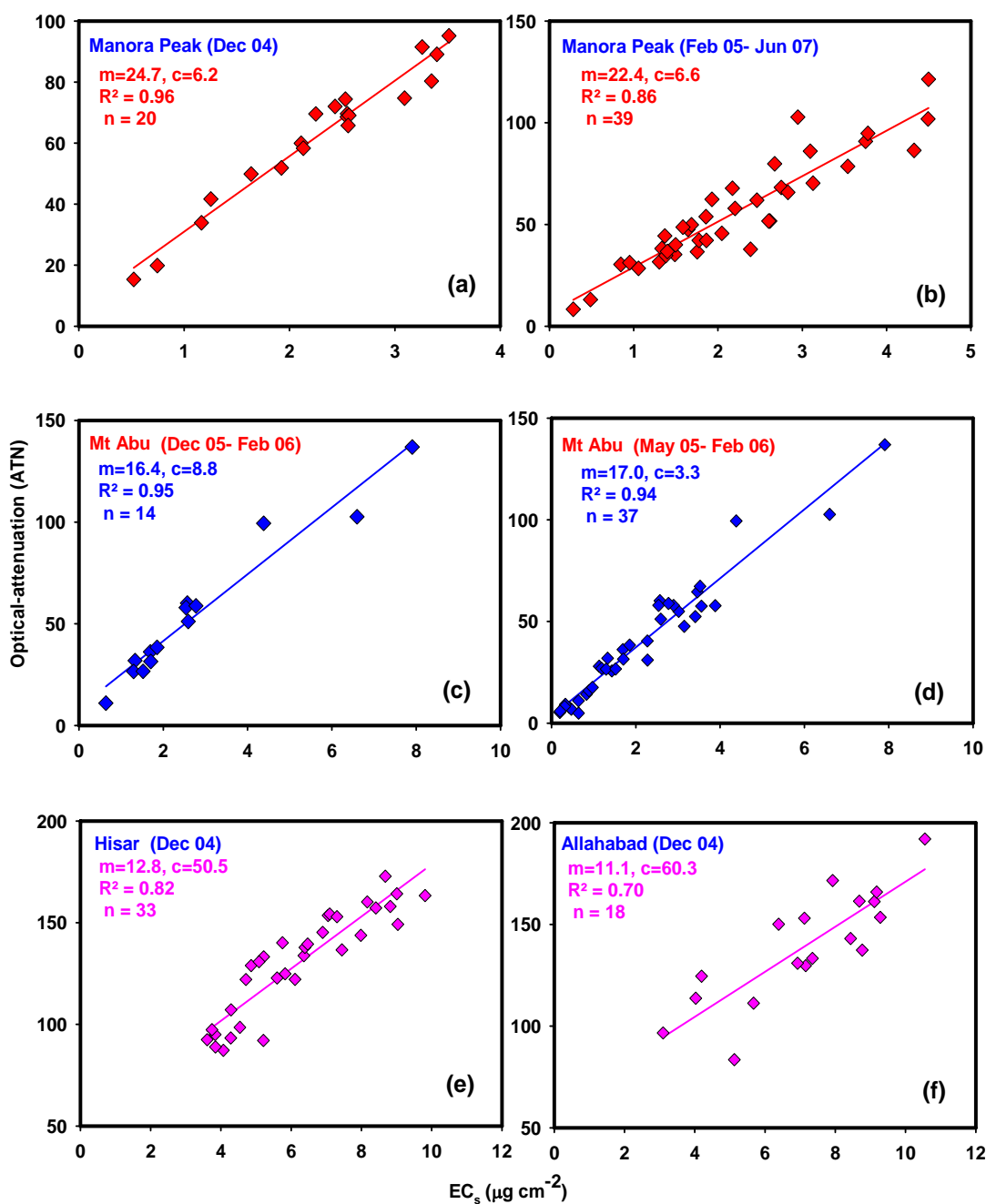


Fig. 6.1: Linear relationships between optical-attenuation (ATN) and surface EC concentration (EC_s , in unit of $\mu\text{gC cm}^{-2}$), indicating the validity of Beer-Lambert's law: (a) and (c) data from high-altitude sites during the wintertime; (b) and (d) represent extended sampling at two high-altitude locations; (e) and (f) represent data for the two urban sites in India. The regression parameters m and c represent slope and intercept of the best-fit line, respectively.

The lower absorption characteristics of dust is further supported by relatively non-absorbing nature of Asian dust observed during the ACE-Asia campaign (<http://www.igac.noaa.gov/newsletter>; Issue No. 28). Also, Carrico *et al.* [2003b] have reported a mean value of 0.94 ± 0.03 for single scattering albedo (SSA) for polluted dust air mass during the ACE-Asia experiment. Organic carbon (OC) mainly scatters the radiation but freshly emitted OC, particularly from biomass burning emissions having significant amount of brown carbon and humic-like substances (HULIS), can contribute to total aerosol absorption at a lower wavelength (ultraviolet) region of the spectrum [Andreae and Gelencser, 2006; Dinar *et al.*, 2008; Hoffer *et al.*, 2006; Kirchstetter *et al.*, 2004; Yang *et al.*, 2009]. The biomass burning emissions from wood and agricultural crop-waste dominate the atmospheric loading of carbonaceous species in India [Ram *et al.*, 2008; Venkataraman *et al.*, 2005]; it is, thus, suggested that freshly emitted OC could be a potential absorbing component in aerosols at the two urban sites.

6.2.2 Inter-comparison of attenuation coefficient derived by the EC-OC analyser ($b_{\text{ATN-ECOC}}$) and the Aethalometer ($b_{\text{ATN-Aeth}}$)

The BC mass concentrations at 880 nm, using Aethalometer based measurements during Dec 2004 campaign [Pant *et al.*, 2006], have been multiplied by the attenuation cross-section ($16.6 \text{ m}^2\text{g}^{-1}$) to obtain $b_{\text{ATN-Aeth}}$ values and are presented in Table 6.1. Although absorption coefficient (b_{abs}) has been used throughout this paper, attenuation coefficient (b_{ATN}) is more suitable parameter (independent of C and R(ATN)) for inter-comparison of absorption measurements by the two analytical instruments. The attenuation coefficient ($b_{\text{ATN-ECOC}}$) assessed by the EC-OC analyser at 678 nm has been corrected to 880 nm (using a value of unity for wavelength dependence of Ångström exponent) in order to match $b_{\text{ATN-Aeth}}$ at 880 nm. The wavelength dependence of b_{ATN} is normally assumed to be a power law where the exponent depends on type of absorbing species ($b_{\text{ATN}} \propto \lambda^{-\alpha}$ where α is the Ångström exponent). The values of the α range from 1 to 3 for wavelengths between 300 nm to 1000 nm but a value of unity have been accepted for Ångström exponent

due to light absorbing carbon [Bergstrom *et al.*, 2004]. The measurement of attenuation coefficient (b_{ATN}) by two independent analytical methods yields a good correlation ($R^2=0.82$, $n=24$, Fig. 6.2) with a slope of unity for samples collected at high-altitude site, Manora Peak; attesting the validity of our approach for b_{ATN} determination.

Table 6.1: Attenuation coefficient (b_{ATN}): Inter-comparison of Aethalometer and EC-OC analyzer.

Sample ID	Sampling dates	BC [#] $\mu\text{gC m}^{-3}$	EC $\mu\text{gC m}^{-3}$	$b_{\text{ATN-Aeth}}^{\text{@}}$ Mm^{-1}	$b_{\text{ATN-ECOC}}^{\text{\$}}$ Mm^{-1}
MNP-8	11-Dec-04	0.96	0.59	15.9	13.9
MNP-9	13-Dec-04	1.42	1.27	23.6	27.4
MNP-12	17-Dec-04	1.61	1.01	26.7	21.0
MNP-13	19-Dec-04	1.84	1.19	30.5	24.1
MNP-14	21-Dec-04	1.70	1.40	28.2	25.9
MNP-16	23-Dec-04	1.27	0.74	21.0	15.3
MNP-17	25-Dec-04	1.27	0.99	21.0	18.4
MNP-18	27-Dec-04	1.70	1.28	28.2	25.4
MNP-19	29-Dec-04	0.58	0.34	9.7	7.0
MNP-20	31-Dec-04	0.54	0.40	8.9	9.1
MNP-46	11-Jun-06	0.84	0.88	13.9	13.5
MNP-47	14-Jun-06	0.81	0.92	13.5	16.9
MNP-51	28-Jul-06	0.33	0.40	5.5	8.9
MNP-52	16-Aug-06	0.26	0.26	4.3	5.4
MNP-54	14-Sep-06	0.94	0.52	15.7	12.3
MNP-55	28-Sep-06	1.24	1.51	20.5	26.4
MNP-57	30-Oct-06	1.57	0.88	26.1	23.7
MNP-68	12-Jun-07	1.16	0.73	19.2	13.1
MNP-69	23-Jun-07	0.52	0.39	8.6	7.8
MNP-71	27-Jul-07	0.54	0.61	9.0	10.0
MNP-72	15-Aug-07	0.58	0.61	9.6	8.8
MNP-73	26-Aug-07	0.74	0.66	12.4	13.1
MNP-75	25-Sep-07	0.96	0.67	15.9	16.8
MNP-78	12-Nov-07	1.08	1.55	18.0	18.6

[#] Ambient BC mass concentration for Dec 2004 [Pant *et al.*, 2006] and for the years 2006-2008; [@]Aethalometer based attenuation coefficient ($b_{\text{ATN_Aeth}}$) derived from BC concentration and attenuation cross-section ($16.6 \text{ m}^2\text{g}^{-1}$) [Pant *et al.*, 2006]; ^{\\$} This study, Attenuation coefficient measured at 678 nm ($b_{\text{ATN_EC-OC}}$) is been corrected to match Aethalometer data (880 nm) assuming inverse dependence of wavelength ($b_{\text{ATN}} \propto \lambda^{-1}$).

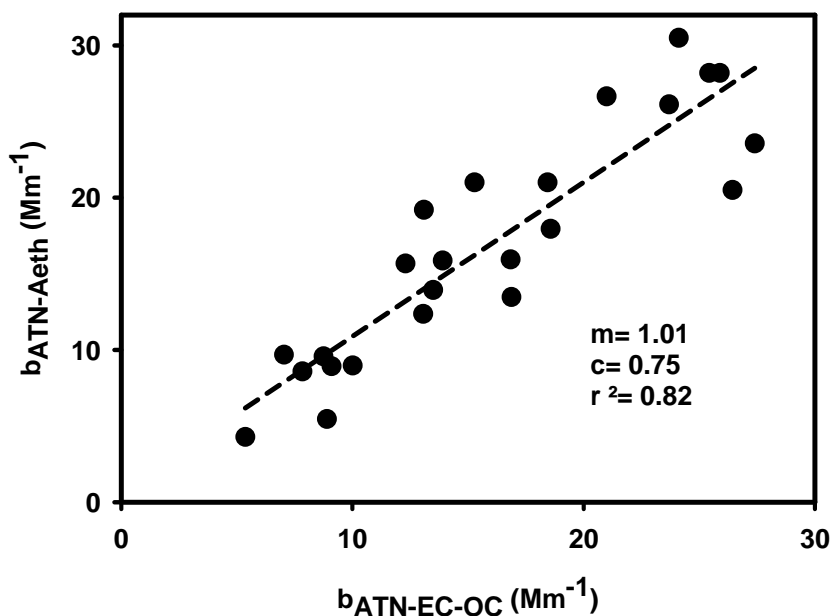


Fig. 6.2: Inter-comparison of attenuation coefficient derived from the two different instrumental techniques (EC-OC analyser and Aethalometer) indicate good agreement. The regression parameters m and c represent slope and intercept of the best-fit line, respectively.

6.2.3 Spatial and temporal variation of absorption coefficient (b_{abs})

The measured ATN at 678 nm has been used to calculate absorption coefficient (b_{abs}) for different sampling sites in northern-India (Table 6.2).

Table 6.2. Absorption coefficient (b_{abs}) and site-specific mass absorption efficiency (σ_{abs}) of EC at different geographical locations in northern India.

Sampling Time	Sites	n	OC/EC	EC $\mu\text{gC m}^{-3}$	b_{abs} Mm^{-1}	σ_{abs} m^2g^{-1}
Jan 07-Mar 08	Kanpur	66	7.4 ± 3.5	3.8 ± 2.3	42.7 ± 17.9	12.7 ± 3.8
Feb 05 - July 08	Manora Peak	86	7.3 ± 3.4	1.3 ± 1.2	13.7 ± 7.3	12.3 ± 2.9
Dec-04	Manora Peak	20	6.0 ± 1.9	0.9 ± 0.3	12.9 ± 4.6	14.5 ± 1.1
May 05-Feb 06	Mt Abu	41	6.6 ± 2.1	0.5 ± 0.5	5.8 ± 4.3	9.8 ± 2.1
Dec 05 - Feb 06	Mt Abu	14	6.1 ± 2.0	0.8 ± 0.6	8.0 ± 5.5	10.4 ± 1.4
Dec-04	Jaduguda	7	3.1 ± 0.6	11.6 ± 2.0	69.7 ± 19.6	6.1 ± 2.0
Dec-04	Hisar	40	8.5 ± 2.2	3.8 ± 1.4	39.9 ± 9.1	11.3 ± 2.2
Dec-04	Allahabad	19	8.1 ± 1.7	6.2 ± 2.0	66.1 ± 17.2	11.1 ± 2.6

The b_{abs} shows a large spatial and temporal variability, varying by an order of magnitude, for the entire sampling period and is related to the difference in chemical and optical characteristics of carbonaceous species derived from different emission sources (Table 6.2). The b_{abs} values at Mt Abu are lower compared to that at Manora Peak. Among urban sites, b_{abs} at Hisar ($39.9 \pm 9.1 \text{ Mm}^{-1}$, $n=41$) is lower compared to Allahabad ($66.1 \pm 17.2 \text{ Mm}^{-1}$, $n=19$) during wintertime (Dec 2004) and the highest was observed for rural sampling site, Jaduguda ($69.7 \pm 19.6 \text{ Mm}^{-1}$, $n=7$). The average values of the absorption coefficient, mass absorption efficiency and EC mass concentrations for the different sampling sites in India are presented in Fig 6.3.

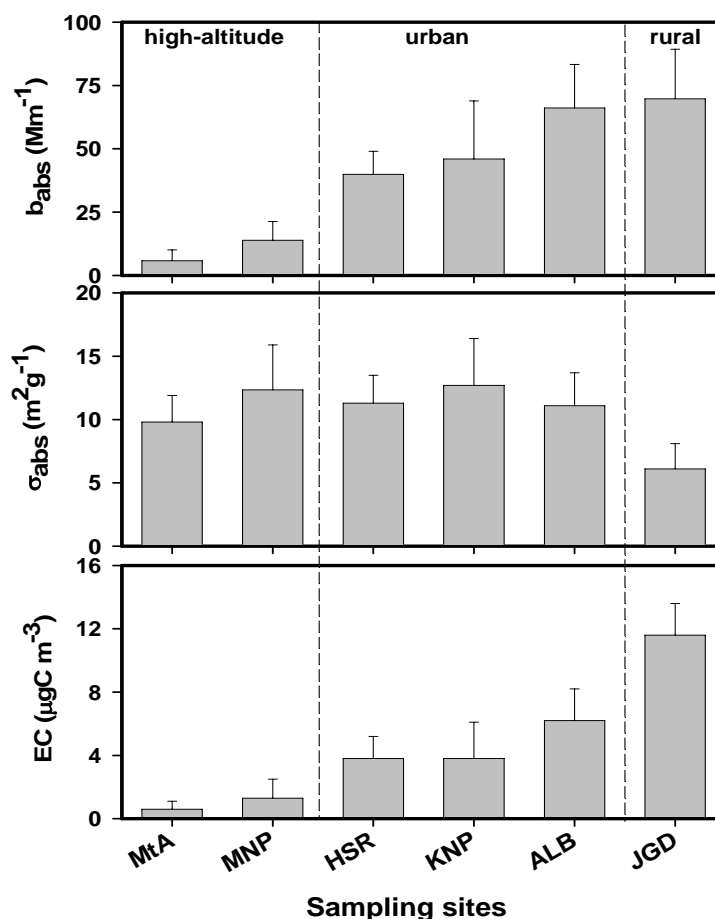


Fig. 6.3: Spatial variability of the absorption coefficient, mass absorption efficiency and EC mass concentrations for the different sampling sites, representing high-altitude (Mt A: Mt Abu and MNP: Manora Peak), urban (HSR: Hisar; KNP: Kanpur and ALB: Allahabad) and rural (JGD: Jaduguda) sites in India.

The EC concentration at Jaduguda is $11.6 \pm 2.0 \mu\text{gC m}^{-3}$, about a factor of two higher than that at Allahabad ($6.2 \pm 2.0 \mu\text{gC m}^{-3}$); whereas OC/EC ratios are higher at Allahabad compared to that at Jaduguda (Table 6.2). These results indicate that emission sources, chemical and optical properties of carbonaceous aerosols are quite different at Allahabad and Jaduguda. Earlier studies have also documented the dominance of coal-based emissions in the eastern part of India [Prasad *et al.*, 2006; Reddy and Venkataraman, 2002]. In fact, OC/EC ratios at Jaduguda are lowest among all sampling locations in northern India (Table 6.2). Thus, relatively low σ_{abs} values ($6.1 \pm 2.1 \text{ m}^2\text{g}^{-1}$) and high EC concentration at Jaduguda is, thus, attributed to coal-based emissions.

The b_{abs} at Manora Peak show a large temporal variability, ranging from 0.9 to 33.2 Mm^{-1} (Fig 6.4a); with lower values occurring in summer (Apr-June) and monsoon season (July-Aug) due to relatively low EC content in aerosol (Fig. 6.4b). The predominantly higher b_{abs} values during post-monsoon (Sep-Nov) and wintertime (Dec-March) are attributed to enhanced biomass burning activities resulting in higher EC concentration [Ram *et al.*, 2008]. The b_{abs} at Manora Peak during wintertime (Dec 2004) varies from 4.4 to 20.9 Mm^{-1} with an average value of $12.9 \pm 4.6 \text{ Mm}^{-1}$ ($n=20$, 1σ), a factor of three lower than the reported value of $44.6 \pm 26.4 \text{ Mm}^{-1}$ ($n=9$) during Dec 2003 from Taipei by Chou *et al.* [2005]. Although, b_{abs} values show a large variability during Feb 05- July 08 sampling period (range: 0.9- 33.2 Mm^{-1}), average b_{abs} ($12.2 \pm 6.6 \text{ Mm}^{-1}$, $n=86$) is similar to that obtained in Dec 2004 (Table 6.2).

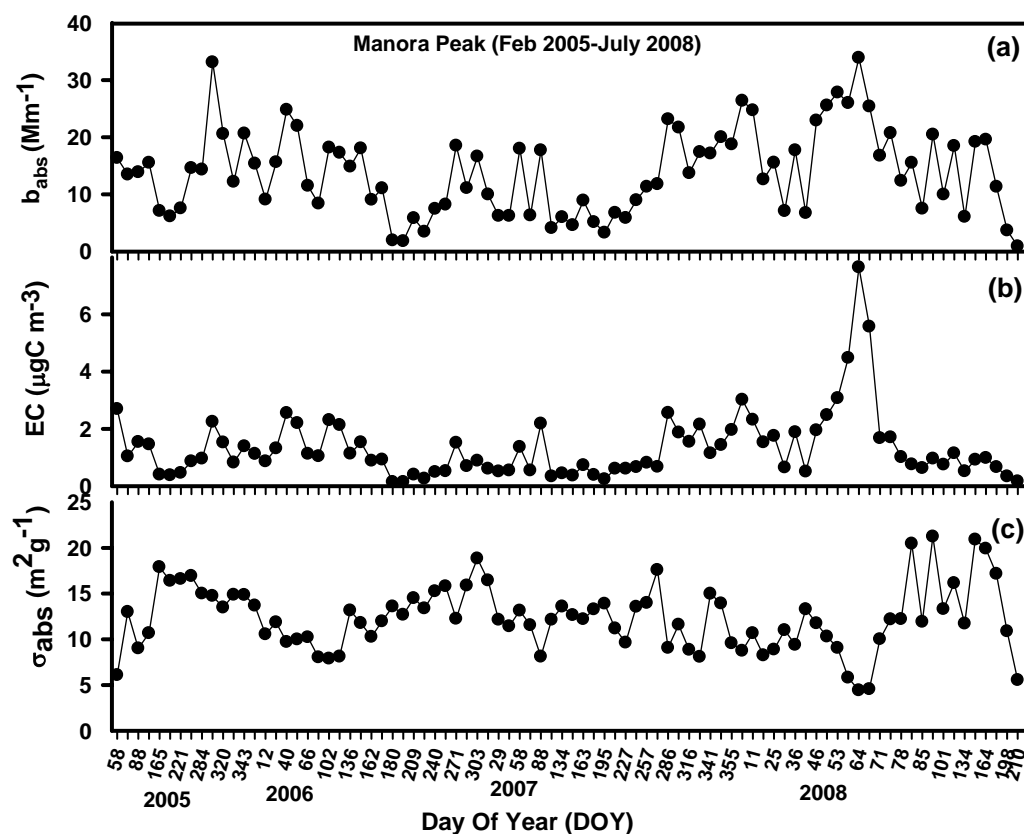


Fig. 6.4: The temporal variability of (a) absorption coefficient (b_{abs}), (b) EC mass concentration and (c) mass absorption efficiency (σ_{abs}) at Manora Peak.

The optical parameters vary on temporal as well as on spatial scale and depend on physical properties (e.g. Refractive Index, density and the mixing state) and chemical composition of aerosol. The aerosol chemical composition at Manora Peak is dominated by mineral dust and carbonaceous aerosol; total carbonaceous aerosol (TCA) contributing about 25% of TSP with significantly lower contribution from absorbing EC (~1-2% of TSP) [Ram *et al.*, 2008]. The observed b_{abs} values at Manora Peak are similar to those reported during the ACE-Asia experiment (e.g. 15 Mm^{-1} [Bergstrom *et al.*, 2004]). Recently, Hyvärinen *et al.* [2009] have reported that b_{abs} values measured using the Aethalometer varies from 4.5 to 23.2 Mm^{-1} during Sep 2005- Sep 2007 at Mukteshwar, a high-altitude site in northern India located nearby Manora Peak. The BC mass concentrations, based on Aethalometer based measurement, also exhibit a large spatio-temporal variability over Indian regions

[*Beegum et al.*, 2009]. If BC mass concentrations are converted to b_{abs} , one can find that b_{abs} values at Manora Peak are an order of magnitude lower compared to those in the Indo-Gangetic Plain [*Ram and Sarin*, 2009]. Furthermore, the annual average b_{abs} values at Manora Peak are factor of two higher than those at Mt Abu, another high-altitude site in western India [*Ram and Sarin*, 2009].

6.2.4 Site-specific mass absorption efficiency of EC (MAE, σ_{abs}): Temporal variability and influence of different emission sources

The biomass burning is characterized by relatively high σ_{abs} values compared to that from fossil-fuel emissions [*Martins et al.*, 1998]. Recently, *Schwarz et al.* [2008] have reported a value of $13 \pm 3 \text{ m}^2\text{g}^{-1}$ for σ_{abs} derived from biomass burning sources. The MAE of EC (σ_{abs}) exhibits a large spatial and temporal variability, varying from $3.4 - 21.2 \text{ m}^2\text{g}^{-1}$ during sampling period at different geographical locations in India. During wintertime (Dec 2004), average values of σ_{abs} at different sampling sites are: $6.1 \pm 2.0 \text{ m}^2\text{g}^{-1}$ at Jaduguda (rural), $14.5 \pm 1.1 \text{ m}^2\text{g}^{-1}$ at Manora Peak (high-altitude), $10.4 \pm 1.4 \text{ m}^2\text{g}^{-1}$ at Mt Abu (high-altitude) and $11.1 \pm 2.6 \text{ m}^2\text{g}^{-1}$ at Allahabad (urban) and $11.3 \pm 2.2 \text{ m}^2\text{g}^{-1}$ Hisar (urban). The long-term average σ_{abs} at Manora Peak for Feb 05-July 08 sampling period is $12.3 \pm 2.9 \text{ m}^2\text{g}^{-1}$. However, the σ_{abs} values at Manora Peak ranges from 4.3 to $21.2 \text{ m}^2\text{g}^{-1}$ for the sampling period (Fig. 6.4c). Despite of a large temporal and sample-to-sample variability in σ_{abs} values, measured b_{abs} values and thermal EC (in unit of $\mu\text{gC m}^{-3}$) show a good correlation for the data with $\text{EC} < 2.0 \mu\text{gC m}^{-3}$ and/or $b_{\text{abs}} < 25 \text{ Mm}^{-1}$ ($R^2 = 0.72$, $n = 73$, Fig. 6.5) and the slope of the best-fit line provides a value of $10.3 \text{ m}^2\text{g}^{-1}$. However, the linearity ceases for the data with $\text{EC} > 2.0 \mu\text{gC m}^{-3}$ and/or $b_{\text{abs}} > 25 \text{ Mm}^{-1}$. Most of these data points represent collection of aerosol samples during wintertime (Fig. 6.5).

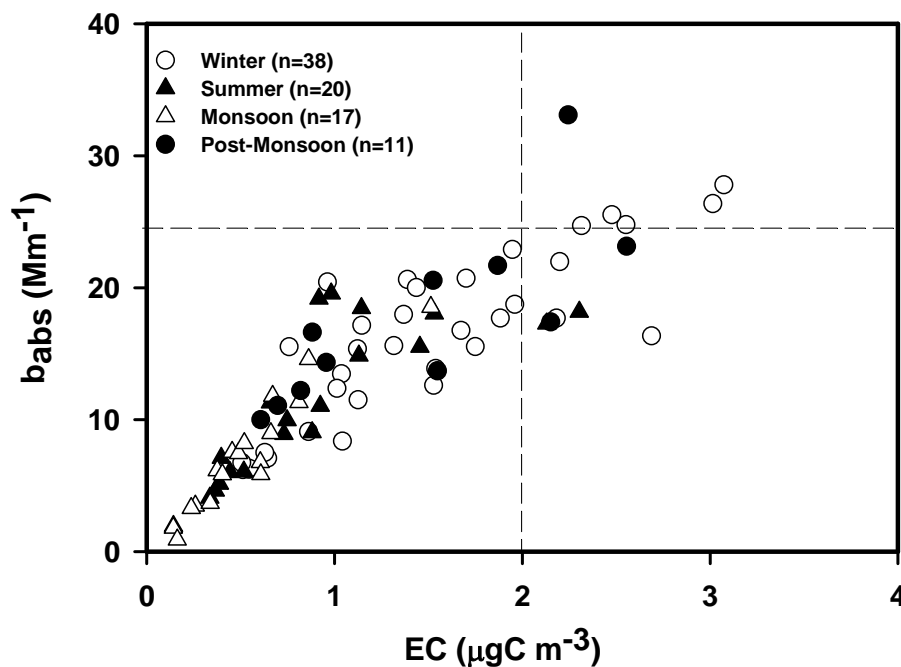


Fig.6.5: The scatter plot between b_{abs} and EC concentration exhibit significant correlation up to $25 Mm^{-1}$ (shown by horizontal dashed line) and $2.0 \mu gC m^{-3}$ (shown by vertical dashed line). The linearity ceases at higher EC concentrations and high b_{abs} values.

A large variability in σ_{abs} values, ranging from $2 - 25 m^2 g^{-1}$, has been reported in literature depending on location, composition and the mixing state of BC in aerosols [Lioussé *et al.*, 1993]. For example, Sharma *et al.* [2002] have reported that median values for site-specific attenuation cross-section ranges from 6.4 to $28.3 m^2 g^{-1}$ for different sites in Canada and have interpreted this variability in terms of distribution of sources and processes contributing to carbonaceous species at sampling sites. An average of $10 m^2 g^{-1}$ is generally taken for σ_{abs} [Sharma *et al.*, 2002]; however, Bond and Bergstrom [2006] had suggested a value of $7.5 \pm 1.2 m^2 g^{-1}$ at $550 nm$ for uncoated soot particles. The relatively high EC concentration ($11.6 \pm 2.0 \mu gC m^{-3}$) and low OC/EC ratio (3.1 ± 0.6) (Table 6.2) indicates dominance of coal-based emissions at Jaduguda, resulting in low σ_{abs} value ($6.1 \pm 2.0 m^2 g^{-1}$). The higher σ_{abs} values obtained at Manora Peak, Hisar and Allahabad could be attributed

to the predominance of aerosol species derived from biomass burning emissions. The samples collected during wintertime have relatively lower σ_{abs} values compared to those for other seasons (Fig. 6.6).

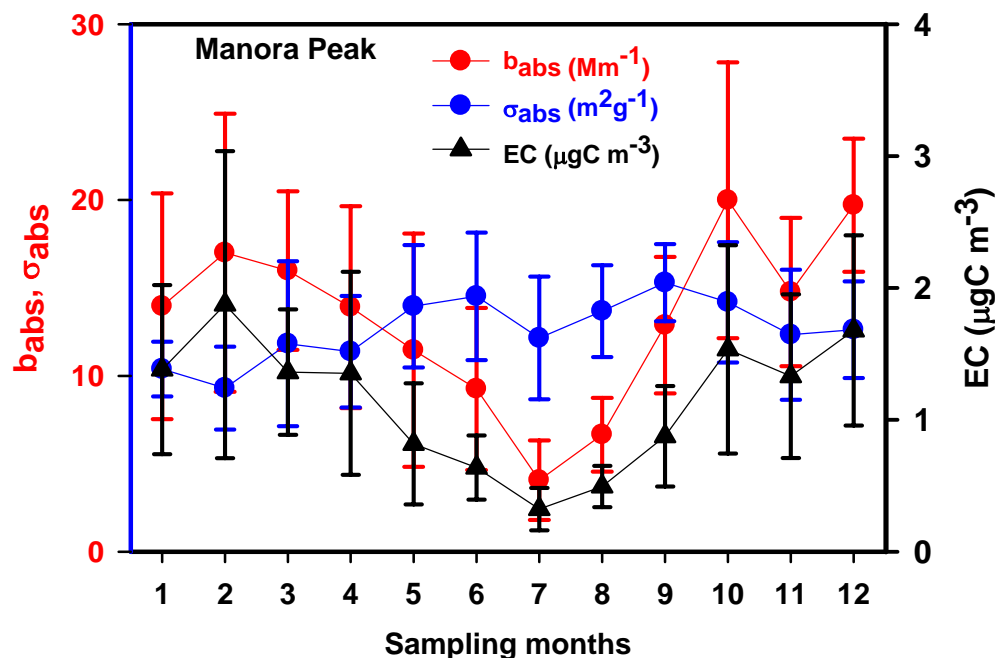


Fig. 6.6: The monthly average values of b_{abs} , σ_{abs} and EC concentration at Manora Peak during the sampling period (Feb 2005-July 2008).

The mixing state of aerosols (external or internal) could be a probable reason for observed seasonal variability in the mass absorption efficiency at Manora Peak. Recently, *Cozic et al.* [2008] also found that σ_{abs} values shows a seasonal variability for the samples collected at a high altitude site (Jungfrauoch) with an average values of $7.6 \pm 0.2 \text{ m}^2\text{g}^{-1}$ (winter) and $11.1 \pm 0.2 \text{ m}^2\text{g}^{-1}$ (summer) and suggested that higher σ_{abs} values in summer probably resulted because of greater coating of BC due to the photochemical activity. The aerosol particles collected at Manora Peak (during winter) are relatively drier, located near the source regions (i.e. freshly emitted) and may exist as an external mixture of aerosols and thus, probably have lower σ_{abs} values. On the other hand, aerosol particles collected during summer months are aged and chemically processed during the transport processes and may exist as an

internally mixed particle, thus resulting in higher σ_{abs} values. However, the reasons for the variability in mass absorption efficiency of EC need to further investigated. A comparison of σ_{abs} values obtained in the present study and those reported in literature is presented in Table 6.3.

The σ_{abs} values, obtained in this study, are higher than those reported during the PRIDE-PRD 2004 experiment, e.g. $7.7 \text{ m}^2\text{g}^{-1}$ [Andreae *et al.*, 2008]; 7.2 ± 1.0 and $9.3 \pm 1.4 \text{ m}^2\text{g}^{-1}$ for PM_1 and PM_{10} aerosols [Cheng *et al.*, 2008]. Bond and Bergstrom [2006] have suggested a value of $7.5 \pm 1.2 \text{ m}^2\text{g}^{-1}$ for the σ_{abs} at 550 nm for the freshly emitted soot particles. However, if we assume an enhancement of 50% in the absorption for coated and aged aerosols [Bond *et al.*, 2006]; the observed σ_{abs} value is in the similar range as suggested in the literature. The average σ_{abs} value at Manora Peak is higher than the commonly cited value of $10.0 \text{ m}^2\text{g}^{-1}$ and that used in the Particle Soot Absorption Photometer (PSAP) for the determination of BC mass concentrations [Sharma *et al.*, 2002]. In a recent study, Miyazaki *et al.* [2008] have reported σ_{abs} as $9.8 \pm 0.1 \text{ m}^2\text{g}^{-1}$ for a suburban site in Thailand based on a newly designed Continuous Soot Monitoring System (COSMOS) for the measurement of BC. Based on Aerosol Robotic Network (AERONET) retrievals, Schuster *et al.* [2005] have derived an average values of 10.5 and $10.0 \text{ m}^2\text{g}^{-1}$ were obtained for Asian continental aerosols for the years 2000 and 2001. Dey and Tripathi [2006] have reported σ_{abs} as 7.9 ± 1.8 , 9.7 ± 3.4 and $12.7 \pm 2.9 \text{ m}^2\text{g}^{-1}$ at an urban location (Kanpur) in northern India, for the years 2001, 2002 and 2003 respectively. The average σ_{abs} at Manora Peak, obtained in this study, is similar to those reported for Asian aerosols derived based on the AERONET retrievals.

Table 6.3: Spatio-temporal variability in mass absorption efficiency (MAE, σ_{abs}): Inter-comparison with literature-based studies.

Location	Type	Analytical methods		σ_{abs} m^2g^{-1}	σ_{abs}		References
		Optical	Thermal		Min.	Max.	
Jaduguda	Rural	TOT [@] , Sunset	Sunset	6.1 ± 2.0	3.4	9.1	This study
Hisar	Urban	TOT, Sunset	Sunset	11.3 ± 2.2	6.1	16.4	This study
Allahabad	Urban	TOT, Sunset	Sunset	11.1 ± 2.6	7.5	16.8	This study
Mt Abu	High-altitude	TOT, Sunset	Sunset	10.4 ± 1.4	8.1	12.2	This study
Manora Peak	High-altitude	TOT, Sunset	Sunset	12.3 ± 2.9	6.1	19.1	This study
	Diesel emitted	Aethalometer	IMPROVE*- TOR**	8.5			<i>Moosmuller et al.</i> [2001]
Baltimore and Washington	suburban ambient	Aethalometer	IMPROVE-TOR	7.1			<i>Chen et al.</i> [2002]
Six sites across Canada	Remote, urban, rural	Aethalometer	IMPROVE-TOR	6.4	28.3		<i>Sharma et al.</i> [2002]
Six sites across Canada	and suburban	Photoacoustic	Cachier/NIOSH [#]	3.2	11.6		<i>Sharma et al.</i> [2002]
Fresno supersite, CA	Urban ambient	Aethalometer	IMPROVE-TOR	11.4 ± 0.7			<i>Watson and Chow</i> [2002]
INDOEX	biofuel and fossil fuel emission	PSAP ^{###}	EGA ^{\$}	8.1 ± 0.7	5.6	10.8	<i>O.L. Mayol-Bracero et al.</i> [2002]
INDOEX	INDOEX	PSAP	Sunset	11 ± 5	5	40	<i>Mader et al.</i> [2002]
ACE-Asia experiment	polluted aerosol mixed with dust	PSAP	NIOSH		3	9	<i>Huebert et al.</i> [2003]
National Park, S. Texas		Photoacoustic	Aethalometer		8.4	9.9	<i>Arnott et al.</i> [2003]
ACE-Asia experiment	ACE-Asia	PSAP	Sunset	7.0 ± 2			<i>Clarke et al.</i> [2004]
Rochester and Philadelphia	Traffic impacted	Aethalometer	Sunset		5.9	54.8	<i>Jeong et al.</i> [2004]
ACE-Asia experiment	Marine, pollution and dust mixed	PSAP	NIOSH		5	25	<i>Quinn et al.</i> [2004]

		AERONET ^{\$\$}		9.9	7.7	12.5	<i>Schuster et al. [2005]</i>
Mexico city		AERONET		8.9 or 8.2	7.8	9.5	<i>Barnard et al. [2005]</i>
Vienna	urban	Aethalometer and MAAP ⁺	several thermal methods		6.8	8.7	<i>Hitzenberger et al. [2006]</i>
Tokyo, Japan		PSAP	Sunset	8.9			<i>Kondo et al. [2006]</i>
Mexico city	T1	PAS	Sunset	8.7			<i>Doran et al. [2007]</i>
Mexico city	T2	PAS	Sunset	10.8			<i>Doran et al. [2007]</i>
		PSAP	TOA	8.5			<i>Kirchstetter and Novakov [2007]</i>
	Jungfrauoch, high-altitude	MAAP	Sunset	7.6 ± 0.2			<i>Cozic et al. [2008]</i>
	Jungfrauoch	MAAP	Sunset	11.1 ± 0.2			<i>Cozic et al. [2008]</i>
Northern-China	rural site	PAS ⁺⁺	Aethalometer	8.28			<i>Yan et al. [2008]</i>
China		Aethalometer	IMPROVE-TOR	11.7			<i>Zhang et al. [2008]</i>
France		Aethalometer	Sunset	10.5			<i>Sciare et al. [2008]</i>
	urban aerosols	SP2 ⁻ and PSAP		7.5 ± 2.0			<i>Schwarz et al. [2008]</i>
	Biomass burning aerosols	SP2 and PSAP		13.3 ± 3.0			<i>Schwarz et al. [2008]</i>
	Background continental air	SP2 and PSAP		9.3 ± 2.0			<i>Schwarz et al. [2008]</i>
South-Asia	Biomass fuel combustion	Integrating Plate method	Sunset		7	15	<i>Habib et al. [2008]</i>
Mexico City Metropolitan Area		PSAP	SP2	10.5			<i>Subramanian et al. [2009]</i>

TOT[@]: Thermal Optical Transmittance; IMPROVE^{*}: Interagency Monitoring of Protected Visual Environments; TOR^{**}: Thermal Optical Reflectance; NIOSH[#]-National Institute for Occupational Safety and Health; PSAP^{##}: Particle Soot Absorption Photometer; EGA^{\$}: Evolved Gas Analysis; AERONET^{\$\$}: Aerosol Robotics Network; MAAP⁺: Multi-Angle Absorption Photometry; PAS⁺⁺: Photo- Acoustic Spectrometer; SP2⁻: Single Particle Soot Photometer

6.3 Summary

The major conclusions drawn from this chapter are listed below:

- A novel approach for the determination of aerosol absorption coefficient (b_{abs} , Mm^{-1}) and mass absorption efficiency (σ_{abs} , m^2g^{-1}) of elemental carbon (EC) is proposed, wherein simultaneously measured optical-attenuation (ATN, equivalent to initial transmittance) of 678 nm laser source, using thermo-optical EC-OC analyzer, has been used for the determination of σ_{abs} and absorption coefficient. This method can serve as a reliable and relatively effective off-line measurement of aerosol optical parameters.
- At high-altitude sites, measured ATN and surface EC loading (EC_s , $\mu\text{gC cm}^{-2}$) on the filters exhibit linear positive relationship ($R^2=0.86 - 0.96$), suggesting EC as a principal absorbing component. However, relatively large scatter in regression analyses for the data from urban sites suggests contribution from other species.
- The representative MAE of EC, during wintertime (Dec 2004), at a rural site (Jaduguda) is $6.1 \pm 2.0 \text{ m}^2\text{g}^{-1}$. In contrast, MAE at the two high-altitude sites is 14.5 ± 1.1 (Manora Peak) and 10.4 ± 1.4 (Mt Abu); and that at urban sites is 11.1 ± 2.6 (Allahabad) and $11.3 \pm 2.2 \text{ m}^2\text{g}^{-1}$ (Hisar). The long-term average MAE at Manora Peak (Feb 2005 to July 2008) is $12.3 \pm 2.9 \text{ m}^2\text{g}^{-1}$ (range: 4.3 to $20.9 \text{ m}^2\text{g}^{-1}$). These results are unlike the constant conversion factor used for MAE in optical instruments for the determination of BC mass concentration.
- A large temporal and spatial variability in the absorption coefficient is observed over the urban, rural and high-altitude sites in India. The lower absorption coefficient values are typical of the high-altitude sites and higher values for the urban and rural atmosphere.
- The results presented in this study have relevance for the climate studies over south Asian region where measurements of aerosol optical properties are lacking in the literature.

SYNTHESIS AND SCOPE OF FUTURE RESEARCH

7.1 Synthesis

The chemical composition and optical properties of atmospheric aerosols are highly variable in space and time due to the changes in the source characteristics (types and emission strength), meteorological conditions and transport of aerosols. The study on the chemical characterization of ambient aerosols provides an effective tool to understand the formation of secondary aerosols, atmospheric chemical processes, transport and the aging of aerosols. On the other hand, in-situ measurements of aerosol optical properties (along with chemical composition) can be used for the better estimation of direct aerosol radiative forcing on a regional scale. Furthermore, ground and long-term measurements of atmospheric chemical constituents can also be used for the validation of aerosol optical properties retrieved from the satellite data. In order to understand the spatio-temporal variabilities in aerosol mass concentration, chemical constituents and optical properties; a long-term ambient aerosol sampling was performed from selected locations representing urban (Kanpur: Jan 2007-March 2008) and the two high-altitude sites (Mt Abu: May 2005-Feb 2006 and Manora Peak: Feb 2005-July 2008) in northern and western India. Furthermore, these observations have been compared with a short-term aerosol sampling carried out during Dec 2004 from urban (Hisar, Allahabad), rural (Jaduguda) and the high-altitude site (Manora Peak) in the Indo-Gangetic Plain (IGP).

The PM_{10} mass concentration exhibits a large temporal variability and ranged from 42 to 312 $\mu\text{g m}^{-3}$ during a one-year sampling period at Kanpur. Total carbonaceous aerosols (TCA) and water-soluble inorganic species (WSIS) contribute nearly two-third of the PM_{10} mass during wintertime whereas their contribution is only ~35% during summer. Boundary layer dynamics, varying sources and their emission strength,

secondary aerosol formation and transport of aerosols all contribute to the seasonal trend in aerosol mass concentrations at Kanpur. Based on the chemical tracers (K^+ concentrations, K^+/OC and OC/EC ratios), biomass burning emission (wood-fuels and agricultural waste) has been identified as a major source of carbonaceous aerosols at urban and high-altitude sites in northern India.

At high-altitude sites, the total suspended particulate (TSP) mass also exhibits large temporal variability; varying from 13 to 432 $\mu\text{g m}^{-3}$ (at Mt Abu) and 13 to 272 $\mu\text{g m}^{-3}$ (at Manora Peak). Simultaneous measurements of aerosol optical depth (AOD), at Manora Peak, also exhibit a significant increase during summer months. On annual-scale, TCA and WSIS contribute nearly 25% and 10% of TSP mass, respectively. The chemical analyses of ambient aerosols from high-altitude sites suggest the dominance of mineral aerosols throughout the sampling period. However, the dominance of mineral aerosols (to TSP and AOD values) is significantly pronounced during summer months (April-June) under the prevailing south-westerly winds when long-range transport of aerosols originating from the desert regions in the middle-East and the Thar Desert (in western India). The long-range transport of mineral aerosols was established with the help of water-soluble Ca (Ca^{2+}) in aerosols and back trajectory analysis of the air-masses reaching at respective sampling locations.

The mass concentrations of OC, EC and WSOC at urban and rural locations in the IGP are an order of magnitude higher than those at the high-altitude sites. The enhancement in their mass concentrations is largest during wintertime when biomass burning emission strength is highest and a boundary layer height help in trapping the aerosols more efficiently. The increase in the biomass burning emission strength is also reflected by the seasonal trend in the mass concentrations of OC and EC at Kanpur when concentrations are a factor of two-to-three higher in the wintertime (compared to those during summer months). A characteristic feature of the carbonaceous species in aerosol samples from the urban and high altitude sites is also reflected in the OC/EC ratios ($A_v=7.8 \pm 3.4$). This is in sharp contrast to their mass ratio from a rural site, influenced by coal-based emissions, in the north-eastern part of India (range: 2.1–4.0, $A_v=3.1 \pm 0.6$, $n=7$).

The WSOC/OC ratios are fairly uniform (~ 0.35 – 0.40) in aerosols over urban and rural sites in the IGP. However, WSOC/OC ratios at high-altitude site (~ 0.55) and those in the IGP during summer months (~ 0.50) are much higher compared to that during wintertime suggesting a significant contribution from the secondary organic aerosol (SOA). The SOA formation is further corroborated by the elevated WSOC/OC ratios in the daytime samples (0.66 ± 0.11) compared to that in the nighttime samples (0.47 ± 0.07) at Kanpur. However, secondary inorganic aerosols (NO_3^- , SO_4^{2-} and NH_4^+) were prominent during wintertime (Dec-Feb), under the prevailing meteorological conditions (low ambient temperature and high relative humidity). The enhanced contribution from carbonaceous and inorganic species and their hygroscopic growth could be a possible cause for the fog and haze weather conditions during wintertime over northern India.

At high-altitude sites, measured optical-attenuation (ATN) and surface EC loading (EC_s , $\mu\text{gC cm}^{-2}$) on the filters exhibit linear positive relationship ($R^2=0.86$ – 0.96), suggesting EC as a principal absorbing component. However, relatively large scatter in regression analyses for the data from urban sites suggests contribution from other absorbing species. The representative mass absorption efficiency (σ_{abs}) of EC, during wintertime (Dec 2004), at a rural site (Jaduguda) is $6.1 \pm 2.0 \text{ m}^2\text{g}^{-1}$. In contrast, the σ_{abs} values at the two high-altitude sites is 14.5 ± 1.1 (Manora Peak) and 10.4 ± 1.4 (Mt Abu); and that at urban sites is 11.1 ± 2.6 (Allahabad) and $11.3 \pm 2.2 \text{ m}^2\text{g}^{-1}$ (Hisar). The spatial variability in σ_{abs} values are attributed to the sources (biomass burning emissions and urban and rural sites vs coal-based emissions at the rural site) and the mixing state of aerosols. These results are unlike the constant conversion factor used for MAE in optical instruments for the determination of BC mass concentration. A large spatio-temporal variability is observed for the aerosols absorption coefficient (b_{abs} , at 678 nm); the lower values are typical of the high-altitude sites and higher values for the urban and rural atmosphere. The average aerosol absorption coefficients, at the high-altitude sites, are an order of magnitude lower than those at urban and rural sites in northern India. Such large variability documented for the absorption parameters suggests the need for their suitable parameterization in the assessment of direct aerosol radiative forcing on a regional scale.

7.2 Scope for the future research

7.2.1 Evaluation of organic aerosols

This study has provided the chemical characteristics of ambient aerosols (bulk, PM_{2.5} and PM₁₀) from urban, rural and high-altitude sites in India. Biomass burning emissions has been inferred as a major source of carbonaceous aerosols based on selected tracers (measured K⁺ concentration, OC/EC and K⁺/OC ratios). However, the source information needs to be better constrained with the help of radiocarbon (¹⁴C) analysis of ambient aerosols and selected tracers such as levoglucosan (for biomass burning emission). Future investigations on the emission inventories of primary and secondary organic aerosols (POA and SOA, respectively) and the measurements of poly-aromatic hydrocarbon (PAHs) would be required to constrain the organic aerosol budget from south-Asian region.

Based on an increase in the WSOC/OC ratios during summer, this study has provided an evidence for the secondary organic aerosol (SOA) formation. The formation mechanism and the aging of organic aerosols during the transport could be another important area of research in the future [Jimenez *et al.*, 2009; Zhang *et al.*, 2007]. This could be easily achieved with the real-time measurements using an Aerosol mass spectrometer (AMS). Furthermore, the measurements of volatile organic compounds (VOCs) and oxidizing species (O₃, OH, NO_x radicals), low molecular weight carboxylic acids (C₂–C₆) can provide an insight for the evolution of organic aerosols over the Indo-Gangetic Plain, a highly polluted environment in northern India [Agarwal *et al.*, 2010; Miyazaki *et al.*, 2009]. It is well known the water-soluble organic carbon (WSOC) can act as cloud condensation nuclei (CCN). The hygroscopic growth, cloud activation and droplet formation needs to be understood for the precipitation processes and the semi-direct effect of aerosols. For such studies, the measurements of surface tension of the surfactant (water-soluble aerosols) will be an important parameter [Padró *et al.*, 2010]. Furthermore, measurements of the CCN properties and size-distribution (using a Scanning Mobile Particle Sizer; SMPS) will be helpful to understand the new-particle formation events under high relative humidity (RH) conditions and in the presence of secondary aerosols.

The pure snow is highly reflective of the solar radiation. The deposition of aerosols on the ice surfaces can act as a catalyst for the melting of the ice-sheets. The presence of relatively high amounts of absorbing black carbon (BC), in ambient aerosols over south-east Asia, can further enhance the melting of the Himalayan glaciers [Yasunari *et al.*, 2010]. The quantification of BC and dust deposition in the Himalayan glaciers and their possible linkage with melting needs to be explored in the future.

7.2.2 Aerosol chemistry

The present study has established that secondary inorganic aerosols (SIA; NH_4^+ , SO_4^{2-} and NO_3^-) constitute ~30% of the aerosol mass, during wintertime, over urban atmospheres of northern India. The future research should focus on the formation mechanism of SIAs, through the simultaneous measurements of gaseous pollutants (sulfur dioxide; SO_2 , nitrogen oxides; $\text{NO}_x = \text{NO} + \text{NO}_2$, ammonia; NH_3 , sulfuric acid; H_2SO_4 and nitric acids; HNO_3), and their partitioning into the solid-phase aerosols. In this regard, a study on the conversion mechanism of sulfur and nitrogen species and conversion ratios should be focused. The secondary formation of particulate NO_3^- , in an urban atmosphere, is of significant interest because it regulates NO_x , O_3 abundances and their life-times. In the daytime photochemical reaction, NO_x act as a catalyst in the formation of O_3 ; whereas it acts as a sink for O_3 in the troposphere during nighttime [Brown *et al.*, 2004; Brown *et al.*, 2006]. The photochemical formation of NO_3^- in the daytime also facilitates the oxidation of volatile organic compounds (VOCs) to form secondary organic aerosols (SOA), which in turn increases the hygroscopicity of ambient aerosols. Thus, the formation of NO_3^- would be an important area of research in the future. It is also observed that the mass concentrations of secondary inorganic aerosols and carbonaceous species (EC, OC and WSOC) show three to four-fold increase during haze days over the IGP. The secondary aerosol formation under the favorable environmental condition and their hygroscopic growth should be looked into as possible causes for the fog-haze formation over the IGP during wintertime.

7.2.3 Studies on optical properties and radiative forcing

This study has provided a novel approach for the measurements of aerosol absorption properties using a thermo-optical EC-OC analyzer and has documented a large spatio-temporal variability in aerosol absorption coefficient (b_{abs}) over the Indian sites. The aerosol absorption has been firmly attributed to the presence of elemental carbon (EC). However, the absorption from humic-like substances (HULIS), produced during biomass burning emission (a major source of carbonaceous aerosols in the IGP), should be investigated in the future. Although, earlier studies have suggested a weak absorption characteristics of Asian mineral aerosols; the absorption from mineral dust needs to be quantified in the future.

Another important optical parameter, namely scattering coefficient (b_{scat}), is widely used for the estimation of single scattering albedo (SSA; the ratio of scattering coefficient to the sum of scattering and absorption coefficients) and the radiative impact of aerosols. Unlike the EC (solely absorbing particulate species); all the chemical species scatter the solar radiation and thus, scattering coefficient depends on the chemical composition of aerosols. Thus, the measurements of the chemical species (provided in this study) can be used for the estimation of aerosol scattering coefficient. Furthermore, the enhancement in the scattering properties due to hygroscopic growth of aerosols should be studied. Finally, these optical parameters can be used for the inter-comparison with other techniques/measurements and more importantly, for the validation of satellite based retrievals which can provide a global coverage.

The chemical reactions, which occur on aerosol surfaces, can turn the initially hydrophobic particles (e.g. soot) into hydrophilic by adding a coating of soluble substances. Therefore the composition of individual particles, i.e. their mixing state, is an important factor for determining whether an aerosol particle can act as cloud condensation nuclei (CCN). The scanning electron microscope (SEM) analysis of aerosols can, thus, provide an insight to the coating of soluble species on aerosol surfaces. This information can be then used to infer the mixing state and the extent of chemical processing and for the prediction of CCN activity.

REFERENCES

- Ackerman, A. S., O. B. Toon, D. E. Stevens, A. J. Heymsfield, V. Ramanathan, and E. J. Welton (2000), Reduction of tropical cloudiness by soot, *Science*, 288(5468), 1042-1047.
- Adhikary, B., G. R. Carmichael, Y. Tang, L. R. Leung, Y. Qian, J. J. Schauer, E. A. Stone, V. Ramanathan, and M. V. Ramana (2007), Characterization of the seasonal cycle of south Asian aerosols: A regional-scale modeling analysis, *J. Geophys. Res.*, 112, D22S22, doi:10.1029/2006JD008143.
- Agarwal, S., S. G. Aggarwal, K. Okuzawa, and K. Kawamura (2010), Size distributions of dicarboxylic acids, ketoacids, dicarbonyls, sugars, WSOC, OC, EC and inorganic ions in atmospheric particles over Northern Japan: implication for long-range transport of Siberian biomass burning and East Asian polluted aerosols, *Atmos. Chem. Phys. Discuss.*, 10, 6713–6754.
- Albinet, A., E. Leoz-Garziandia, H. Budzinski, E. Villenave, and J.-L. Jaffrezo (2008), Nitrated and oxygenated derivatives of polycyclic aromatic hydrocarbons in the ambient air of two French alpine valleys Part 1: Concentrations, sources and gas/particle partitioning, *Atmos. Environ.*, 42, 43–54.
- Ali, K., G. A. Momin, S. Tewari, P. D. Safai, D. M. Chate, and P. S. P. Rao (2004), Fog and precipitation chemistry at Delhi, north India, *Atmos. Environ.*, 38, 4215–4222.
- Allen, G. A., J. Lawrence, and P. Koutrakis (1999), Field validation of a semi-continuous method for aerosol black carbon (aethalometer) and temporal patterns of summertime hourly black carbon measurements in southwestern PA, *Atmos. Environ.*, 33(5), 817-823.
- Ammann, M., M. Kalberer, D. T. Jost, L. Tobler, E. Rossler, D. Piguet, H. W. Gaggeler, and U. Baltensperger (1998), Heterogeneous production of nitrous acid on soot in polluted air masses, *Nature*, 395(6698), 157-160.

- Andreae, M. O. (1983), Soot carbon and excess fine potassium: long-range transport of combustion-derived aerosols, *Science*, 220(4602), 1148-1151.
- Andreae, M. O., and A. Gelencser (2006), Black carbon or brown carbon? the nature of light-absorbing carbonaceous aerosols, *Atmos. Chem. Phys.*, 6(10), 3131-3148.
- Andreae, M. O., and Crutzen. P. J. (1997), Atmospheric Aerosols: Biogeochemical Sources and Role in Atmospheric Chemistry, *Science*, 276, 1052-1058, DOI: 10.1126/science.1276.5315.1052.
- Andreae, M. O., and P. Merlet (2001), Emission of trace gases and aerosols from biomass burning, *Global Biogeochem. Cycles*, 15(4), 955-966.
- Andreae, M. O., O. Schmid, H. Yang, D. Chand, J. Z. Yu, L.-M. Zeng, and Y.-H. Zhang (2008), Optical properties and chemical composition of the atmospheric aerosol in urban Guangzhou, China, *Atmos. Environ.*, 42, 6335–6350.
- Arnott, W. P., H. Moosmuller, C. F. Rogers, T. Jin, and R. Bruch (1999), Photoacoustic spectrometer for measuring light absorption by aerosols: Instrument description, *Atmos. Environ.*, 33(17), 2845-2852.
- Arnott, W. P., H. Moosmuller, P. J. Sheridan, J. A. Ogren, R. Raspet, W. V. Slaton, J. L. Hand, S. M. Kreidenweis, and J. L. Collett Jr. (2003), Photoacoustic and filter-based ambient aerosol light absorption measurements: Instrument comparisons and the role of relative humidity, *J. Geophys. Res.*, 108, 4034, doi:10.1029/2002JD002165.
- Babu, S. S., and K. K. Moorthy (2002), Aerosol black carbon over a tropical station in India, *Geophys. Res. Lett.*, 29 (23), 2098, doi:10.1029/2002GL015662.
- Babu, S. S., S. K. Satheesh, and K. K. Moorthy (2002), Aerosol radiative forcing due to enhanced black carbon at an urban site in India, *Geophys. Res. Lett.*, 29 (18), 1880, doi:10.1029/2002GL015826.
- Badarinath, K. V. S., K. M. Latha, T. R. K. Chand, R. R. Reddy, K. R. Gopal, L. S. S. Reddy, K. Narasimhulu, and K. R. Kumar (2007), Black carbon aerosols and gaseous pollutants in an urban area in North India during a fog period, *Atmos. Res.*, 85, 209-216.

- Bahrman, C. P., and V. Saxena (1998), Influence of air mass history on black carbon concentrations and regional climate forcing in southeastern United States, *J. Geophys. Res.*, *103(D18)*, 23153-23161.
- Barnard, J. C., E. I. Kassianov, T. P. Ackerman, S. Frey, K. Johnson, B. Zuberi, L. T. Molina, M. J. Molina, J. S. Gaffney, and N. A. Marley (2005), Measurements of Black Carbon Specific Absorption in the Mexico City Metropolitan Area during the MCMA 2003 Field Campaign, *Atmos. Chem. Phys.*, *5*, 4083-4113.
- Beegum, I. N., K. K. Moorthy, S. S. Babu, S. K. Satheesh, V. Vinoj, K. V. S. Badarinath, P. D. Safai, P. C. S. Devara, S. Singh, Vinod, U. C. Dumka, and P. Pant (2009), Spatial distribution of aerosol black carbon over India during pre-monsoon season, *Atmos. Environ.*, *43*, 1071–1078.
- Bergstrom, R. W., P. Pilewskie, J. Pommier, M. Rabbette, P. B. Russell, B. Schmid, J. Redemann, A. Higurashi, T. Nakajima, and P. K. Quinn (2004), Spectral absorption of solar radiation by aerosols during ACE-Asia, *J. Geophys. Res.*, *109*, *D19S15*, doi:10.1029/2003JD004467.
- Birch, M. E. (1998), Analysis of carbonaceous aerosols: Interlaboratory comparison, *Analyst*, *123(5)*, 851-857.
- Birch, M. E., and R. A. Cary (1996), Elemental carbon-based method for monitoring occupational exposures to particulate diesel exhaust, *Aerosol Sci. Technol.*, *25(3)*, 221-241.
- Bizjak, M., J. Tursic, M. Lesnjak, and T. Cegnar (1999), Aerosol black carbon and ozone measurements at Mt. Krvavec EMEP/GAW station, Slovenia, *Atmos. Environ.*, *33(8)*, 2783-2787.
- Bodhaine, B. A. (1995), Aerosol absorption measurements at Barrow, Mauna Loa and the south pole, *J. Geophys. Res.*, *100(D5)*, 8967-8975.
- Bond, T. C., and R. W. Bergstrom (2006), Light absorption by carbonaceous particles: An investigative review, *Aerosol Sci. Technol.*, *40(1)*, 1-41.
- Bond, T. C., E. Bhardwaj, R. Dong, R. Jogani, S. Jung, C. Roden, D. G. Streets, and N. M. Trautmann (2007), Historical emissions of black and organic carbon aerosol from energy-related combustion, 1850-2000, *Global Biogeochem. Cycles*, *21(2)*, doi:10.1029/2006GB002840.

- Bond, T. C., G. Habib, and R. W. Bergstrom (2006), Limitations in the enhancement of visible light absorption due to mixing state, *J. Geophys. Res.*, *111*, D20211, doi:10.1029/2006JD007315.
- Brown, S. S., J. E. Dibb, H. Stark, M. Aldener, M. Vozella, S. Whitlow, E. J. Williams, B. M. Lerner, R. Jakoubek, A. M. Middlebrook, J. A. DeGouw, C. Warneke, P. D. Goldan, W. C. Kuster, W. M. Angevine, D. T. Sueper, P. K. Quinn, T. S. Bates, J. F. Meagher, F. C. Fehsenfeld, and A. R. Ravishankara (2004), Nighttime removal of NO_x in the summer marine boundary layer, *Geophys. Res. Lett.*, *31*, L07108, doi:10.1029/2004GL019412.
- Brown, S. S., T. B. Ryerson, A. G. Wollny, C. A. Brock, R. Peltier, A. P. Sullivan, R. J. Weber, W. P. Dube, M. Trainer, J. F. Meagher, F. C. Fehsenfeld, and A. R. Ravishankara (2006), Variability in nocturnal nitrogen oxide processing and its role in regional air quality, *Science*, *311*(5757), 67-70.
- Cabada, J. C., S. N. Pandis, R. Subramanian, A. L. Robinson, A. Polidori, and B. Turpin (2004), Estimating the secondary organic aerosol contribution to PM_{2.5} using the EC tracer method, *Aerosol Sci. Technol.*, *38*, 140-155.
- Cachier, H., M.-P. Bremond, and P. Buat-Menard (1989), Determination of atmospheric soot carbon with a sample thermal method, *Tellus*, *41B*(3), 379-390.
- Cao, J.-J., B.-Q. Xu, J.-Q. He, X.-Q. Liu, Y.-M. Han, G.-H. Wang, and C.-S. Zhu (2009), Concentrations, seasonal variations, and transport of carbonaceous aerosols at a remote Mountainous region in western China, *Atmos. Environ.*, *43*(29), 4444-4452.
- Cao, J. J., S. C. Lee, K. F. Ho, X. Y. Zhang, S. C. Zou, K. Fung, J. C. Chow, and J. G. Watson (2003), Characteristics of carbonaceous aerosol in Pearl River Delta Region, China during 2001 winter period, *Atmos. Environ.*, *37*(11), 1451-1460.
- Cao, J. J., S. C. Lee, K. F. Ho, S. C. Zou, K. Fung, Y. Li, J. G. Watson, and J. C. Chow (2004), Spatial and seasonal variations of atmospheric organic carbon and elemental carbon in Pearl River Delta Region, China, *Atmos. Environ.*, *38*(27), 4447-4456.
- Carmichael, G. R., B. Adhikary, S. Kulkarni, A. DAllura, Y. Tang, D. Streets, Q. Zhang, T. C. Bond, V. Ramanathan, A. Jamroensan, and P. Marrapu (2009), Asian

- aerosols: Current and year 2030 distributions and implications to human health and regional climate change, *Environ. Sci. Technol.*, *43*(15), 5811-5817.
- Carrico, C. M., M. H. Bergin, A. B. Shrestha, J. E. Dibb, L. Gomes, and J. M. Harris (2003a), The importance of carbon and mineral dust to seasonal aerosol properties in the Nepal Himalaya, *Atmos. Environ.*, *37*(20), 2811-2824.
- Carrico, C. M., P. Kus, M. J. Rood, P. K. Quinn, and T. S. Bates (2003b), Mixtures of pollution, dust, sea salt, and volcanic aerosol during ACE-Asia: Radiative properties as a function of relative humidity, *J. Geophys. Res.*, *108* (D23), 8650, doi:10.1029/2003JD003405.
- Castro, L. M., C. A. Pio, R. M. Harrison, and D. J. T. Smith (1999), Carbonaceous aerosol in urban and rural European atmospheres: Estimation of secondary organic carbon concentrations, *Atmos. Environ.*, *33*(17), 2771-2781.
- Chang, S.-C., and C.-T. Lee (2007), Secondary aerosol formation through photochemical reactions estimated by using air quality monitoring data in Taipei City from 1994 to 2003, *Atmos. Environ.*, *41*(19), 4002-4017.
- Charlson, R. J., S. E. Schwartz, J. M. Hales, R. D. Cess, J. A. Coakley Jr., J. E. Hansen, and D. J. Hofmann (1992), Climate forcing by anthropogenic aerosols, *Science*, *255*(5043), 423-430.
- Chen, L.-W. A., B. G. Doddridge, R. R. Dickerson, J. C. Chow, and R. C. Henry (2002), Origins of fine aerosol mass in the Baltimore-Washington corridor: Implications from observation, factor analysis, and ensemble air parcel back trajectories, *Atmos. Environ.*, *36*(28), 4541-4554.
- Cheng, Y. F., A. Wiedensohler, H. Eichler, H. Su, T. Gnauk, E. Brüggemann, H. Herrmann, J. Heintzenber, J. Slanina, T. Tuch, M. Hu, and Y. H. Zhang (2008), Aerosol optical properties and related chemical apportionment at Xinken in Pearl River Delta of China, *Atmos. Environ.*, *42*, 6351-6372.
- Chester, R. (1990), *Marine Geochemistry*, 698 pp., Unwin Hyman, London.
- Cheung, H.-C., T. Wang, K. Baumann, and H. Guo (2005), Influence of regional pollution outflow on the concentrations of fine particulate matter and visibility in the coastal area of southern China, *Atmos. Environ.*, *39*, 6463-6474.

- Chinnam, N., S. Dey, S. N. Tripathi, and M. Sharma (2006), Dust events in Kanpur, northern India: Chemical evidence for source and implications to radiative forcing, *Geophys. Res. Lett.*, *33*, L08803, doi:10.1029/2005GL025278.
- Chou, C. C.-K., T.-K. Chen, S.-H. Huang, and S. C. Liu (2003), Radiative absorption capability of Asian dust with black carbon contamination, *Geophys. Res. Lett.*, *30*(12), 1616, doi:10.1029/2003GL017076.
- Chou, C. C.-K., W.-N. Chen, S.-Y. Chang, T.-K. Chen, and S.-H. Huang (2005), Specific absorption cross-section and elemental carbon content of urban aerosols, *Geophys. Res. Lett.*, *32*, L21808, doi:10.1029/2005GL024301.
- Chowdhury, Z., M. Zheng, J. J. Schauer, R. J. Sheesley, L. G. Salmon, G. R. Cass, and A. G. Russell (2007), Speciation of ambient fine organic carbon particles and source apportionment of PM_{2.5} in Indian cities, *J. Geophys. Res.*, *112*, D15303, doi:10.1029/2007JD008386.
- Clarke, A. D., Y. Shinozuka, V. N. Kapustin, S. Howell, B. Huebert, S. Doherty, T. Anderson, D. Covert, J. Anderson, X. Hua, K. G. Moore II, C. McNaughton, G. Carmichael, and R. Weber (2004), Size distributions and mixtures of dust and black carbon aerosol in Asian outflow: Physiochemistry and optical properties, *J. Geophys. Res.*, *109*, D15S09, doi:10.1029/2003JD004378.
- Cong, Z., S. Kang, S. Dong, X. Liu, and D. Qin (2008), Elemental and individual particle analysis of atmospheric aerosols from high Himalayas, *Environ. Monit. Assessment*, *160*, 323-335.
- Cozic, J., B. Verheggen, E. Weingartner, J. Crosier, K. Bower, M. Flynn, H. Coe, S. Henning, M. Steinbacher, M. C. Coen, A. Petzold, and U. Baltensperger (2008), Chemical composition of free tropospheric aerosol for PM₁ and coarse mode at the high alpine site Jungfraujoeh, *Atmos. Chem. Phys.*, *8*, 407-423.
- Dall'Osto, M., R. M. Harrison, H. Coe, and P. Williams (2009), Real-time secondary aerosol formation during a fog event in London, *Atmos. Chem. Phys.*, *9*, 2459–2469.
- Das, S. K., A. Jayaraman, and A. Misra (2008), Fog-induced variations in aerosol optical and physical properties over the Indo-Gangetic Basin and impact to aerosol radiative forcing, *Annales Geophysicae*, *26*, 1345–1354.

- Decesari, S., M. C. Facchini, C. Carbone, L. Giulianelli, M. Rinaldi, E. Finessi, S. Fuzzi, A. Marinoni, P. Cristofanelli, R. Duchi, P. Bonasoni, E. Vuillermoz, J. Cozic, J. L. Jaffrezo, and P. Laj (2010), Chemical composition of PM₁₀ and PM₁ at the high-altitude Himalayan station Nepal Climate Observatory-Pyramid (NCO-P) (5079m a.s.l.), *Atmos. Chem. Phys.*, *10*, 4583–4596, doi:4510.5194/acp-4510-4583-2010.
- Dey, S., and S. N. Tripathi (2006), Retrieval of black carbon and specific absorption over Kanpur city, northern India during 2001–2003 using AERONET data, *Atmos. Environ.*, *40*, 445–456.
- Dey, S., and S. N. Tripathi, (2008), Aerosol direct radiative effects over Kanpur in the Indo-Gangetic basin, northern India: Long-term (2001–2005) observations and implications to regional climate, *J. Geophys. Res.*, *113*, D04212, doi:10.1029/2007JD009029.
- Dinar, E., A. A. Riziq, C. Spindler, C. Erlick, G. Kiss, and Y. Rudich (2008), Optical properties of absorbing aerosols containing model and atmospheric HULIS, *Faraday Discuss.*, *137*, 279 - 295.
- Doran, J. C., J. C. Barnard, W. P. Arnott, R. Cary, R. Coulter, J. D. Fast, E. I. Kassianov, L. Kleinman, N. S. Laulainen, T. Martin, G. Paredes-Miranda, M. S. Pekour, W. J. Shaw, D. F. Smith, S. R. Springston, and X.-Y. Yu (2007), The T₁-T₂ study: evolution of aerosol properties downwind of Mexico City, *Atmos. Chem. Phys.*, *7*, 1585–1598.
- Draxler, R. R., and G. D. Rolph (2003), HYSPLIT (HYbrid Single-Particle Lagrangian Integrated Trajectory) Model access via NOAA ARL READY Website (<http://www.arl.noaa.gov/ready/hysplit4.html>). NOAA Air Resources Laboratory, Silver Spring, MD.
- Duan, F., X. Liu, T. Yu, and H. Cachier (2004), Identification and estimate of biomass burning contribution to the urban aerosol organic carbon concentrations in Beijing, *Atmos. Environ.*, *38*(9), 1275-1282.
- Duan, F. K., K. B. He, Y. L. Ma, F. M. Yang, X. C. Yu, S. H. Cadle, T. Chan, and P. A. Mulawa (2006), Concentration and chemical characteristics of PM_{2.5} in Beijing, China: 2001-2002, *Sci. Total Environ.*, *355*, 264-275.

- Dumka, U. C., S. K. Satheesh, P. Pant, P. Hegde, and K. K. Moorthy (2006), Surface changes in solar irradiance due to aerosols over central Himalayas, *Geophys. Res. Lett.*, *33*, L20809, doi:10.1029/2006GL027814.
- Echalar, F., A. Gaudichet, H. Cachier, and P. Artaxo (1995), Aerosol emissions by tropical forest and savanna biomass burning: characteristic trace elements and fluxes, *Geophys. Res. Lett.*, *22*(22), 3034–3042.
- Favez, O., H. Cachier, J. Sciare, S. C. Alfaro, T. M. El-Araby, M. A. Harhash, and M. M. Abdelwahab (2008a), Seasonality of major aerosol species and their transformations in Cairo megacity, *Atmos. Environ.*, *42*, 1503–1516.
- Favez, O., J. Sciare, H. Cachier, S. C. Alfaro, and M. M. Abdelwahab (2008b), Significant formation of water-insoluble secondary organic aerosols in semi-arid urban environment, *Geophys. Res. Lett.*, *35*, L15801, doi:10.1029/2008GL034446.
- Fuzzi, S., M. O. Andreae, B. J. Huebert, M. Kulmala, T. C. Bond, M. Boy, S. J. Doherty, A. Guenther, M. Kanakidou, K. Kawamura, V.-M. Kerminen, U. Lohmann, L. M. Russell, and U. Poschl (2006), Critical assessment of the current state of scientific knowledge, terminology, and research needs concerning the role of organic aerosols in the atmosphere, climate, and global change, *Atmos. Chem. Phys.*, *6*, 2017–2038.
- Ganguly, D., P. Ginoux, V. Ramaswamy, D. M. Winker, B. N. Holben, and S. N. Tripathi (2009), Retrieving the composition and concentration of aerosols over the Indo-Gangetic basin using CALIOP and AERONET data, *Geophys. Res. Lett.*, *36*, L13806, doi:10.1029/2009GL038315.
- Ganguly, D., A. Jayaraman, T. A. Rajesh, and H. Gadhavi (2006), Wintertime aerosol properties during foggy and non-foggy days over urban center Delhi and their implications for shortwave radiative forcing, *J. Geophys. Res.*, *111*, D15217, doi:10.1029/2005JD007029.
- Gautam, R., N. C. Hsu, M. Kafatos, and S.-C. Tsay (2007), Influences of winter haze on fog/low cloud over the Indo-Gangetic plains, *J. Geophys. Res.*, *112*, D05207, doi:10.1029/2005JD007036.

- Gelencser, A., B. May, D. Simpson, A. Sanchez-Ochoa, A. Kasper-Giebl, H. Puxbaum, A. Caseiro, C. Pio, and M. Legrand (2007), Source apportionment of PM_{2.5} organic aerosol over Europe: Primary/secondary, natural/anthropogenic, and fossil/biogenic origin, *J. Geophys. Res.*, *112*, D23S04, doi:10.1029/2006JD008094.
- Geng, H., Y. Park, H. Hwang, S. Kang, and C.-U. Ro (2009), Elevated nitrogen-containing particles observed in Asian dust aerosol samples collected at the marine boundary layer of the Bohai Sea and the Yellow Sea, *Atmos. Chem. Phys.*, *9*, 6933–6947.
- Gobbi, G. P., F. Angelini, P. Bonasoni, G. P. Verza, A. Marinoni, and F. Barnaba (2010), Sunphotometry of the 2006–2007 aerosol optical/radiative properties at the Himalayan Nepal Climate Observatory – Pyramid (5079m a.s.l.), *Atmos. Chem. Phys. Discuss.*, *10*, 1193–1220.
- Guo, S., M. Hu, Z. B. Wang, J. Slanina, and Y. L. Zhao (2010), Size-resolved aerosol water-soluble ionic compositions in the summer of Beijing: implication of regional secondary formation, *Atmos. Chem. Phys.*, *10*, 947–959.
- Gustafsson, Ö., M. Kruså, Z. Zencak, R. J. Sheesley, L. Granat, E. Engström, P. S. Praveen, P. S. P. Rao, C. Leck, and H. Rodhe (2009), Brown Clouds over South Asia: Biomass or Fossil Fuel Combustion?, *Science*, *323*, 495-498.
- Habib, G., C. Venkataraman, T. C. Bond, and J. J. Schauer (2008), Chemical, Microphysical and Optical Properties of Primary Particles from the Combustion of Biomass Fuels, *Environ. Sci. Technol.*, *42*(23), 8829-8834.
- Han, Y. M., Z. W. Han, J. J. Cao, J. C. Chow, J. G. Watson, Z. S. An, S. X. Liu, and R. J. Zhang (2008), Distribution and origin of carbonaceous aerosol over a rural high-mountain lake area, Northern China and its transport significance, *Atmos. Environ.*, *42*(10), 2405-2414.
- Haywood, J., and O. Boucher (2000), Estimates of the direct and indirect radiative forcing due to Tropospheric aerosols: A review, *Rev. Geophys.*, *38*(4), 513–543; doi:10.1029/1999RG000078.

- He, K., F. Yang, Y. Ma, Q. Zhang, X. Yao, C. K. Chan, S. Cadle, T. Chan, and P. Mulawa (2001), The characteristics of PM_{2.5} in Beijing, China, *Atmos. Environ.*, *35*(29), 4959-4970.
- Hegde, P., P. Pant, and Y. B. Kumar (2008), An integrated analysis of lidar observations in association with optical properties of aerosols from a high altitude location in central Himalayas, *Atmos. Sci. Lett.*, *10*(1), 48 - 57.
- Hegde, P., P. Pant, M. Naja, U. C. Dumka, and R. Sagar (2007), South Asian dust episode in June 2006: Aerosol observations in the central Himalayas, *Geophys. Res. Lett.*, *34*, L23802, doi:10.1029/2007GL030692.
- Hitzenberger, R., A. Berner, H. Giebl, R. Kromp, S. M. Larson, A. Rouc, A. Koch, S. Marischka, and H. Puxbaum (1999), Contribution of carbonaceous material to cloud condensation nuclei concentrations in European background (Mt. Sonnblick) and urban (Vienna) aerosols, *Atmos. Environ.*, *33*(17), 2647-2659.
- Hitzenberger, R., A. Petzold, H. Bauer, P. Ctyroky, P. Pouresmaeil, L. Laskus, and H. Puxbaum (2006), Intercomparison of thermal and optical measurement methods for elemental carbon and black carbon at an urban location, *Environ. Sci. Technol.*, *40*(20), 6377-6381.
- Hoffer, A., A. Gelencser, P. Guyon, G. Kiss, O. Schmid, G. P. Frank, P. Artaxo, and M. O. Andreae (2006), Optical properties of humic-like substances (HULIS) in biomass-burning aerosols, *Atmos. Chem. Phys.*, *6*(11), 3563-3570.
- Horvath, H. (1993), Atmospheric light absorption - A review, *Atmos. Environ. - Part A General Topics*, *27* A(3), 293-317.
- Hoyle, C. R., T. Berntsen, G. Myhre, and S. A. Isaksen (2007), Secondary organic aerosol in the global aerosol – chemistry transport model Oslo CTM2, *Atmos. Chem. Phys.*, *5*, 9053–9092.
- Huebert, B. J., T. Bates, P. B. Russell, G. Shi, Y. J. Kim, K. Kawamura, G. Carmichael, and T. Nakajima (2003), An overview of ACE-Asia: Strategies for quantifying the relationships between Asian aerosols and their climatic impacts, *J. Geophys. Res.*, *108* (D23), 8633, doi:10.1029/2004JD004700.
- Hyvärinen, A. P., H. Lihavainen, M. Komppula, V. P. Sharma, V.-M. Kerminen, T. S. Panwar, and Y. Viisanen (2009), Continuous measurements of optical properties

- of atmospheric aerosols in Mukteshwar, Northern India, *J. Geophys. Res.*, *114*, D08207, doi:10.1029/2008JD011489.
- IPCC (2007), Summary for Policymakers, In: Climate Change 2007: The Physical Science Basis. Contribution of Working Group I to the Fourth Assessment Report of the Intergovernmental Panel on Climate Change, [Solomon, S., D. Qin, M. Manning, Z. Chen, M. Marquis, K.B. Averyt, M.Tignor and H.L. Miller (eds.)], Cambridge University Press, Cambridge, United Kingdom and New York, NY, USA.
- Jacobson, M. C., H.-C. Hansson, K. J. Noone, and R. J. Charlson (2000), Organic atmospheric aerosols: Review and state of the science, *Rev. Geophys.*, *38*(2), 267-294.
- Jacobson, M. Z. (2001), Strong radiative heating due to the mixing state of black carbon in atmospheric aerosols, *Nature*, *409*(6821), 695-697.
- Jeong, C. H., P. K. Hopke, E. Kim, and D. W. Lee (2004), The comparison between thermal-optical transmittance elemental carbon and Aethalometer black carbon measured at multiple monitoring sites, *Atmos. Environ.*, *38*, 5193-5204.
- Jethva, H., S. K. Satheesh, and J. Srinivasan (2005), Seasonal variability of aerosols over the Indo-Gangetic basin, *J. Geophys. Res.*, *110*, D21204, doi:10.1029/2005JD005938.
- Jickells, T. D., Z. S. An, K. K. Andersen, A. R. Baker, G. Bergametti, N. Brooks, J. J. Cao, P. W. Boyd, R. A. Duce, K. A. Hunter, H. Kawahata, N. Kubilay, J. laRoche, P. S. Liss, N. Mahowald, J. M. Prospero, A. J. Ridgwell, I. Tegen, and R. Torres (2005), Global iron connections between desert dust, ocean biogeochemistry, and climate, *Science*, *308*, 67-71.
- Jimenez, J. L., M. R. Canagaratna, N. M. Donahue, A. S. H. Prevot, Q. Zhang, J. H. Kroll, P. F. DeCarlo, J. D. Allan, H. Coe, N. L. Ng, A. C. Aiken, K. S. Docherty, I. M. Ulbrich, A. P. Grieshop, A. L. Robinson, J. Duplissy, J. D. Smith, K. R. Wilson, V. A. Lanz, C. Hueglin, Y. L. Sun, J. Tian, A. Laaksonen, T. Raatikainen, J. Rautiainen, P. Vaattovaara, M. Ehn, M. Kulmala, J. M. Tomlinson, D. R. Collins, M. J. Cubison, E. J. Dunlea, J. A. Huffman, T. B. Onasch, M. R. Alfarra, P. I. Williams, K. Bower, Y. Kondo, J. Schneider, F.

- Drewnick, S. Borrmann, S. Weimer, K. Demerjian, D. Salcedo, L. Cottrell, R. Griffin, A. Takami, T. Miyoshi, S. Hatakeyama, A. Shimono, J. Y. Sun, Y. M. Zhang, K. Dzepina, J. R. Kimmel, D. Sueper, J. T. Jayne, S. C. Herndon, A. M. Trimborn, L. R. Williams, E. C. Wood, A. M. Middlebrook, C. E. Kolb, U. Baltensperger, and D. R. Worsnop (2009), Evolution of organic aerosols in the atmosphere, *Science*, *325*, 1525-1529, DOI: 1510.1126/science.1180353.
- Junker, C., S. G. Jennings, and H. Cachier (2006), Aerosol light absorption in the North Atlantic: trends and seasonal characteristics during the period 1989 to 2003, *Atmos. Chem. Phys.*, *6*, 1913-1925.
- Kanakidou, M., J. H. Seinfeld, S. N. Pandis, I. Barnes, F. J. Dentener, M. C. Facchini, R. Van Dingenen, B. Ervens, A. Nenes, C. J. Nielsen, E. Swietlicki, J. P. Putaud, Y. Balkanski, S. Fuzzi, J. Horth, G. K. Moortgat, R. Winterhalter, C. E. L. Myhre, K. Tsigaridis, E. Vignati, E. G. Stephanou, and J. Wilson (2005), Organic aerosol and global climate modelling: A review, *Atmos. Chem. Phys.*, *5*(4), 1053-1123.
- Kirchstetter, T. W., and T. Novakov (2007), Controlled generation of black carbon particles from a diffusion flame and applications in evaluating black carbon measurement methods, *Atmos. Environ.*, *41*(9), 1874-1888.
- Kirchstetter, T. W., T. Novakov, and P. V. Hobbs (2004), Evidence that the spectral dependence of light absorption by aerosols is affected by organic carbon, *J. Geophys. Res.*, *109*, D21208, doi:10.1029/2004JD004999.
- Kondo, Y., Y. Komazaki, Y. Miyazaki, N. Moteki, N. Takegawa, D. Kodama, S. Deguchi, M. Nogami, M. Fukuda, T. Miyakawa, Y. Morino, M. Koike, H. Sakurai, and K. Ehara (2006), Temporal variations of elemental carbon in Tokyo, *J. Geophys. Res.*, *111*, D12205, doi:10.1029/2005JD006257.
- Kondo, Y., Y. Miyazaki, N. Takegawa, T. Miyakawa, R. J. Weber, J. L. Jimenez, Q. Zhang, and D. R. Worsnop (2007), Oxygenated and water-soluble organic aerosols in Tokyo, *J. Geophys. Res.*, *109*, D01203, doi:10.1029/2006JD007056.
- Kumar, A., and M. M. Sarin (2009), Mineral aerosols from western India: Temporal variability of coarse and fine atmospheric dust and elemental characteristics, *Atmos. Environ.*, *43*, 4005-4013.

- Kumar, A., M. M. Sarin, and B. Srinivas (2010), Aerosol iron solubility over Bay of Bengal: Role of anthropogenic sources and chemical processing, *Mar. Chem.*, doi:10.1016/j.marchem.2010.1004.1005
- Kumar, A., M. M. Sarin, and A. K. Sudheer (2008), Mineral and anthropogenic aerosols in Arabian Sea–atmospheric boundary layer: Sources and spatial variability, *Atmos. Environ.*, *42*, 5169–5181.
- Kundu, S., K. Kawamura, T. W. Andreae, A. Hoffer, and M. O. Andreae (2010), Diurnal variation in the water-soluble inorganic ions, organic carbon and isotopic compositions of total carbon and nitrogen in biomass burning aerosols from the LBA-SMOCC campaign in Rondônia, Brazil, *J. Aerosol Sci.*, *41*, 118-133.
- Lary, D., A. Lee, R. Toumi, M. Newchurch, M. Pirre, and J. Renard (1997), Carbon aerosols and atmospheric photochemistry, *J. Geophys. Res.*, *102(D3)*, 3671-3682.
- Lary, D. J., D. E. Shallcross, and R. Toumi (1999), Carbonaceous aerosols and their potential role in atmospheric chemistry, *J. Geophys. Res.*, *104(D13)*, 15929-15940.
- Latha, K. M., and K. V. S. Badarinath (2003), Black carbon aerosols over tropical urban environment: A case study, *Atmos. Res.*, *69*, 125– 133.
- Lee, Y. L., and R. Sequeira (2002), Water-soluble aerosol and visibility degradation in Hong Kong during autumn and early winter, 1998, *Environ. Pollut.*, *116*, 225–233.
- Lelieveld, J., P. J. Crutzen, V. Ramanathan, M. O. Andreae, C. A. M. Brenninkmeijer, T. Campos, G. R. Cass, R. R. Dickerson, H. Fischer, J. A. De Gouw, A. Hansel, A. Jefferson, D. Kley, A. T. J. De Laat, S. Lal, M. G. Lawrence, J. M. Lobert, O. L. Mayol-Bracero, A. P. Mitra, T. Novakov, S. J. Oltmans, K. A. Prather, T. Reiner, H. Rodhe, H. A. Scheeren, D. Sikka, and J. Williams (2001), The Indian Ocean Experiment: Widespread air pollution from South and Southeast Asia, *Science*, *291(5506)*, 1031-1036.
- Lighty, J. S., J. M. Veranth, and A. F. Sarofim (2000), Combustion aerosols: factors governing their size and composition and implications to human health, *J. Air & Waste Manage. Assoc.*, *50(9)*, 1565-1618.

- Lin, C.-Y., Z. Wang, W.-N. Chen, S.-Y. Chang, C. C. K. Chou, N. Sugimoto, and X. Zhao (2007), Long-range transport of Asian dust and air pollutants to Taiwan: observed evidence and model simulation, *Atmos. Chem. Phys.*, 7(2), 423-434.
- Liousse, C., H. Cachier, and S. G. Jennings (1993), Optical and thermal measurements of black carbon aerosol content in different environments: Variation of the specific attenuation cross-section (σ), *Atmos. Environ. - Part A General Topics*, 27A(8), 1203-1211.
- Mader, B. T., R. C. Flagan, and J. H. Seinfeld (2002), Airborne measurements of atmospheric carbonaceous aerosols during ACE-Asia, *J. Geophys. Res.*, 107(D23), 4704, doi:10.1029/2002JD002221.
- Maenhaut, W. (2008), New Directions: Future needs for global monitoring and research of aerosol chemical composition, *Atmos. Environ.*, 42, 1070–1072.
- Mahowald, N. M., A. R. Baker, G. Bergametti, N. Brooks, R. A. Duce, T. D. Jickells, N. Kubilay, J. M. Prospero, and I. Tegen (2005), Atmospheric global dust cycle and iron inputs to the ocean, *Global Biogeochem. Cycles*, 19, GB4025, doi:10.1029/2004GB002402.
- Mahowald, N. M., S. Engelstaedter, C. Luo, A. Sealy, P. Artaxo, C. Benitez-Nelson, S. Bonnet, Y. Chen, P. Y. Chuang, D. D. Cohen, F. Dulac, B. Herut, A. M. Johansen, N. Kubilay, R. Losno, W. Maenhaut, A. Paytan, J. M. Prospero, L. M. Shank, and R. L. Siefert (2009), Atmospheric iron deposition: Global distribution, variability, and human perturbations, *Annu. Rev. Marine Sci.*, 1, 245-278, doi:10.1146/annurev.marine.010908.163727.
- Malm, W. C., J. V. Molenar, R. A. Eldred, and J. F. Sisler (1996), Examining the relationship among atmospheric aerosols and light scattering and extinction in the Grand Canyon area, *J. Geophys. Res.*, 101(14), 19251-19265.
- Manktelow, P. T., K. S. Carslaw, G. W. Mann, and D. V. Spracklen (2010), The impact of dust on sulfate aerosol, CN and CCN during an East Asian dust storm, *Atmos. Chem. Phys.*, 10, 365–382.
- Martins, J., P. Artaxo, C. Liousse, J. Reid, P. Hobbs, and Y. Kaufman (1998), Effects of black carbon content, particle size, and mixing on light absorption by aerosols from biomass burning in Brazil, *J. Geophys. Res.*, 103 (D24), 32041-32050.

- Mauderly, J. L., and J. C. Chow (2008), Health effects of organic aerosols, *Inhalation Toxicol.*, 20(3), 257 - 288
- Mayol-Bracero, O. L., R. Gabriel, M. O. Andreae, T. W. Kirchstetter, T. Novakov, J. Ogren, P. Sheridan, and D. G. Streets (2002), Carbonaceous aerosols over the Indian Ocean during the Indian Ocean Experiment (INDOEX): Chemical characterization, optical properties, and probable sources, *J. Geophys. Res.*, 107(D19), 8030, doi:10.1029/2000JD000039.
- Mayol-Bracero, O. L., P. Guyon, B. G. Roberts, M. O. Andreae, S. Decesari, M. C. Facchini, S. Fuzzi, and P. Artaxo (2002), Water-soluble organic compounds in biomass burning aerosols over Amazonia, 2, Apportionment of the chemical composition and importance of the polyacidic fraction, *J. Geophys. Res.*, 107(D20), 8047, doi:10.1029/2001JD000522.
- Menon, S., J. Hansen, L. Nazarenko, and Y. Luo (2002), Climate effects of black carbon aerosols in China and India, *Science*, 297(5590), 2250-2253.
- Mishra, S. K., and S. N. Tripathi (2008), Modeling optical properties of mineral dust over the Indian Desert, *J. Geophys. Res.*, 113, D23201, doi:10.1029/2008JD010048.
- Miyazaki, Y., S. G. Agarwal, K. Singh, P. K. Gupta, and K. Kawamura (2009), Dicarboxylic acids and water-soluble organic carbon in aerosols in New Delhi, India in winter: Characteristics and formation processes, *J. Geophys. Res.*, 114, D19206, doi:10.1029/2007JD009116.
- Miyazaki, Y., Y. Kondo, S. Han, M. Koike, D. Kodama, Y. Komazaki, H. Tanimoto, and H. Matsueda (2007), Chemical characteristics of water-soluble organic carbon in the Asian outflow, *J. Geophys. Res.*, 112, D22S30, doi:10.1029/2007JD009116.
- Miyazaki, Y., Y. Kondo, L. K. Sahu, J. Imaru, N. Fukushima, and M. Kanod (2008), Performance of a newly designed Continuous Soot Monitoring System (COSMOS), *J. Environ. Monit.*, 10(10), 1109-1240.
- Moosmuller, H., W. P. Arnott, C. F. Rogers, J. L. Bowen, J. A. Gillies, W. R. Pierson, J. F. Collins, T. D. Durbin, and J. M. Norbeck (2001), Time-resolved characterization of diesel particulate emissions. 2. Instruments for elemental and organic carbon measurements, *Environ. Sci. Technol.*, 35(10), 1935-1942.

- Myhre, G. (2009), Consistency between satellite-derived and modeled estimates of the direct aerosol effect, *Science*, *325*, 187-190, DOI: 110.1126/science.1174461.
- Na, K., A. A. Sawant, C. Song, and D. R. C. III (2004), Primary and secondary carbonaceous species in the atmosphere of Western Riverside County, California, *Atmos. Environ.*, *38*(9), 1345-1355.
- Nair, V. S., K. K. Moorthy, D. P. Alappattu, P. K. Kunhikrishnan, S. George, P. R. Nair, S. S. Babu, B. Abish, S. K. Satheesh, S. N. Tripathi, K. Niranjana, B. L. Madhavan, V. Srikant, C. B. S. Dutt, K. V. S. Badarinath, and R. R. Reddy (2007), Wintertime aerosol characteristics over the Indo-Gangetic Plain (IGP): Impacts of local boundary layer processes and long-range transport, *J. Geophys. Res.*, *112*, D13205, doi:10.1029/2006JD008099.
- Nel, A. (2005), Air pollution-related illness: Effects of particles, *Science*, *308*, 804-806.
- Novakov, T., S. Menon, T. W. Kirchstetter, D. Koch, and J. E. Hansen (2005), Aerosol organic carbon to black carbon ratios: Analysis of published data and implications for climate forcing, *J. Geophys. Res.*, *110*, D21205, doi:10.1029/2005JD005977.
- Novakov, T., and J. E. Penner (1993), Large contribution of organic aerosols to cloud-condensation-nuclei concentrations, *Nature*, *365*, 823-826.
- Padró, L. T., D. Tkacik, T. Latham, C. J. Hennigan, A. P. Sullivan, R. J. Weber, L. G. Huey, and A. Nenes (2010), Investigation of cloud condensation nuclei properties and droplet growth kinetics of the water-soluble aerosol fraction in Mexico City, *J. Geophys. Res.*, *115*, D09204, doi:10.1029/2009JD013195.
- Pant, P., P. Hegde, U. C. Dumka, R. Sagar, S. K. Satheesh, K. K. Moorthy, A. Saha, and M. K. Srivastava (2006), Aerosol characteristics at a high-altitude location in central Himalayas: Optical properties and radiative forcing, *J. Geophys. Res.*, *111*, D17206, doi:10.1029/2005JD006768.
- Pio, C. A., M. Legrand, T. Oliveira, J. Afonso, C. Santos, A. Caseiro, P. Fialho, F. Barata, H. Puxbaum, A. Sanchez-Ochoa, A. Kasper-Giebl, A. Gelencser, S. Preunkert, and M. Schock (2007), Climatology of aerosol composition (organic versus inorganic) at non-urban sites on a west-east transect across Europe, *J. Geophys. Res.*, *112*, D23S02, doi:10.1029/2006JD008038.

- Prasad, A. K., and R. P. Singh (2007), Changes in Himalayan snow and glacier cover between 1972 and 2000, *Eos Trans. AGU*, 88, 33, doi:10.1029/2007EO330002.
- Prasad, A. K., R. P. Singh, and M. Kafatos (2006), Influence of coal based thermal power plants on aerosol optical properties in the Indo-Gangetic basin, *Geophys. Res. Lett.*, 33, L05805, doi:10.1029/2005GL023801.
- Puxbaum, H., J. Rendl, R. Allabashi, L. Otter, and M. C. Scholes (2000), Mass balance of the atmospheric aerosol in a South African subtropical savanna (Nylsvley, May 1997), *J. Geophys. Res.*, 105(D16), 20697-20706.
- Quinn, P. K., D. J. Coffman, T. S. Bates, E. J. Welton, D. S. Covert, T. L. Miller, J. E. Johnson, S. Maria, L. Russell, R. Arimoto, C. M. Carrico, and M. J. Rood (2004), Aerosol optical properties measured on board the Ronald H. Brown during ACE-Asia as a function of aerosol chemical composition and source region, *J. Geophys. Res.*, 109, D19S01, doi:10.1029/2003JD004010.
- Ram, K., and M. M. Sarin (2009), Absorption coefficient and site-specific mass absorption efficiency of elemental carbon in aerosols from urban, rural and high-altitude sites in India, *Environ. Sci. Technol.*, 43, 8233-8239.
- Ram, K., and M. M. Sarin, (2010), Spatio-temporal variability in atmospheric abundances of EC, OC and WSOC over northern India, *J. Aerosol Sci.*, 41(1), 88-98.
- Ram, K., M. M. Sarin, and P. Hegde (2008), Atmospheric abundances of primary and secondary carbonaceous species at two high-altitude sites in India: Sources and temporal variability, *Atmos. Environ.*, 42(28), 6785-6796.
- Ramachandran, S., and T. A. Rajesh (2007), Black carbon aerosol mass concentrations over Ahmedabad, an urban location in western India: Comparison with urban sites in Asia, Europe, Canada, and the United States, *J. Geophys. Res.*, 112, D06211, doi:10.1029/2006JD007488.
- Ramachandran, S., R. Rengarajan, A. Jayaraman, M. M. Sarin, and S. K. Das (2006), Aerosol radiative forcing during clear, hazy, and foggy conditions over a continental polluted location in north India, *J. Geophys. Res.*, 111, D20214, doi:10.1029/2006JD007142.

- Ramana, M. V., V. Ramanathan, I. A. Podgorny, B. B. Pradhan, and B. Shrestha (2004), The direct observations of large aerosol radiative forcing in the Himalayan region, *Geophys. Res. Lett.*, *31*, L05111, doi:10.1029/2003GL018824.
- Ramanathan, V., and G. Carmichael (2008), Global and regional climate changes due to black carbon, *Nature Geosci.*, *1*, 221-227.
- Ramanathan, V., P. J. Crutzen, J. T. Kiehl, and D. Rosenfeld (2001), Aerosols, climate, and the hydrological cycle, *Science*, *294*(5549), 2119-2124.
- Ramanathan, V., and M. V. Ramana (2005), Persistent, widespread, and strongly absorbing haze over the Himalayan foothills and the Indo-Gangetic plains, *Pure Appl. Geophys.*, *162*, 1609 – 1626.
- Ramanathan, V., M. V. Ramana, G. Roberts, D. Kim, C. Corrigan, C. Chung, and D. Winker (2007), Warming trends in Asia amplified by brown cloud solar absorption, *Nature*, *448*, 575-578, doi:510.1038/nature06019.
- Rastogi, N., and M. M. Sarin (2006), Chemistry of aerosols over a semi-arid region: Evidence for acid neutralization by mineral dust, *Geophys. Res. Lett.*, *33*, L23815, doi:10.1029/2006GL027708.
- Reddy, M. S., and C. Venkataraman (2002), Inventory of aerosol and sulphur dioxide emissions from India: I - Fossil fuel combustion, *Atmos. Environ.*, *36*(4), 677-697.
- Rengarajan, R., M. M. Sarin, and A. K. Sudheer (2007), Carbonaceous and inorganic species in atmospheric aerosols during wintertime over urban and high-altitude sites in North India, *J. Geophys. Res.*, *112*, D21307, doi:10.1029/2006JD008150.
- Rissman, T. A., A. Nenes, and J. H. Seinfeld (2004), Chemical amplification (or Dampening) of the Twomey effect: Conditions derived from droplet activation theory, *J. Atmos. Sci.*, *61*, 919-930.
- Rolph, G. D. (2010), Real-time Environmental Applications and Display sYstem (READY) Website (<http://ready.arl.noaa.gov>), NOAA Air Resources Laboratory, Silver Spring, MD.
- Rosenfeld, D., J. Dai, X. Yu, Z. Yao, X. Xu, X. Yang, and C. Du (2007), Inverse relations between amounts of air pollution and orographic precipitation, *Science*, *315*(5817), 1396-1398.

- Saarikoski, S., H. Timonen, K. Saarnio, M. Aurela, L. Jarvi, P. Keronen, V.-M. Kerminen, and R. Hillamo (2008), Sources of organic carbon in fine particulate matter in northern European urban air, *Atmos. Chem. Phys.*, *8*, 6281–6295.
- Sagar, R., B. Kumar, U. C. Dumka, K. K. Moorthy, and P. Pant (2004), Characteristics of aerosol spectral optical depths over Manora Peak: A high-altitude station in the central Himalayas, *J. Geophys. Res.*, *109*, D06207, doi:10.1029/2003JD003954.
- Sandradewi, J., A. S. H. Prévôt, E. Weingartner, R. Schmidhauser, M. Gysel, and U. Baltensperger (2008a), A study of wood burning and traffic aerosols in an Alpine valley using a multi-wavelength Aethalometer, *Atmos. Environ.*, *42*(1), 103-112.
- Sandradewi J., A. S. H. Prévôt, S. Szidat, N. Perron, M. Rami Alfarra, V. A. Lanz, E. Weingartner, U. Baltensperger (2008b), Using aerosol light absorption measurements for the quantitative determination of wood burning and Traffic emission contributions to particulate matter, *Environ. Sci. Technol.*, *42* (9), 3316-3323.
- Satheesh, S. K., and V. Ramanathan (2000), Large differences in tropical aerosol forcing at the top of the atmosphere and Earth's surface, *Nature*, *405*(6782), 60-63.
- Schauer, J. J., W. F. Rogge, L. M. Hildemann, M. A. Mazurek, G. R. Cass, and B. R. T. Simoneit (1996), Source apportionment of airborne particulate matter using organic compounds as tracers, *Atmos. Environ.*, *30*(22), 3837-3855.
- Schmid, O., P. Artaxo, W. P. Arnott, D. Chand, L. V. Gatti, G. P. Frank, A. Hoffer, M. Schnaiter, and M. O. Andreae (2006), Spectral light absorption by ambient aerosols influenced by biomass burning in the Amazon Basin. I: Comparison and field calibration of absorption measurement techniques, *Atmos. Chem. Phys.*, *6*(11), 3443-3462.
- Schuster, G. L., O. Dubovik, B. N. Holben, and E. E. Clothiaux (2005), Inferring black carbon content and specific absorption from Aerosol Robotic Network (AERONET) aerosol retrievals, *J. Geophys. Res.*, *110*, D10S17, doi:10.1029/2004JD004548.
- Schwartz, S. E., Harshvardhan, and C. M. Benkovitz (2002), Influence of anthropogenic aerosol on cloud optical depth and albedo shown by satellite measurements and chemical transport modeling, *Proc. Natl. Acad. Sci. USA* *99*, 1784–1789.

- Schwarz, J., R. Gao, J. R. Spackman, L. Watts, D. S. Thomson, D. W. Fahey, T. B. Ryerson, J. Peischl, J. S. Holloway, M. K. Trainer, G. J. Frost, T. Baynard, D. Lack, J. A. DeGouw, C. Warneke, and L. A. D. Negro (2008), Measurement of the mixing state, mass, and optical size of individual black carbon particles in urban and biomass burning emissions, *Geophys. Res. Lett.*, *35*, L13810, doi:10.1029/2008GL033968.
- Sciare, J., H. Cachier, K. Oikonomou, P. Ausset, R. Sarda-Estève, and N. Mihalopoulos (2003), Characterization of carbonaceous aerosols during the MINOS campaign in Crete, July–August 2001: a multi-analytical approach, *Atmos. Chem. Phys.*, *3*, 1743-1757.
- Sciare, J., K. Oikonomou, O. Favez, E. Liakakou, Z. Markaki, H. Cachier, and N. Mihalopoulos (2008), Long-term measurements of carbonaceous aerosols in the Eastern Mediterranean: evidence of long-range transport of biomass burning, *Atmos. Chem. Phys.*, *8*, 5551-5563.
- Seinfeld, J. H., and S. N. Pandis (1998), *Atmospheric Chemistry and Physics: From Air Pollution to Climate Change*, John Wiley & Sons, Inc, Hoboken, New Jersey.
- Sharma, S., J. R. Brook, H. Cachier, J. Chow, A. Gaudenzi, and G. Lu (2002), Light absorption and thermal measurements of black carbon in different regions of Canada, *J. Geophys. Res.*, *107*(D24), 4771, doi:10.1029/2002JD002496.
- Sheesley, R. J., J. J. Schauer, Z. Chowdhury, G. R. Cass, and B. R. T. Simoneit (2003), Characterization of organic aerosols emitted from the combustion of biomass indigenous to South Asia, *J. Geophys. Res.*, *108* (D9), 4285, doi:10.1029/2002JD002981.
- Sillanpaa, M., A. Frey, R. Hillamo, A. S. Pennanen, and R. O. Salonen (2005), Organic, elemental and inorganic carbon in particulate matter of six urban environments in Europe, *Atmos. Chem. Phys.*, *5*(11), 2869-2879.
- Singh, R. P., S. Dey, S. N. Tripathi, V. Tare, and B. N. Holben (2004), Variability of aerosol parameters over Kanpur, northern India, *J. Geophys. Res.*, *109*, D23206, doi:10.1029/2004JD004966.

- Singh, S., S. Nath, R. Kohli, and R. Singh (2005), Aerosols over Delhi during pre-monsoon months: Characteristics and effects on surface radiation forcing, *Geophys. Res. Lett.*, *32*, L13808, doi:10.1029/2005GL023062.
- Snyder, D. C., and J. J. Schauer (2007), An inter-comparison of two black carbon aerosol instruments and a semi-continuous elemental carbon instrument in the urban environment, *Aerosol Sci. Technol.*, *41*(5), 463-474.
- Song, C. H., C. M. Kim, Y. J. Lee, G. R. Carmichael, B. K. Lee, and D. S. Lee (2007), An evaluation of reaction probabilities of sulfate and nitrate precursors onto East Asian dust particles, *J. Geophys. Res.*, *112*, D18206, doi:10.1029/2006JD008092.
- Streets, D. G., T. C. Bond, T. Lee, and C. Jang (2004), On the future of carbonaceous aerosol emissions, *J. Geophys. Res.*, *109*, D24212, doi:10.1029/2004JD004902.
- Subramanian, R., E. Winijkul, T. C. Bond, W. Thiansathit, N. T. K. Oanh, I. Paw-armart, and K. G. Duleep (2009), Climate-relevant properties of diesel particulate emissions: Results from a Piggyback study in Bangkok, Thailand, *Environ. Sci. Technol.*, *43*(11), 4213–4218.
- Sudheer, A. K., and M. M. Sarin (2008), Carbonaceous aerosols in MABL of Bay of Bengal: Influence of continental outflow, *Atmos. Environ.*, *42*(18), 4089–4100.
- Sun, J., and P. A. Ariya (2006), Atmospheric organic and bio-aerosols as cloud condensation nuclei (CCN): A review, *Atmos. Environ.*, *40*(5), 795-820.
- Tare, V., S. N. Tripathi, N. Chinnam, A. K. Srivastava, S. Dey, M. Manar, V. P. Kanawade, A. Agarwal, S. Kishore, R. B. Lal, and M. Sharma (2006), Measurements of atmospheric parameters during Indian Space Research Organization-Geosphere Biosphere Program Land Campaign II at a typical location in the Ganga Basin: 2. Chemical properties, *J. Geophys. Res.*, *111*, D23210, doi:10.1029/2006JD007279.
- Tripathi, S. N., S. Dey, V. Tare, and S. K. Satheesh (2005a), Aerosol black carbon radiative forcing at an industrial city in northern India, *Geophys. Res. Lett.*, *32*, L08802, doi:10.1029/2005GL022515.
- Tripathi, S. N., S. Dey, V. Tare, S. K. Satheesh, S. Lal, and S. Venkataramani (2005b), Enhanced layer of black carbon in a north Indian industrial city, *Geophys. Res. Lett.*, *32*, L12802, doi:10.1029/2005GL022515.

- Turpin, B. J., and J. J. Huntzicker (1995), Identification of secondary organic aerosol episodes and quantitation of primary and secondary organic aerosol concentrations during SCAQS, *Atmos. Environ.*, *29*(23), 3527-3544.
- Turpin, B. J., and H.-J. Lim (2001), Species contributions to PM_{2.5} mass concentrations: Revisiting common assumptions for estimating organic mass, *Aerosol Sci. Technol.*, *35*(1), 602-610.
- Venkataraman, C., G. Habib, A. Eiguren-Fernandez, A. H. Miguel, and S. K. Friedlander (2005), Residential biofuels in South Asia: Carbonaceous aerosol emissions and climate impacts, *Science*, *307*(5714), 1454-1456.
- Venkataraman, C., C. K. Reddy, S. Josson, and M. S. Reddy (2002), Aerosol size and chemical characteristics at Mumbai, India, during the INDOEX-IFP (1999), *Atmos. Environ.*, *36*(12), 1979-1991.
- Wang, C., D. Kim, A. M. L. Ekman, M. C. Barth, and P. J. Rasch (2009), Impact of anthropogenic aerosols on Indian summer monsoon, *Geophys. Res. Lett.*, *36*, L21704, doi:10.1029/2009GL040114.
- Watson, J. G., and J. C. Chow (2002), Comparison and evaluation of in situ and filter carbon measurements at the Fresno Supersite, *J. Geophys. Res.*, *107*(D21), 8341, doi:10.1029/2001JD000573.
- Weber, R. J., A. P. Sullivan, R. E. Peltier, A. Russell, B. Yan, M. Zheng, J. de Grouw, C. Warneke, C. Brock, J. S. Holloway, E. L. Atlas, and E. Edgerton (2007), A study of secondary organic aerosol formation in the anthropogenic-influenced southeastern United States, *J. Geophys. Res.*, *112*, D13302, doi:10.1029/2007JD008408.
- Weingartner, E., H. Saathoff, M. Schnaiter, N. Streit, B. Bitnar, and U. Baltensperger (2003), Absorption of light by soot particles: Determination of the absorption coefficient by means of aethalometers, *J. Aerosol Sci.*, *34*(10), 1445-1463.
- Yan, P., J. Tang, J. Huang, J. T. Mao, X. J. Zhou, Q. Liu, Z. F. Wang, and H. G. Zhou (2008), The measurement of aerosol optical properties at a rural site in Northern China, *Atmos. Chem. Phys.*, *8*, 2229-2242.
- Yang, M., S. G. Howell, J. Zhuang, and B. J. Huebert (2009), Attribution of aerosol light absorption to black carbon, brown carbon, and dust in China – interpretations of

- atmospheric measurements during EAST-AIRE, *Atmos. Chem. Phys.*, *9*, 2035–2050.
- Yasunari, T. J., P. Bonasoni, P. Laj, K. Fujita, E. Vuillermoz, A. Marinoni, P. Cristofanelli, R. Duchi, G. Tartari, and K.-M. Lau (2010), Preliminary estimation of black carbon deposition from Nepal Climate Observatory-Pyramid data and its possible impact on snow albedo changes over Himalayan glaciers during the pre-monsoon season, *Atmos. Chem. Phys. Discuss.*, *10*, 9291-9328.
- Zhang, Q., J. L. Jimenez, M. R. Canagaratna, J. D. Allan, H. Coe, I. Ulbrich, M. R. Alfarra, A. Takami, A. M. Middlebrook, Y. L. Sun, K. Dzepina, E. Dunlea, K. Docherty, P. F. DeCarlo, D. Salcedo, T. Onasch, J. T. Jayne, T. Miyoshi, A. Shimono, S. Hatakeyama, N. Takegawa, Y. Kondo, J. Schneider, F. Drewnick, S. Borrmann, S. Weimer, K. Demerjian, P. Williams, K. Bower, R. Bahreini, L. Cottrell, R. J. Griffin, J. Rautiainen, J. Y. Sun, Y. M. Zhang, and D. R. Worsnop (2007), Ubiquity and dominance of oxygenated species in organic aerosols in anthropogenically-influenced Northern Hemisphere mid-latitudes, *Geophys. Res. Lett.*, *34*, L13801, doi:10.1029/2007GL029979.
- Zhang, Q., J. Zhang, and H. Xue (2010), The challenge of improving visibility in Beijing, *Atmos. Chem. Phys. Discuss.*, *10*, 6199–6218.
- Zhang, X. Y., Y. Q. Wang, X. C. Zhang, W. Guo, T. Niu, S. L. Gong, Y. Yin, P. Zhao, J. L. Jin, and M. Yu (2008), Aerosol monitoring at multiple locations in China: contributions of EC and dust to aerosol light absorption, *Tellus*, *60*(4), 647-656.

LIST OF PUBLICATIONS

(i) Papers published in peer reviewed International Journals:

- 1. Kirpa Ram, M. M. Sarin and P. Hegde (2008)**, Atmospheric abundances of primary and secondary carbonaceous species at two high-altitude sites in India: Sources and temporal variability, **Atmospheric Environment**, *42*, 6785-6795, doi:10.1016/j.atmosenv.2008.01.031
- 2. Kirpa Ram and M. M. Sarin (2009)**, Absorption coefficient and site-specific mass absorption efficiency of elemental carbon in atmospheric aerosols from urban, rural and high-altitude sites in India, **Environmental Science and Technology** *43*, 8233-8239; doi:10.1021/es9011542.
- 3. Kirpa Ram and M. M. Sarin (2010)**, Spatio-temporal variability in atmospheric abundances of EC, OC and WSOC over northern India, **Journal of Aerosol Science** *41*, 88-98; doi:10.1016/j.jaerosci.2009.11.004
- 4. Kirpa Ram, M. M. Sarin and P. Hegde (2010)**, Long-term record of aerosol optical properties and chemical composition from a high-altitude site (Manora Peak) in Central Himalaya, **Atmospheric Chemistry and Physics Discussions**, *10*, 7435-7467.
- 5. Kirpa Ram, M. M. Sarin, S. N. Tripathi (2010)**, Atmospheric black carbon and attenuation coefficient from an urban location in northern India: Inter-comparison of thermal and optical methods, **Atmospheric Research**, doi: 10.1016/j.atmosres.2010.04.06 (Available online).
- 6. Kirpa Ram, M.M. Sarin and S. N. Tripathi (2010)**, One-year record of carbonaceous aerosols from an urban location (Kanpur) in the Indo-Gangetic Plain: Characterization, sources and temporal variability, **Journal of Geophysical Research-Atmospheres (revised, 2010)**

7. **Kirpa Ram** and M. M. Sarin (2010), Day-night variability of EC, OC, WSOC and inorganic ions in PM_{2.5} and PM₁₀ over urban site in the Indo-Gangetic Plain: Implications to secondary aerosol formation, **Atmospheric Environment (under review)**

(ii) Abstracts in International/National Conferences:

1. **Kirpa Ram** and M. M. Sarin (2010), Secondary aerosol formation over urban atmosphere in the Indo-Gangetic Plain, northern India, **ICACGP-IGAC-2010**: 11-16th July 2010, Halifax, Canada.
2. **Kirpa Ram**, M. M. Sarin and Prashant Hegde (2009), Absorption properties of atmospheric aerosols from a high-altitude site in northern India, **European Aerosol Conference-2009**: 6-11 Sept 2009, Karlsruhe, Germany, Abstract T091A27.
3. **Kirpa Ram**, M.M. Sarin and S.N. Tripathi (2009), One-year record of carbonaceous aerosols from urban location (Kanpur) in the Indo-Gangetic Plain (IGP), **European Aerosol Conference-2009**: 6-11 Sept 2009, Karlsruhe, Germany, Abstract T059A16.
4. **Kirpa Ram**, A. K. Sudheer and M. M. Sarin (2009), Chemical characteristics of aerosols during foggy and clear days: Case study from northern India, **European Aerosol Conference-2009**: 6-11 Sept 2009, Karlsruhe, Germany, Abstract T042A09.
5. **Kirpa Ram** and M. M. Sarin (2009), Site-specific mass absorption efficiency of EC in atmospheric aerosols from urban, rural and high-altitude sites in India, **MOCA-2009**: July 19-29, 2009, Montreal, Canada.
6. **Kirpa Ram** and M. M. Sarin (2008), Carbonaceous aerosols in urban and high-altitude environment of north-India, **International Conference on Carbonaceous Aerosols (ICCPA-2008)**: 12-14th Aug 2008, Berkeley, California.

7. **Kirpa Ram**, R. Rengarajan, M. M. Sarin and A. K. Sudheer (2008), Relevance of soot particles in the present-day context of atmospheric carbon cycle and climate change, **International Conference on Terrestrial Planets: Evolution through time**: 22-25 January, 2008, Ahmedabad, India.
8. **Kirpa Ram**, M. M. Sarin and Prashant Hegde (2007), Carbonaceous species in atmospheric aerosols from high-altitude sites in India: Role of secondary organic carbon, **International Symposium on Aerosol-Chemistry-Climate Interactions**: 20-22 Nov 2007, Ahmedabad, India.
9. **Kirpa Ram** and M. M. Sarin (2007), Causes for temporal variability of atmospheric ^{210}Pb & ^7Be in a semi-arid region: Implications to Stratosphere-Troposphere exchange, **International Symposium on Aerosol-Chemistry-Climate Interactions**: 20-22 Nov 2007, Ahmedabad, India.
10. **Kirpa Ram** and M. M. Sarin (2007), Atmospheric carbonaceous species (EC, OC): Temporal variability over a high-altitude site in semi-arid region of western India, **Indian Aerosol Science and Technology Association (IASTA)-2007 conference**: 14-16 Nov, 2007, New Delhi, India

APPENDIX-1: ACRONYMS

ACE-Asia	Asian Aerosol Characterization Experiment
AMS	Aerodyne Mass Spectrometry
AOD	Aerosol Optical Depth
BL	Boundary Layer
b_{abs}	Aerosol Absorption Coefficient
b_{scat}	Aerosol Scattering Coefficient
CCN	Cloud Condensation Nuclei
EC	Elemental Carbon
IPCC	Intergovernmental Panel on Climate Change
OC	Organic Carbon
PAH	Poly Aromatic Hydrocarbons
PM _{2.5}	Particulate Matter of aerodynamic diameter less than or equal to 2.5 μm
PM ₁₀	Particulate Matter of aerodynamic diameter less than or equal to 10 μm
POA	Primary Organic Aerosol
PPM	Parts Per Million
PPB	Parts Per Billion
STP	Standard temperature (25° C) and pressure (760 mm)
SOA	Secondary Organic Aerosol
SOC	Secondary Organic Carbon
SEM	Scanning Electron Microscopy
σ_{abs}	Mass Absorption Efficiency of EC
TCA	Total carbonaceous aerosols
TEM	Transmission Electron Microscopy
TOF-MS	Time-Of-Flight Mass Spectrometry
TSP	Total suspended particulate
VOC	Volatile Organic Compound
WIOC	Water-Insoluble Organic Carbon
WSOC	Water-Soluble Organic Carbon